Geochemical-Exploration Studies in the Coeur d'Alene District, Idaho and Montana

---

GEOLOGICAL SURVEY PROFESSIONAL PAPER 1116

Geochemical-Exploration Studies in the Coeur d'Alene District, Idaho and Montana

By GARLAND B. GOTT *and* JOHN B. CATHRALL

GEOLOGICAL SURVEY PROFESSIONAL PAPER 1116

The geochemistry of the Coeur d'Alene mining district, including the modifications that have been made by postore faulting, have been investigated

U.S. DEPARTMENT OF THE INTERIOR
March 3, 1849

UNITED STATES GOVERNMENT PRINTING OFFICE, WASHINGTON : 1980

UNITED STATES DEPARTMENT OF THE INTERIOR
CECIL D. ANDRUS, *Secretary*

GEOLOGICAL SURVEY
H. William Menard, *Director*

Library of Congress Cataloging in Publication Data
Gott, Garland Bayard, 1912–
Geochemical-exploration studies in the Coeur d'Alene District, Idaho and Montana.
(Geological Survey Professional Paper 1116)
Bibliography: p. 40
1. Geochemical prospecting–Coeur d'Alene Mining District. I. Cathrall, John B., joint author.
II. Title. III. Series: United States Geological Survey Professional Paper 1116.
TN270.G67 622'.1 79-607002

For sale by the Superintendent of Documents, U.S. Government Printing Office
Washington, D.C. 20402

CONTENTS

ILLUSTRATIONS

[Plates are in pocket]

TABLES

[Tables 3-6 at end of text]

GEOCHEMICAL-EXPLORATION STUDIES IN THE COEUR D'ALENE DISTRICT, IDAHO AND MONTANA

By GARLAND B. GOTT and JOHN B. CATHRALL

ABSTRACT

The principal ore deposits in the Coeur d'Alene district are lead-zinc-silver replacement veins in Precambrian rocks of the Belt Supergroup. The main ore minerals are galena, tetrahedrite, and sphalerite. The host rocks are mainly quartzite, siltite, and argillite. Cretaceous quartz monzonite locally intrudes the Belt rocks.

The geochemical investigations reported here were carried out to determine if geochemical methods would be useful in the search for concealed ore deposits. About 8,700 soil samples and 4,000 rock samples were collected from a 300-square-mile (780 square kilometer) area for this study. The samples were analyzed for 35 elements.

Antimony, silver, lead, manganese, and copper form dispersion patterns and halos that are related to many of the ore deposits within the district, and these same elements were found to be most useful in delineating the known mineral belts that contain most of the orebodies. The dispersion patterns are probably primary, having only minor modifications due to secondary redistribution of the ore-forming elements.

The mineral belts and geochemical-dispersion patterns have been laterally offset, perhaps as much as 16 miles (26 km), by postore faulting. Prefault dispersion patterns can be restored by adjusting the geochemical maps along the postore faults to match the dispersion patterns across the fault trace. The reconstructed dispersion patterns of antimony, arsenic, lead, sulfur, and the ratio of cadmium to zinc form concentric halos around the restored position of the Gem stocks. Most of the Coeur d'Alene ore has been mined from this halo. It appears that the geochemical exploration methods reported here successfully delineate the major mineral belts and indicate unexplored areas in which to search for new deposits.

INTRODUCTION

The Coeur d'Alene district is in the Bitterroot Mountains in the panhandle of northern Idaho and a small area in western Montana (fig. 1). The first recorded production within the district was in 1884 and since that time the area has become one of the most important mining districts in the world, having produced, through 1978, approximately 28.2×10^9 g (grams) of silver, 6,860,101 t (metric tons) of lead, 2,980,733 t of zinc, and 139,850 t of copper for a total value of \$3,251,827,000 (Donald C. Springer, Consulting Geologist, Osburn, Idaho, personal commun.). It is one of the few districts in the world in which a significant amount of ore is produced principally for its silver content.

Past exploration for ore deposits within the district probably has resulted in the discovery of all the economically mineable deposits that are exposed at the surface. The discovery of additional ore deposits within the district has, therefore, become increasingly difficult and costly. For this reason the geochemical investigations reported here were carried out to determine if geochemical methods can be used successfully in the search for concealed ore deposits of the Coeur d'Alene type. Geochemical techniques have been successfully used elsewhere to investigate large disseminated deposits concealed under shallow cover, but the Coeur d'Alene deposits have different characteristics. They are steeply dipping replacement veins, many of which are very narrow at their suboutcrop. Many others terminate before they reach the surface. Moreover, the veins are enclosed by structurally complex rocks in an extremely rugged terrain that is generally covered by several feet (as much as several meters) of subsoil and moderately heavy to heavy vegetation. Exposures of bedrock in most places are sparse. Nevertheless, the geochemical survey described here has revealed dispersion patterns of ore-forming metals in the soil and weathered rock that are related to the mineralized rock below. Samples collected at intervals of 300–500 ft (feet) (100–166 m (meters)) along many traverses show the presence of zones that contain relatively narrow sulfide-bearing veins. Some elements, especially lead, silver, antimony, copper and manganese, are useful in defining the known linear mineral belts and their possible extensions. In addition, the most volatile elements are zoned in concentric patterns marginal to monzonite stocks.

The area investigated is centered on the established Coeur d'Alene district and covers about 300 mi^2 (square miles) (780 km^2 (square kilometers)). Approximately 8,700 soil samples and 4,000 rock samples were collected and analyzed for as many as 35 elements. The resulting geochemical data were evaluated in relation to known ore deposits, mineral belts, extensions of mineral belts, and potential mineral belts that are as yet unexplored.

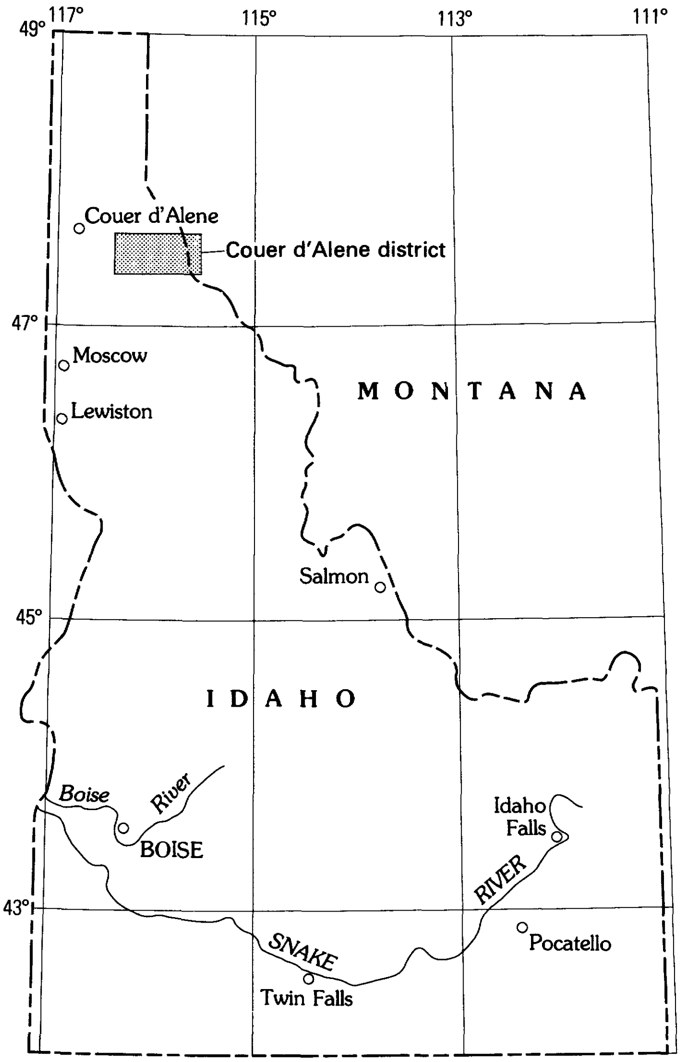

FIGURE 1.—Index map showing the location of the Coeur d'Alene district, Shoshone County, Idaho, and Mineral County, Mont.

ACKNOWLEDGMENTS

We gratefully acknowledge the helpful cooperation of all the mining companies and geologists who generously shared with us their knowledge and ideas about the geology and ore deposits of the Coeur d'Alene district. We particularly wish to thank the American Smelting and Refining Co., Bunker Hill Co., Callahan Mining Corp., Day Mines, Inc., Hecla Mining Co., Sidney Mining Co., and Sunshine Mining Co. We are particularly indebted to Garth M. Crosby, S. Norman Kesten, Stanley Huff, Merle Hutchinson, Donald Springer, Keith Droste, Roger McConnell, Robert L. Meyer, Alfred E. Nugent, A. R. Kinkle, Malcolm Brown, and Donald C. Long.

The comprehensive U.S. Geological Survey Professional Paper by Hobbs, Griggs, Wallace, and Campbell (1965) has been used extensively in these studies. Their detailed descriptions of the 25,000-30,000 ft (7,620-9,144 m) of the Belt Supergroup rocks that are exposed and of the complex structure within the Coeur d'Alene district have given much more direction to these studies than would have otherwise been possible. Likewise, the report by Fryklund (1964) has given the writers a basic understanding of the ore deposits that would otherwise have been difficult to obtain. The earlier publications of Hershey (1916), Ransome and Calkins (1908), and Umpleby and Jones (1923) have given much information about the ore deposits as they were known in the early years of this century. This information has been drawn upon freely. The reader is referred to these publications for more detail about the geology and ore deposits of the district.

We are indebted to Theodore M. Billings, Joseph M. Botbol, Arthur P. Pierce, and Gordon H. Van Sickle for collection of geochemical samples; to Joseph M. Botbol and Jack B. Fife for computer programs; to Theodore M. Billings for retrieval and reduction of analytical data; to George Van Trump, Jr., for computer printouts of cumulative-frequency plots; and to Lennart A. Anderson for interpretation of aeromagnetic data pertaining to the Atlas pluton.

An essential contribution of this study has been made by many analysts in the Denver laboratories of the U.S. Geological Survey and is gratefully acknowledged. The analysts for most of the data used in this report are R. N. Babcock, G. F. Chlumsky, C. A. Curtis, J. V. Desmond, M. S. Erickson, W. H. Ficklin, C. L. Forn, J. G. Frisken, D. J. Grimes, J. R. Hassemer, J. D. Hoffman, R. T. Hopkins, C. L. Jacobson, W. W. Janes, H. D. King, R. W. Leinz, J. M. Motooka, Vania Mello, R. L. Miller, E. L. Mosier, J. C. Negri, S. Noble, R. M. O'Leary, J. Reynolds, Z. C. Stephenson, A. J. Toevs, R. B. Tripp, Susan Truesdell, J. H. Turner, R. L. Turner, L. A. Vinnola, J. R. Watterson, K. C. Watts, and E. P. Welsch.

GEOLOGIC SETTING OF THE ORE DEPOSITS

The ore deposits of the Coeur d'Alene district are confined to rocks of the Belt Supergroup, a huge section of fine-grained clastic rocks consisting largely of quartzite, siltite, and argillite of late Precambrian age (pl. 1). Disseminated dolomite and limestone occur in the upper part of the section. These rocks were laid down in a large geosyncline covering central and northern Idaho, much of western Montana, a large area in southeastern British Columbia, and adjacent Alberta (Hobbs and others, 1965, p. 1). The Coeur d'Alene district lies along the southwestern side of this geosyncline. The thickness of the rocks of the Belt Supergroup in the Coeur d'Alene district is unknown, but at least 21,000 ft (6,400 m) is exposed. An unknown amount at the base is buried, and an indeterminate amount of the upper part has been eroded (Hobbs and Fryklund, 1968). Harrison (1972) reported a thickness of 67,000 ft (20,420 m) of exposed Belt rocks about 75 mi (121 km) southeast of the Coeur d'Alene district near Alberton, Mont., where neither the top nor bottom of the group is exposed. The sedimentary rocks of the Belt Supergroup have been divided into six formations. These formations, together with their major characteristics and general economic significance as host rocks for the ore deposits, are given in table 1 (Hobbs and others, 1965, p. 14). Cretaceous monzonite, known as the Gem and Dago Peak stocks, intrude the Belt rocks. In addition, there are two episodes of intrusives represented by diabase and lamprophyre dikes.

The structure as mapped by Hobbs, Griggs, Wallace, and Campbell (1965) shows that the rocks in the Coeur d'Alene district have been folded and faulted into a complex pattern of blocks and slices. The southeast-trending Osburn fault, which bisects the district, has large components of strike-slip and vertical movements and is the most pronounced structural feature within the district. The northwest-trending Kellogg fault, west of the town of Kellogg, may be a branch of the Osburn fault along which considerable strike-slip movement occurred. Several geochemical dispersion patterns suggest that the Paymaster fault may also be a strand of the Osburn fault. The Placer Creek fault, roughly parallel to the Osburn and 3–4 mi (4.8–6.4 km) south of it, also has right-lateral strike-slip movement. Many other northwest-trending faults that are steeply dipping to the southwest connect the Osburn and Placer Creek faults. Some of these connecting faults are normal, others are reverse, and still

TABLE 1.—*Characteristics of Belt Supergroup, Coeur d'Alene District*

[Stratigraphic data from Hobbs and others 1965. p. 14]

Group	Formation		Lithology	Thickness		Ore-bearing
				(ft)	(m)	
Missoula	Striped Peak Formation		Interbedded quartzite and argillite with some arenaceous dolomitic beds. Purplish gray and pink to greenish gray. Ripple marks, mud cracks common. Top eroded.	1,500+	457+	No.
	Wallace Formation	Upper part	Mostly medium- to greenish-gray finely laminated argillite. some arenaceous dolomite and impure quartzite, and minor gray dolomite and limestone in the middle part.	4,500–6,500	1,372–1,981	Yes, but limited.
		Lower part	Light-gray more or less dolomitic quartzite interbedded with greenish-gray argillite. Ripple marks, mud cracks abundant.			
Ravalli	St. Regis Formation	Upper part	Light greenish-yellow to light green-gray argillite; thinly laminated. Some carbonate-bearing beds.	1,400–2,000	427–610	Yes.
		Lower part	Gradational from interbedded argillite and impure quartzite at top to thick-bedded pure quartzite at base. Red-purple color characteristic; some green-gray argillite. Some carbonate-bearing beds. Ripple marks, mud cracks, and mud-chip breccia common.			
	Revett Formation		Thick-bedded vitreous light yellowish-gray to nearly white pure quartzite. Grades into nearly pure and impure quartzite at top and bottom. Cross-stratification common.	1,200–3,400	366–1,036	Yes.
	Burke Formation		Light greenish-gray impure quartzite. Some pale red and light yelowish-gray pure to nearly pure quartzite. Ripple marks, swash marks and pseudoconglomerate.	2,200–3,000	571–914	Yes
	Prichard Formatin	Upper part	Interbedded medium-gray argillite and quartrose argillite and light-gray impure to pure quartzite. Some mud cracks and ripple marks.	12,000+	3,658+	Yes.
		Lower part	Thin- to thick-bedded, medium gray argillite and quartrose argillite; laminated in part. Pyrite abundant. Some discontinuous quartzite zones. Base buried.			

others have strike-slip components of movement. There are two sets of high-angle faults north of the Osburn fault. A northwest-trending set is adjacent to and subparallel to the Osburn fault, and another is a north-trending set. The normal Dobson Pass fault bisects the northern part of the district and dips westward at an angle of about 30°. To the west of the Dobson Pass fault, the reverse Carpenter Gulch and Blackcloud faults dip westward at relatively low angles.

The aeromagnetic map shown in figure 2 (U.S. Geological Survey, 1969a, b) strikingly outlines the position and general shape of the known Gem and Dago Peak stocks and strongly suggests that a buried pluton, possibly having a composition similar to that of the Gem stocks, exists near the Atlas mine south of Mullan. Lennart Anderson (oral commun., 1971) of the U.S. Geological Survey has estimated that the top of this pluton is about 3,500 ft (1,067 m) below the surface. To simplify later discussions the pluton is here referred to as the Atlas pluton.

PROBLEMATICAL ORIGIN AND AGE OF THE ORE DEPOSITS

Controversy over the origin and age of the Coeur d'Alene ore deposits has existed from the earliest studies of the district to the present (1975) and is still unresolved. Ransome and Calkins (1908) and Umpleby and Jones (1923) considered that the ore deposits were derived from hydrothermal solutions from a magmatic source related to the Idaho batholith. Fryklund (1964) believed that major proportions of the sulfides were derived from a "deep point source" that is probably below the magmatic zone in the mantle. Hershey (1916) concluded that the source of the lead and zinc in the ore deposits was from disseminations of these metals in the upper part of the Prichard Formation. He expressed the opinion that active circulation of heated waters started by the intrusion of the monzonite stocks dissolved the lead and zinc minerals and transported them upward and deposited them in the veins. He thereby concluded that the ore deposits were older than the monzonite intrusives and that the minor sulfide veins in the monzonite stocks resulted from reworking and incorporation of some of the preexisting sulfide minerals. The widespread occurrences of stratabound copper sulfides in the Belt Supergroup, recently described by Clark (1971), Harrison (1972), and others, provide a possible source for some of the sulfides that may have been remobilized into vein-type deposits.

Extensive studies of the isotope ratios in lead from the Coeur d'Alene deposits as well as from numerous other deposits in the surrounding region by Long, Silverman, and Kulp (1960), Cannon, Pierce, Antweiler, and Buck (1962), and Zartman and Stacey (1971) have convinced these workers that most of the lead is of ancient origin—probably originally derived in Precambrian time. Assuming the interpretation of the age of the lead is correct, the problems related to its original source, its positioning in the various deposits, the amount of possible remobilization, and the time of its final emplacement are subject to various interpretations.

The geochemical data presented here do not unequivocally resolve this problem although the data do support Hershey's (1916) conclusion that some metals were remobilized and redistributed at the time of the monzonite intrusions. Antimony, sulfur, arsenic, cadmium, lead, and possibly other elements form halos around the original position of the Gem stocks; antimony, silver, copper, barium, and manganese form dispersion patterns directly above the postulated Atlas pluton. These dispersion patterns clearly formed in response to the elevated temperatures provided by the invading magmas.

GEOCHEMICAL STUDIES

SAMPLE MATERIAL

A geochemical study of an area as large as the Coeur d'Alene district (approximately 300 mi^2 (780 km^2)) involves the collection and analysis of a large number of samples and the interpretation of a large amount of analytical data. In the Coeur d'Alene district limitations were imposed upon the various sample materials and the conditions for their collection. The principal limitations were contamination of soils resulting from mine and smelter operations spanning the greater part of a century, dense vegetative cover which greatly limits the bedrock exposures, leaching and redistribution of the most soluble metals in the zone of oxidation, and the steep slopes and rough nature of terrain which has resulted in the down-slope movement of detrital material and, locally, large volumes of talus.

Both rocks and roils were sampled in this study (fig. 3, 4). Because of the dense vegetative cover and the steepness of the terrain the traverses were largely restricted to jeep trails and ridge lines. Wherever possible these traverses were oriented normal to the mineralized structues. The sample interval was 0.1 mi (0.16 km) on jeep traverses and generally 300 ft (100 m) on walking traverses.

Special test studies of soil profiles indicated that soil samples collected in the district from depths greater than about 6 in. (inches) (15 cm (centimeters)) below the

A soil horizon are free from contamination except in the vicinity of the smelter at Kellogg. Canney (1959) investigated the extent of soil contamination by lead and zinc derived from the Kellogg Smelter and concluded that contamination by these two elements below about 6 in. (15 cm) is not significant, except near the smelter where samples collected from any depth may be contaminated by metals derived from smelter emissions. All soil samples were collected at or below this depth. Alluvial soils were not collected.

Bedrock samples were collected wherever they were exposed along a line of traverse, and these were supplemented by float samples where bedrock was not exposed. Float samples, however, were collected only where the sample was judged to be near its source.

Approximately 600 samples of conifer twigs and needles, principally from Douglas-fir and western white pine, were collected from the district and are under study.

ANALYTICAL METHODS

Semiquantitative spectrographic analyses were used for iron, magnesium, calcium, titanium, manganese, boron, barium, beryllium, cobalt, chromium, lanthanum, molybdenum, nickel, scandium, strontium, vanadium, yttrium, and zirconium (Grimes and Marranzino, 1968). Atomic-absorption spectrophotometry was used to determine zinc, silver, cadmium, copper, and lead (Ward and others, 1963, 1969). Mercury was determined using flameless atomic-absorption spectrophotometry (Vaughn and McCarthy, 1964). Antimony and arsenic were determined by colorimetry (Ward and others, 1963). The Leco combustion technique was used to determine sulfur. The minus-80-mesh part of the soil samples and the minus-100-mesh or finer part of the rock samples were used for analysis.

The lower limit of detection for each element by the analytical method used, the estimated crustal abundance, and the median concentration level of the elements in the Coeur d'Alene district are shown in table 2.

TABLE 2.—*Lower limit of detection of the elements by analytical methods used in this study, estimated crustal abundance and the median value of the elements in samples from the Coeur d'Alene district*

[Value for Fe, Mg, Ca, and Ti in percent; all other values in parts per million. <, less than]

Element	Lower limit of detection	Crustal abundance (Goldschmidt, 1954)	Median value of concentration in rocks	Median value of concentration in soils
Spectrographic analyses				
Fe	0.05	5	2.4	3.6
Mg	.02	2	.25	.65
Ca	.05	3.6	<.05	.60
Ti	.002	.44	.2	.52
Mn	10	1,000	366	1,333
B	10	10	38	30
Ba	20	430	383	628
Be	1	6	.8	1.2
Co	10	40	<10	11
Cr	20	200	20	35
La	20	18	27	26
Mo	20	2.3	<20	<20
Nb	10	20	<10	<10
Ni	5	100	9	23
Sc	5	5	6	10
Sn	10	40	<10	<10
Sr	100	150	<100	156
V	10	150	21	93
Y	10	28	21	22
Zr	20	220	198	229
Atomic absorption analyses				
Hg	0.02	0.5	0.03	0.1
Cu	25	70	12	28
Pb	25	16	19	43
Zn	25	80	36	95
Ag	.2	.02	.2	.6
Cd	.2	.18	.4	.8
Colorimetry analyses				
As	10	5	<10	<10
Sb	.5	1	1	1.1
Leco combustion analysis				
S	30	520	80	468

DATA POINTS

A computer-implemented graphics technique has been used to illustrate the geochemical relations (Gott and Botbol, 1973). The analytical data for elements was expanded to include ratios and combinations of the more common sulfide-forming elements. All geochemical maps were gridded to a rectangular coordinate system 1,000 ft (305 m) apart.

The original data points (sample localities) were transposed to the grid coordinated or mesh points by drawing a circle around each mesh point and shifting the coordinates of data points to the center of the circle. The value at each point was weighted according to its distance from the mesh point; as a result, close-lying data points have more influence than outlying data points on the final value to be used at the mesh point. After data points have been weighted and projected to a mesh point, all values were averaged, and the average value were used at that point. The map location of the data is the center of the left digit of the value given. The extent of interpolation between mesh points is determined by the size of the search circle

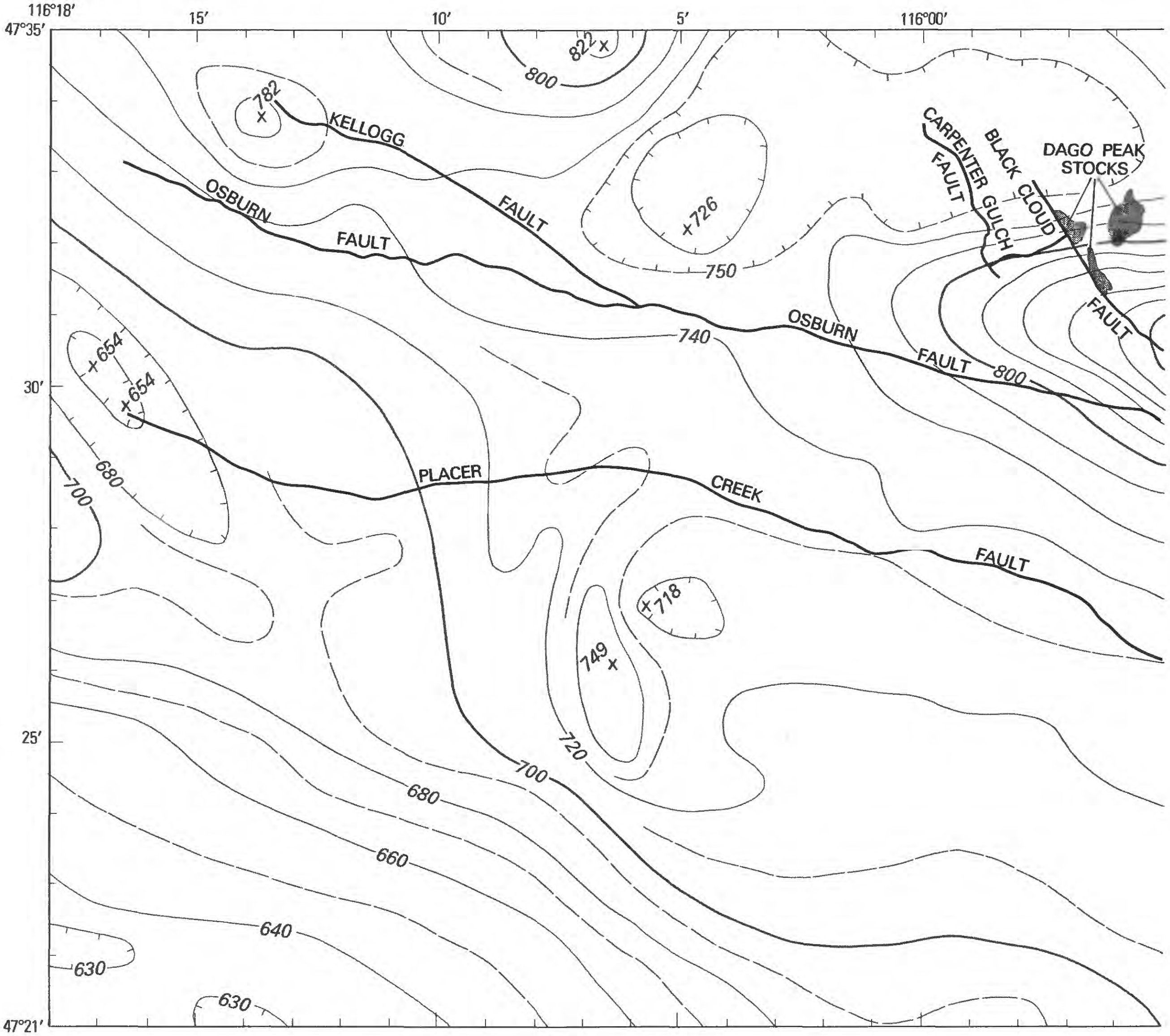

EXPLANATION

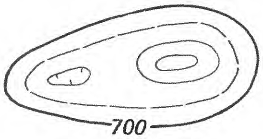

Magnetic contours—Showing total intensity magnetic field of the earth in gammas relative to arbitrary datum. Hachured to indicate closed areas of lower magnetic intensity. Contour interval 20 gammas. Dashed lines are 10 gamma supplemental contours

+749 Measured maximum or minimum intensity within closed high or closed low

——— Fault

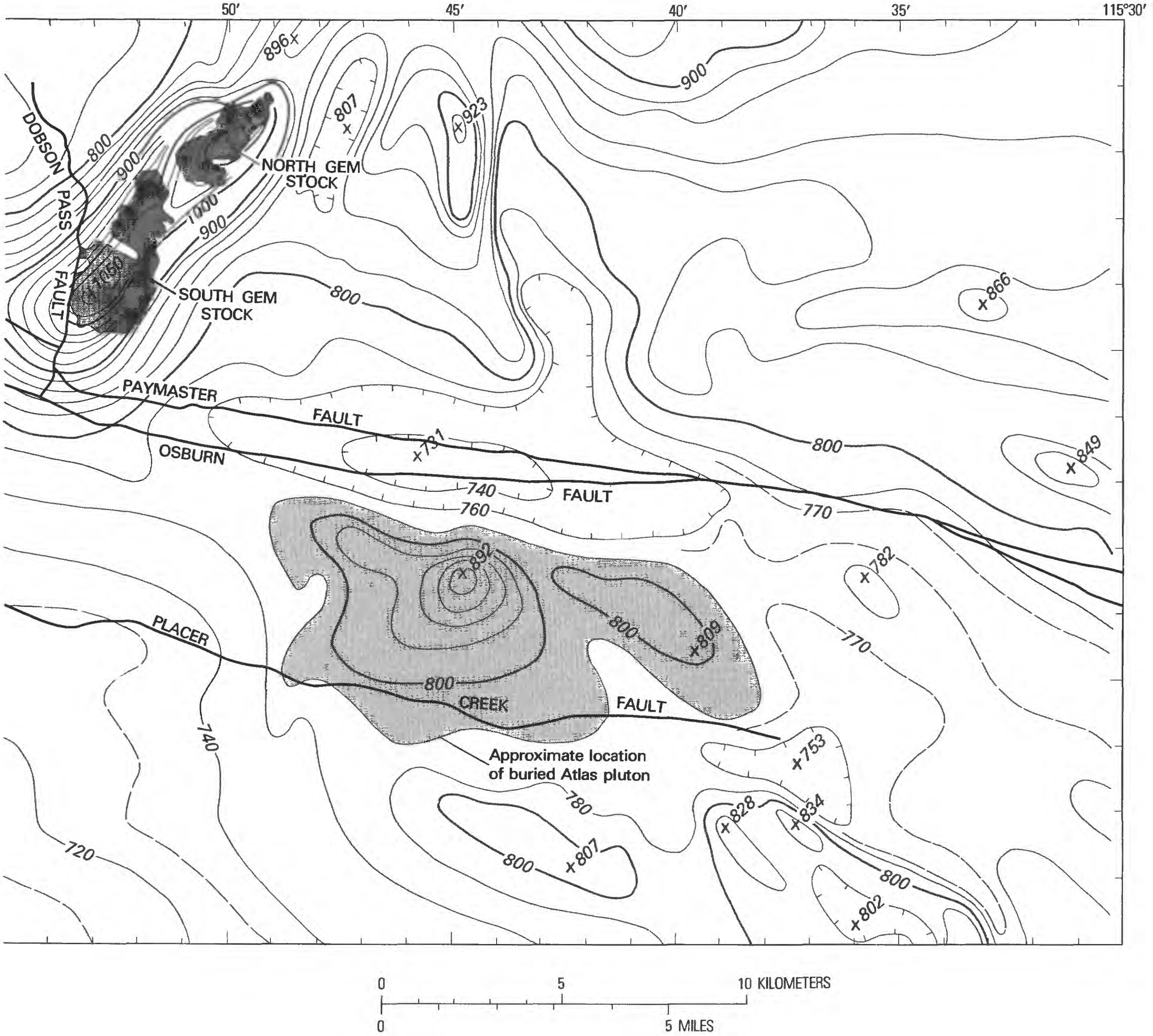

FIGURE 2.—Aeromagnetic map of the Coeur d'Alene district, Idaho and Montana. Magnetic contours compiled from U.S. Geological Survey Geophysical Investigation Maps GP-685 and GP-689 (1969). Faults west of 115°42′30″ modified from Hobbs, Griggs, Wallace, and Campbell (1965); faults east of 115°42′30″ modified from Wallace and Hosterman (1956). Monzonite stocks and associated rocks from Hobbs, Griggs, Wallace, and Campbell (1965, pls. 3, 4).

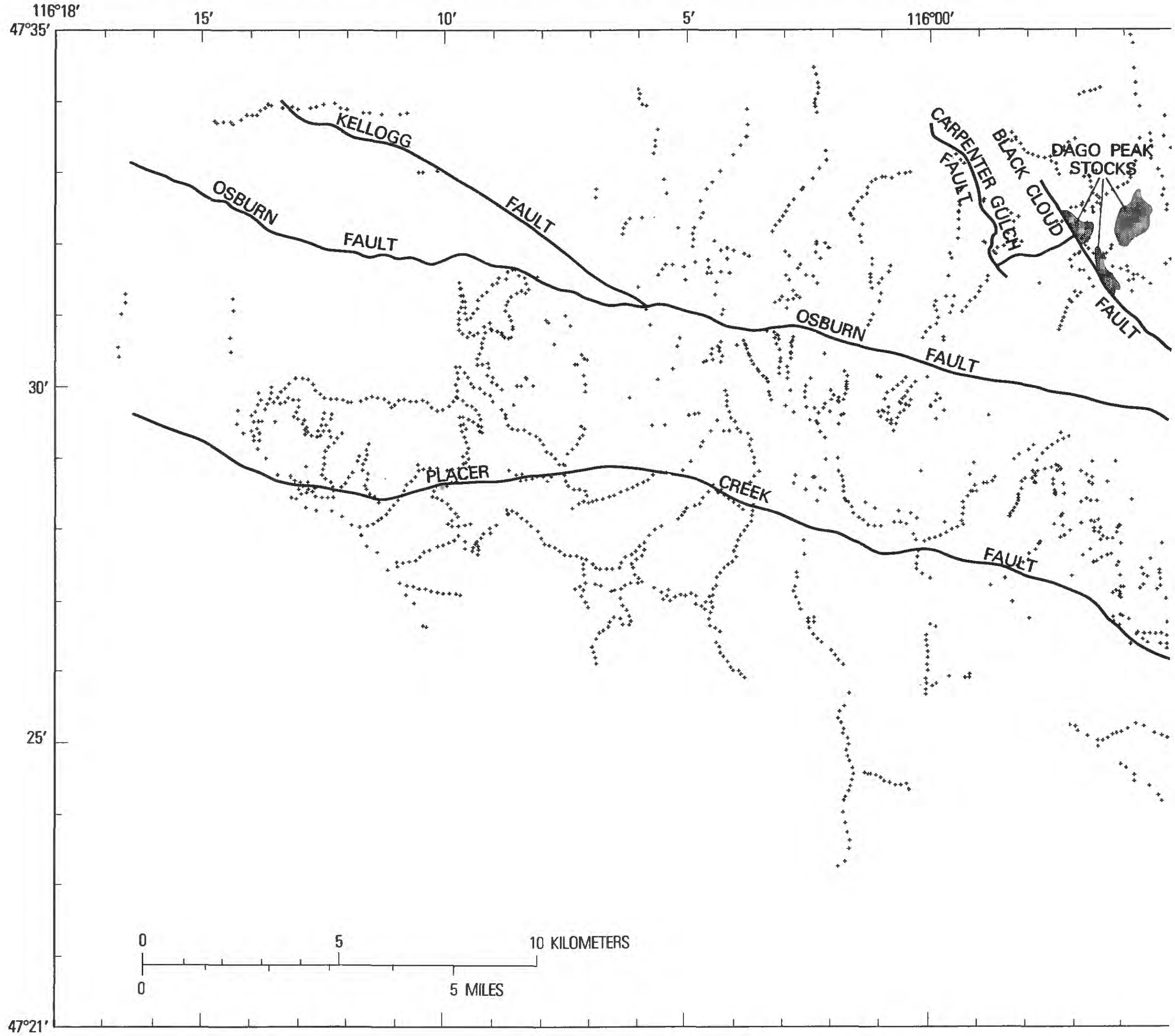

FIGURE 3.—Rock-sample locality map, Coeur d'Alene district, Idaho and Montana. Faults west of 115°42'30" modified

drawn around each mesh point. The larger the radius and circumscribed circle, the larger the number of data points represented by a single value. Thus, larger circle sizes have a smoothing effect on the resulting geochemical surface. For the illustrations presented here a circle radius of 800 ft (244 m) was used.

The computed geochemical values were plotted at coordinate intersections on a X-Y flat-bed plotter equipped with a 50- by 60-in. (127- by 152-cm) table. All contouring of isoconcentration was done manually.

It became necessary to change from an IBM 370 computer to a DEC 1070 computer before processing of the geochemical data was completed. This change means that in moving average type of computations, such as those made by the grid program, there may be a small difference in the output calculations as displayed on the plot maps.

SMELTER CONTAMINATION

Emissions derived from the smelter near Kellogg obviously have been the source of some metals that have been added to the soils and exposed rocks in the vicinity of the smelter. Inasmuch as large ore deposits, such as the Bunker Hill, Page, and other deposits also occur near the smelter, it is difficult to distinguish the relative proportions of elements in surface materials that were derived from the smelter from those derived from the weathering of naturally occurring deposits.

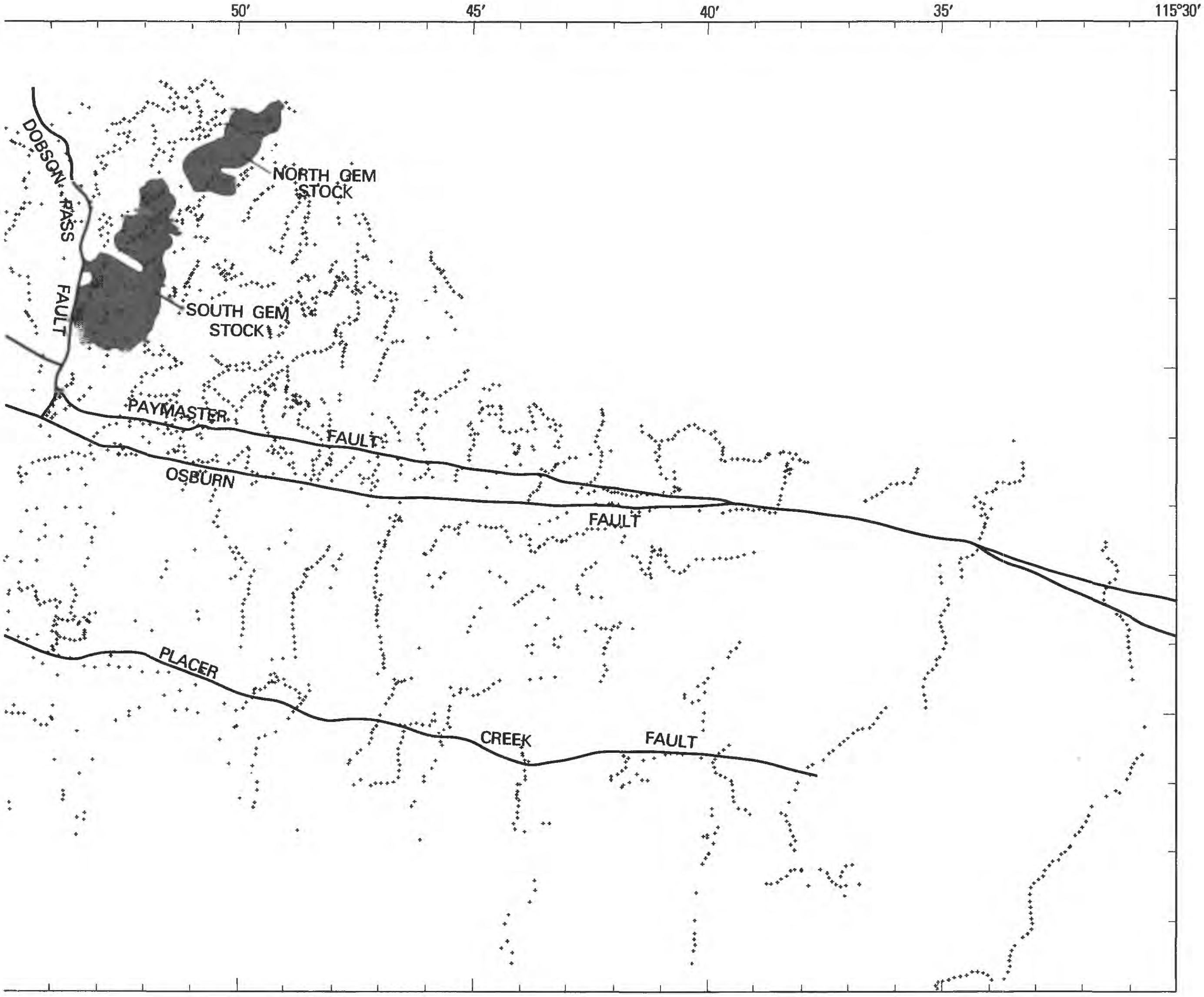

from Hobbs, Griggs, Wallace, and Campbell (1965); faults east of 115°42′30″ modified from Wallace and Hosterman (1956).

The geochemical data presented in this report indicate, however, that in many places beyond the area of smelter contamination the ore-forming metals retained in the soils are the same as those contained in the parent rock from which the soils were formed. In such places, many of the dispersion patterns of the metals in soils have been found to be coextensive with dispersion patterns formed by the same metal in rocks.

This rationalization suggests that the anomalous concentrations of several elements in soils immediately eastward and downwind from the smelter, particularly in the area north of the Osburn fault, may have been wholly or in part derived from smelter contamination. The elements that are present in soil anomalies in this position, without coincident rock anomalies, are antimony, arsenic, boron, copper, lead, mercury, nickel, zinc, and cadmium.

RECONSTRUCTION OF THE GEOCHEMICAL DISPERSION PATTERNS

Geologists who have studied the Coeur d'Alene district have concluded that postore faulting is extensive. The net slip resulting from this faulting is of such magnitude that some of the mineral belts are thought to have been displaced many miles. Vertical displacements of many thousands of feet have also occurred along some faults. Throughout most of the segment of

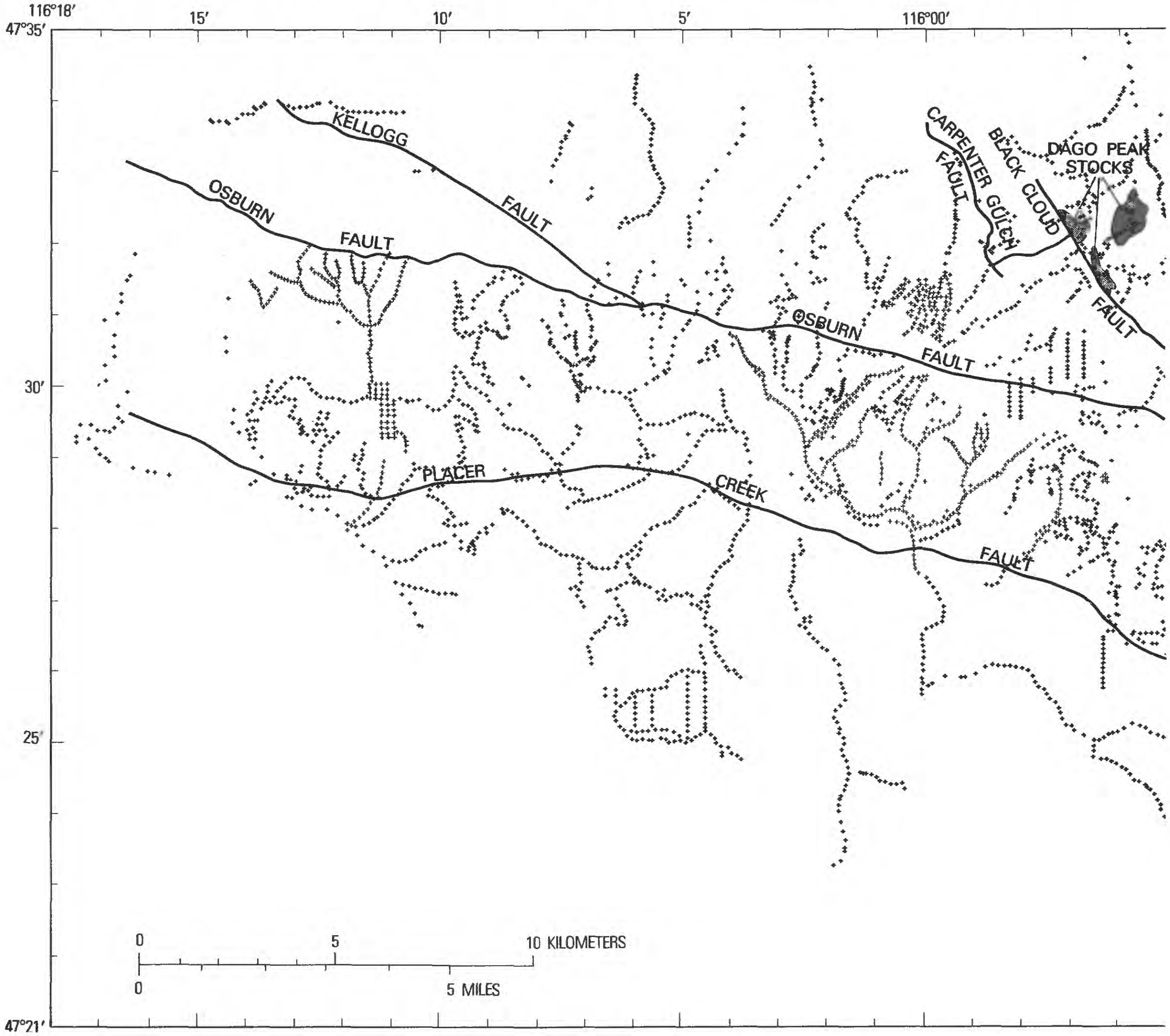

FIGURE 4.—Soil-sample locality map, Coeur d'Alene district, Idaho and Montana. Faults west of 115°42′30″ modified

the Osburn fault between Silverton and Kellogg, the Prichard Formation has been faulted against the Wallace Formation, indicating a minimum stratigraphic displacement of 4,800 ft (1,463 m), according to the thicknesses of the Belt formations given by Hobbs, Griggs, Wallace, and Campbell (1965, p. 14). Hershey (1916, p. 2) estimated that the Osburn fault has a maximum vertical displacement of more than 10,000 ft (3,048 m), and Shenon and McConnel (1939, p. 7) thought that it might have a maximum vertical displacement of more than 15,000 ft (4,572 m). Hershey (1916) and Umpleby (1924) suggested that strike-slip movement of major proportions had occurred.

Hobbs, Griggs, Wallace, and Campbell (1965, p. 73–83) reviewed the evidence pertaining to this structural discontinuity and concluded that the maximum right-lateral strike-slip movement along the fault was probably about 16 mi (26 km) along the segment of the fault eastward from the junction of the Osburn and Dobson Pass faults. West of this junction right-lateral strike-slip movement on the Osburn fault is thought by these authors to be about 12 mi (19 km). The difference in the amount of displacement along the two segments of the same structure is attributed to dip-slip movement along the abutting low-angle Dobson Pass fault. These displacements are largely based on the offset of major fold axes and faults, the differences in lithology of formations on opposite sides of the fault, the position of major mining areas on opposite sides of the fault, and the patterns of ore and gangue-mineral

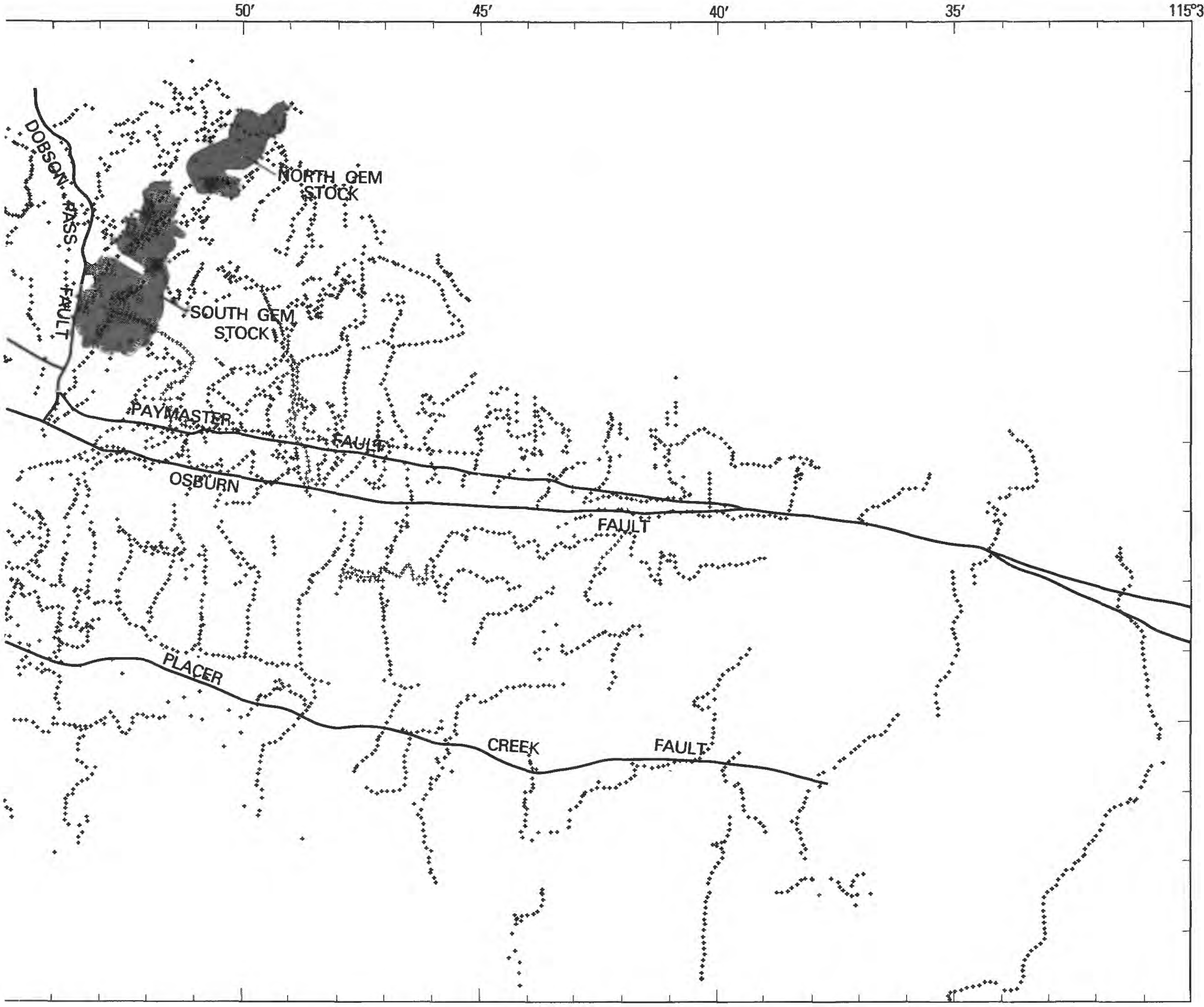

from Hobbs, Griggs, Wallace, and Campbell (1965); faults east of 115°42′30″ modified from Wallace and Hosterman (1956).

distribution within the district. Of these the most striking evidence is the offset of the mineral belts that made up the original center of mineralization, resulting in the location of the major mining area in the Mullan-Burke-Wallace triangle north of the fault and another major mining area in the Kellogg-Wallace area south of the fault. Major movement on some of the other faults in the area has important implications regarding the pattern of ore distribution.

Hobbs, Griggs, Wallace, and Campbell (1965, p. 90) thought that major movement on the Kellogg fault might also have been strike slip and that it might be a branch of the Osburn fault that accommodated some of the strike slip to the east. They also believed that the low-angle, west-dipping normal Dobson Pass fault truncated the tops of the Gem stocks, separating the main igneous bodies as now known from the upper cupolas that form the Dago Peak stocks about 3½ miles (5.6 km) to the west. The termination of geochemical dispersion patterns against the Paymaster fault suggests that strike-slip movement also may have occurred along that fault.

If such large displacements have occurred along the postore faults, the geochemical dispersion patterns that reflect the mineral belts also should be offset. To test the hypothesis that movement along the Osburn, Kellogg, Paymaster, and Dobson Pass faults displaced the mineral belts and geochemical dispersion patterns, several geochemical maps were reconstructed using a computer program to shift the fault blocks and the data points within the blocks to the best geochemical fit (fig. 5). When this was done so that dispersion patterns of antimony, lead, arsenic, sulfur, and the ratio of cadmium to zinc were continuous from one fault block to another, the amount and direction of movement necessary to produce the continuity was remarkably similar to the fault displacements estimated by Hobbs, Griggs, Wallace, and Campbell (1965) from geologic evidence. It seems probable that the reconstruction illustrates the original position of the mineral belts and the concentric geochemical halos that were formed around the prefaulted Gem stocks.

The direction, rotation and manner in which the blocks were reassembled is shown and explained in figure 5 and the results are shown on plates *2B*–*6B*. The rotation accompanying the shifting of the fault blocks resulted in a different group of data points being averaged in the grid blocks in the reconstructed and unreconstructed geochemical maps. Although this means that the values shown on the reconstructed and unreconstructed maps are different, this has not greatly affected the overall geochemical patterns.

The reconstruction of the district to an approximation of the structure that existed at the time of emplacement of the ore deposits shows the geometric relations among the mineral belts. The Dago Peak stocks, before detachment by the Dobson Pass fault (Gott and Botbol, 1975), formed the tops of the Gem stocks and the volatile elements antimony, arsenic, sulfur, cadmium, and lead originally formed concentric halos surrounding the stocks. These halos interrupt the northwest-trending mineral belts which appear to continue to the northwest beyond the west side of the halos, as best shown on plates 2*B*, 3*B*, and 6*B*.

The reconstructed geochemical maps indicate that the spatial relations between the mineral belts as shown by figure 6 has been changed. The Moe–Reindeer Queen mineral belt probably was the southeast continuation of the Rex-Snowstorm belt. The Gem–Gold Hunter mineral belt terminates a short distance south of the present trace of the Osburn fault. The Dayrock, Success, Tamarack-Marsh, and Douglas subbelts are not well defined by the geochemical dispersion patterns. The Lucky Friday, Golconda, and Alice deposits were probably displaced from other mineral belts to the west by movement along postore faults. There appears to be a good possibility that the Page-Galena belt is composed of more than one mineral belt. The mines in the Galena–Coeur d'Alene, Sunshine-Crescent, and Bunker Hill areas may be within different mineral belts rather than constituting segments of the same belt.

PRESENT DISTRIBUTION AND GEOCHEMICAL SIGNIFICANCE OF THE ELEMENTS

The present distribution of the ore-forming and ore-associated elements is considerably different from the original distribution of these elements. The displacement of the mineral belts and geochemical dispersion patterns have changed the geochemical patterns from an orderly fabric marking the mineral belts and the Gem–Dago Peak halo of volatile elements surrounding the stocks, to a fabric in which discontinuous segments dominate the principal geochemical features.

Within individual mineral belts, some of the elements, particularly the sulfide-forming elements, have a similar distribution and thus have positive correlation coefficients. Other elements are not spatially associated and have either no correlation or have a negative correlation coefficient. The degree to which the various elements are associated is indicated by the correlation coefficients given in tables 3 and 4. Where the number of pairs of valid observations are few, the correlation coefficients may have little significance. Concentrations of the elements at the 25th, 50th, 75th, and 90th percentiles are given in tables 5 and 6.

There is considerable disagreement between the preliminary distribution maps of antimony, manganese, and silver in soils as shown by Gott and Botbol (1973) and those shown in this report as illustrated on plate 7*B*, 7*N*, and 7*T*. This disagreement resulted from the addition of considerable new analytical data.

The general distribution and significance of the geochemically most important elements are discussed below.

BACKGROUND AND ANOMALOUS SAMPLES

One of the most difficult problems in geochemical exploration is to distinguish geochemical anomalies related to economically significant mineral deposits from background values that have no relation to such mineral deposits. In order to distinguish anomalous values from background values, a threshold point for each element is generally established. There are at least two populations of many elements in the rocks and in the soils of the Coeur d'Alene district. One population represents background values, and one population represents anomalous values. These populations are shown by cumulative frequency plots on a logarithmic probability scale where each population is represented by a straight line. The intersection of the straight lines represents the point that normally is taken as the threshold between background and anomalous values. Isopleths below the threshold indicated by the cumulative frequency plots, however, show definition to some of the known mineral belts. This relationship suggests that mixed populations of anomalous and background values are present and that the threshold value given by the cumulative frequency plot is a maximum value. Only values above the lower limit of analytical detection were used in plotting.

ANTIMONY

Within the Coeur d'Alene district, antimony occurs principally in tetrahedrite ($(Cu,Fe,Zn,Ag)_{12}(Sb,As)_4S_{13}$) and stibnite ($Sb_2S_3$). Polybasite ($(Ag,Cu)_{10}Sb_2S_{11}$), pyrargyrite ($Ag_3SbS_3$), bournonite ($PbCuSbS_3$), meneghinite ($Pb_3Sb_7S_{23}$), boulangerite ($Pb_5Sb_4S_{11}$), and jamesonite ($PbFeSb_6S_{14}$) have been reported to occur on levels of a few mines below the zone of oxidation. Analyses shown in table 14 indicate that considerable amounts of antimony are also contained in galena.

After galena and sphalerite, tetrahedrite is the third most abundant ore mineral and, therefore, constitutes the most important antimony source within the district. The analyses of five samples, mostly from the Sunshine mine, presented by Fryklund (1964, p. 18) and shown in table 7, indicate that the antimony in the Coeur d'Alene tetrahedrite probably ranges between 20 and 30 percent. The median antimony value in all soils and rocks that were analyzed is about 1 ppm (part per million) (table 8). The threshold value for antimony in both soils and rocks is about 10 ppm which occurs near the 92d percentile level in rocks and the 97th percentile in soils (fig. 7). The median value is somewhat higher in the St. Regis Formation than it is in the other Belt formations.

TABLE 7.—*Analyses of tetrahedrite from the Coeur d'Alene district, (in percent)*

[From Fryklund, 1964, p. 18, table 9. Leaders, (...), no data]

Element	1	2	3	4	5
Cu	29.10	29.10	37.70	33.70	26.2
Fe	5.50	5.50	5.13	5.05	----
Zn	5.09	3.56	3.87	----	----
Ag	3.95	6.15	Tr	5.75	11.12
Bi	0	0	Tr	0	----
Pb	0	0	0	0.20	----
Sb	22.36	22.36	26.81	25.90	26.1
As	10.13	8.59	Tr	1.18	----
S	24.16	24.44	26.49	24.10	----
Total	100.29	99.70	100.0	95.88	----

SAMPLE LOCALITIES

1. Sunshine Mine (Warren, 1934, p. 694, analysis A).
2. Sunshine Mine (Warren, 1934, p. 694, analysis B).
3. Hypotheek Mine (Shannon, 1926, p. 167).
4. Sunshine Mine (Rasor, 1934).
5. Sunshine Mine (Mitcham, 1952, p. 443).

TABLE 8.—*Percentile distribution (in parts per million) of antimony in soils and rocks in the Coeur d'Alene district, by formation*

[Leaders, (---), no data]

Formation	Sample medium	Percentile distribution 25th	50th	75th	90th	Valid observation
Monzonite	Soil	0.4	0.8	1.6	3	192
	Rock	---	---	---	1.1	106
Wallace	Soil	.8	1.1	2.8	5.3	2,178
	Rock	---	1.1	2.8	7.4	992
St. Regis	Soil	.9	1.9	3.8	7	1,544
	Rock	.9	2.2	5	9.5	830
Revett	Soil	.9	1.8	3	6	693
	Rock	---	1.6	4	10	452
Burke	Soil	.5	1	2	4	564
	Rock	---	1.1	3.7	11	402
Prichard	Soil	.8	1	4	8	1,442
	Rock	.5	1.9	4.2	7.8	726
All formations	Soil	.8	1.1	2.9	5.8	8,153
	Rock	---	1	3.5	7.9	3,965

Stibnite has been mined from a few small mines along Pine Creek at the western end of the district and from the Stanley mine near Burke. Stibnite has also been mined from the Houghland mine 8 mi (13 km) northeast of Burke in Sanders County, Mont. (Fryklund, 1964, p. 15).

The dispersion patterns of antimony (pl. 7*A*, *B*) have a relation to the ore deposits, mineral belts, and postore faulting that is best shown by plate 2. Before postore faulting occurred, the original position of the Gem stocks was encircled by a huge antimony halo which interrupted the antimony dispersion patterns that reflected the position of the northwest-trending mineral belts (pl. 2*B*). Postore faulting obliterated this simple geochemical picture by displacement of the antimony dispersion patterns.

The large antimony anomaly about 1 mi (1.6 km) east of the Gem stocks and bisected by long 115°50′ is a segment of the original halo (pl. 7*A*). The antimony anomaly directly west of the Dobson Pass fault is a higher structural and erosional level of the same segment of the halo. The antimony anomaly north of the Osburn fault near long 116° is a segment of the western side of the halo. Antimony dispersion patterns north and northwest of the Dago Peak stocks are probably the northwest extensions of the Gem–Gold Hunter and Rex-Snowstorm mineral belts. Antimony

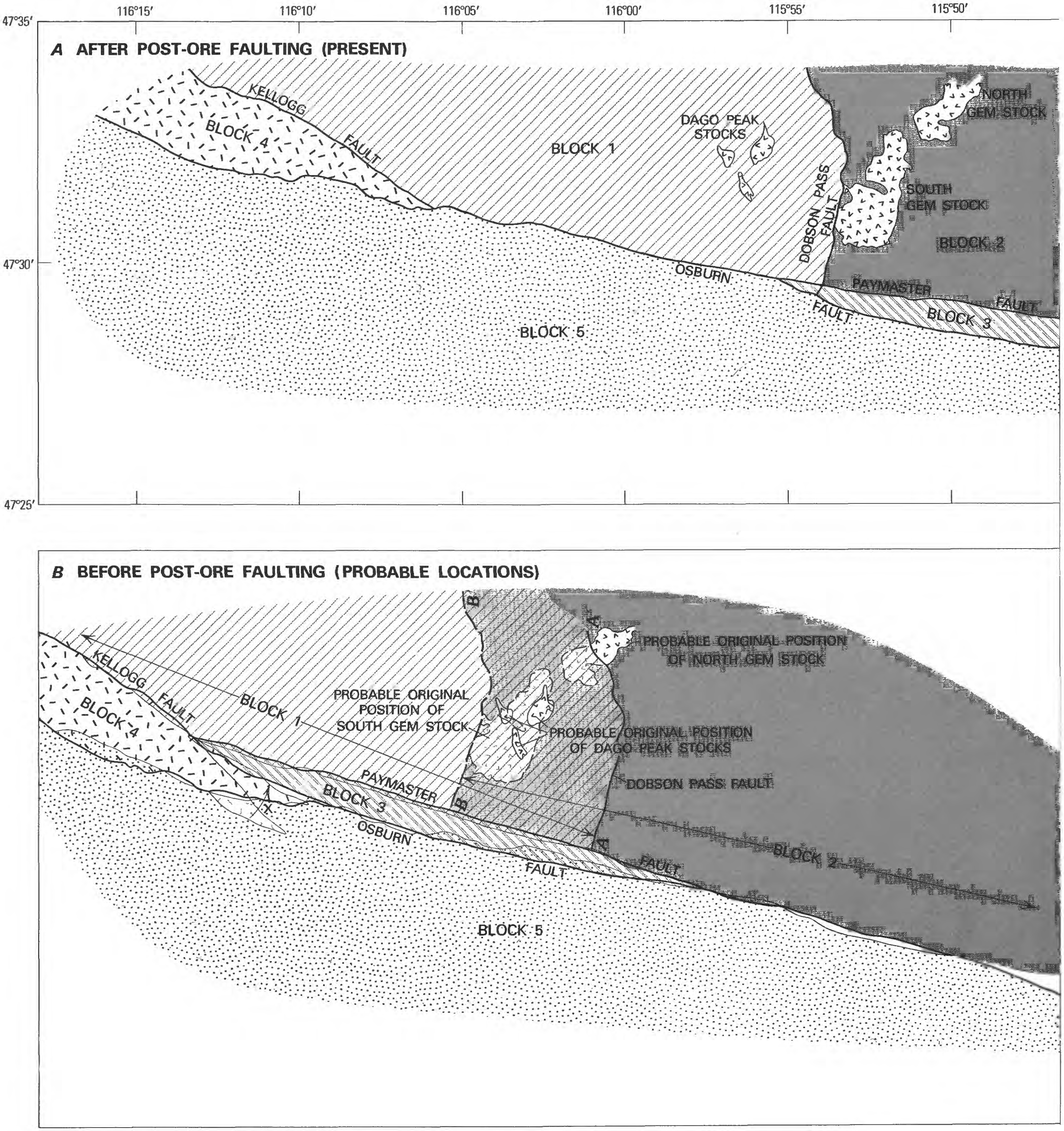
116°15′
116°10′
116°05′
116°00′
115°55′
115°50′
47°35′
47°30′
47°25′
A AFTER POST-ORE FAULTING (PRESENT)
KELLOGG FAULT
BLOCK 4
BLOCK 1
DAGO PEAK STOCKS
NORTH GEM STOCK
SOUTH GEM STOCK
DOBSON PASS FAULT
BLOCK 2
OSBURN
PAYMASTER
FAULT
FAULT
BLOCK 3
BLOCK 5
B BEFORE POST-ORE FAULTING (PROBABLE LOCATIONS)
B
A
PROBABLE ORIGINAL POSITION OF NORTH GEM STOCK
KELLOGG FAULT
BLOCK 1
BLOCK 4
PROBABLE ORIGINAL POSITION OF SOUTH GEM STOCK
PROBABLE ORIGINAL POSITION OF DAGO PEAK STOCKS
DOBSON PASS FAULT
PAYMASTER
BLOCK 3
X
B
A
OSBURN
FAULT
FAULT
BLOCK 2
BLOCK 5

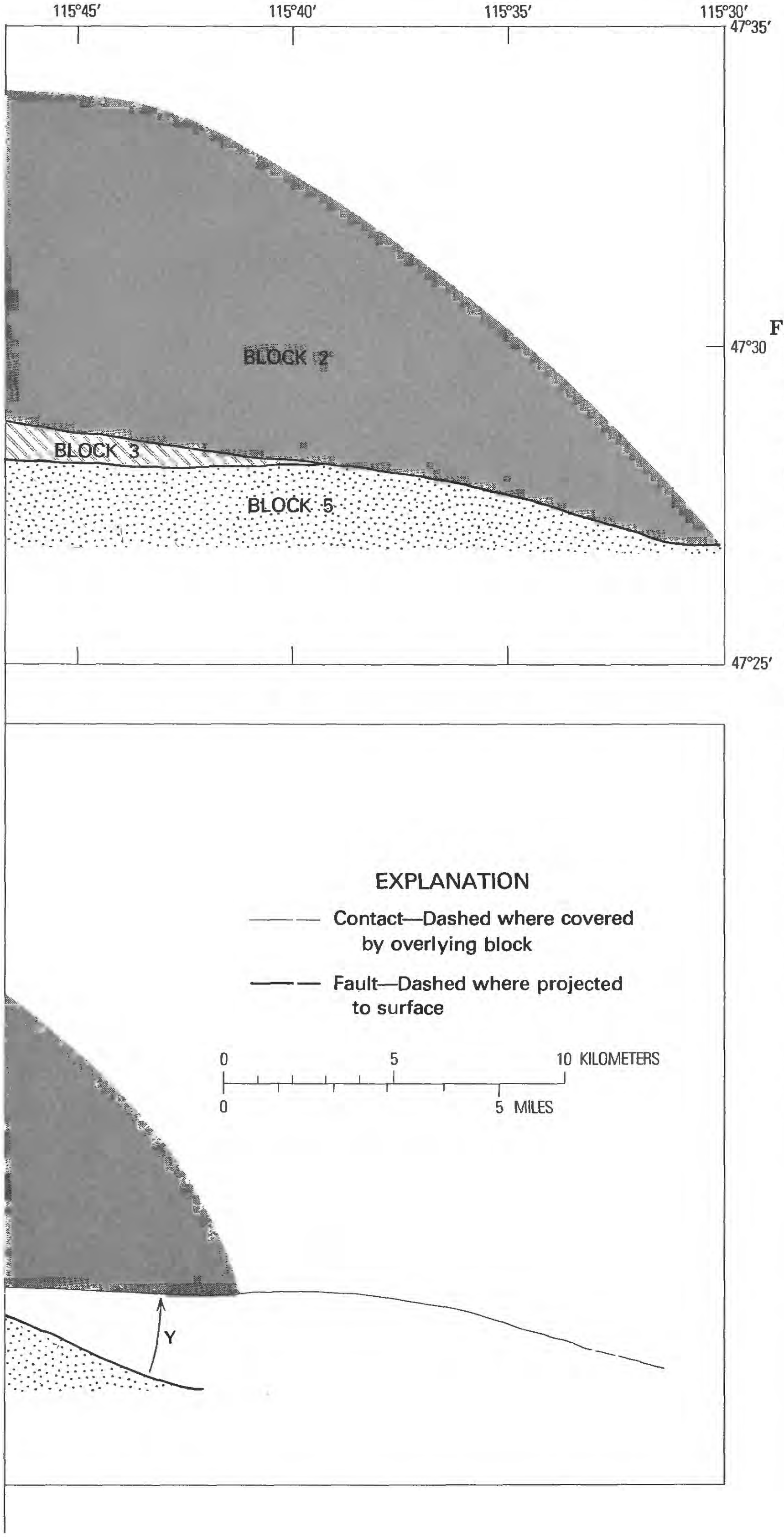

FIGURE 5.—Position of fault blocks before and after postore faulting, Coeur d'Alene district. The fault blocks, shown in *A* as they exist today, have been restored to their prefault positions in *B*. Arrows X and Y (*B*) show the amount of folding required for closest fit. Areas of 2 or more patterns represent overlap, and unpatterned areas represent gaps along the trace of fault blocks (*B*). Block 1 (*A*), bounded by the Kellogg and Osburn faults on the south and the Dobson Pass fault to the east, was moved west 6′45.5″, north 1′48.75″ and was rotated clockwise 4° around its center of gravity. Block 2 (*A*), bounded by the Dobson Pass fault on the west and the Paymaster and Osburn faults to the south, was moved west 11′12.5″, north 1′19″, and was rotated clockwise 7° around its center of gravity. The difference in west and north movement of block 2 compared to movement of block 1 caused the area east of Dobson Pass fault (block 2) to move west under block 1 along the Dobson Pass fault and below the Dago Peak stocks from line *A–A′* to line *B–B′* (*B*). The southeastern end of block 2 (*B*) was rotated counterclockwise as indicated by arrow Y to simulate folding required for the closest fit along the trace of the Osburn fault. Block 3 (*A*), bounded by the Paymaster and Osburn faults, was moved west 18′41″, north 3′04″, and rotated clockwise 8° around its center of gravity. Block 4 (*A*), bounded by the Kellogg fault on the north and Osburn fault on the south, was moved west 4′45″, north 1′00″, and rotated clockwise 13° around its center of gravity. The eastern end of block 4 was further rotated counterclockwise as indicated by arrow X (*B*) to simulate folding required for the closest fit along the traces of the Kellogg and Osburn faults. Block 5, south of the Osburn fault, was not moved or rotated.

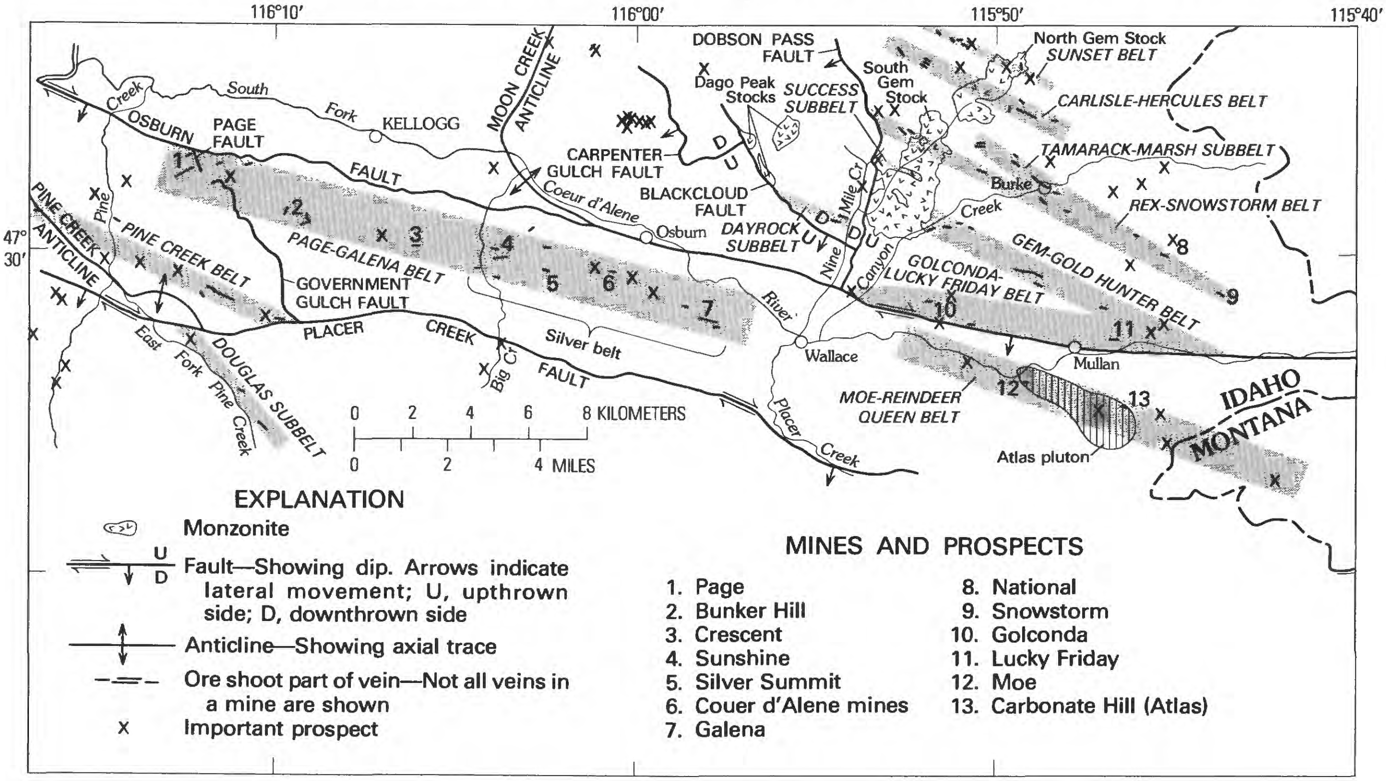

FIGURE 6.—Mineral belts of the Coeur d'Alene district (modified from Hobbs and Fryklund, 1968).

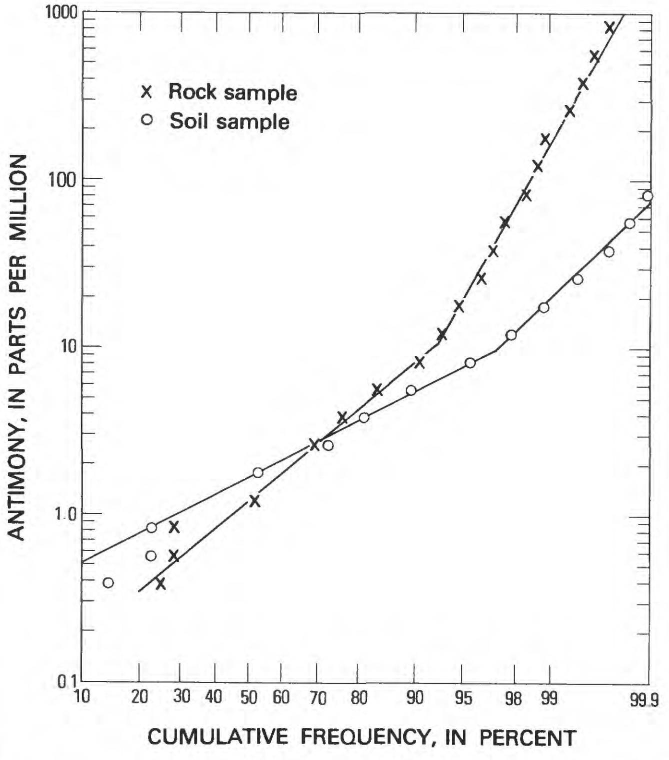

FIGURE 7.—Cumulative frequency plot for antimony, from 3,965 rock samples and 8,153 soil samples.

delineates the Rex-Snowstorm mineral belt moderately well, and the Gem-Gold Hunter belt is defined in some segments. The Moe-Reindeer Queen mineral belt appears to be defined by a strong antimony dispersion pattern about 9 mi (14.5 km) long. The dispersion pattern, however, may also be related to the buried Atlas pluton. The shape and position of this pluton is indicated by the magnetic anomaly shown in figures 2 and 8.

The Page-Galena mineral belt (pl. 2*A*; pl. 7*A*) is defined by a narrow sinuous antimony dispersion pattern extending from the Placer Creek fault at long 115°56′ through the Galena, Coeur d'Alene, Silver Summit, Sunshine, Crescent, Bulker Hill, and Page mines. The southern part of the Gem-Dago Peak halo interrupts the mineral belt in the vicinity of the Sunshine and Crescent mines, and in the area of overlap the two dispersion patterns cannot be distinguished with certainty (pl. 2*B*). The Pine Creek mineral belt is indicated by an inconspicuous antimony dispersion pattern. In an extensive area north of the Osburn fault between long 116°1′ and 116°7′, the soils contain anomalously high amounts of antimony (pl. 7*B*). The soil anomalies, however, do not conform to the antimony patterns in the rock. The soil anomalies probably are caused by contamination from the nearby Kellogg smelter.

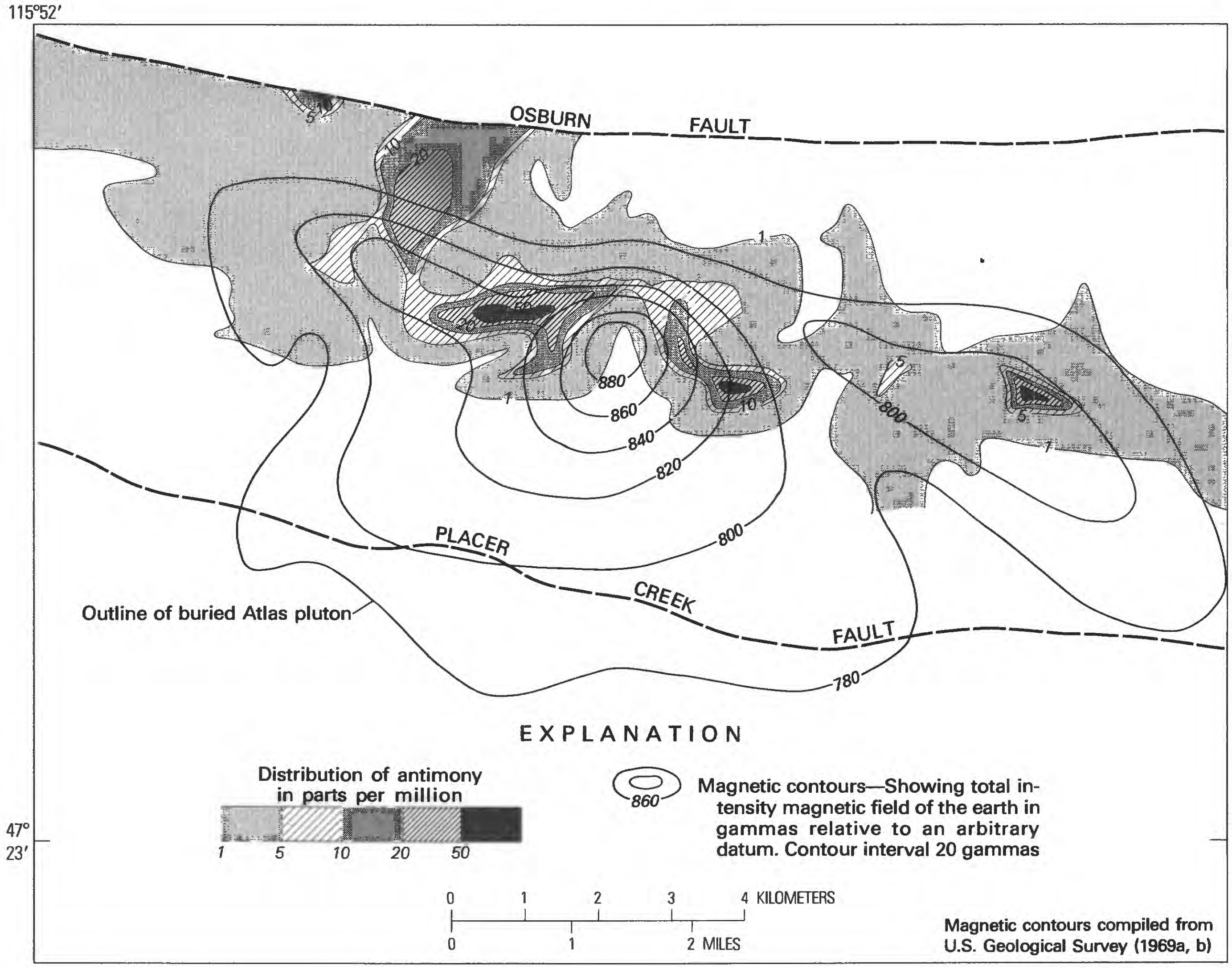

Magnetic contours compiled from U.S. Geological Survey (1969a, b)

FIGURE 8.—Magnetic map and distribution of antimony in rocks in the Atlas pluton area, Coeur d'Alene district.

ARSENIC

The principal arsenic-bearing minerals known to be present in the Coeur d'Alene district are arsenopyrite ($FeAsS$), tetrahedrite ($(Cu,Fe,Zn,Ag)_{12}(SbAs)_4S_{13}$), and gersdorffite ($(Ni,Fe,Co)AsS$) (Fryklund, 1964). These minerals occur most abundantly in the tetrahedrite veins of the Page-Galena mineral belt where arsenic in concentrations of 10 to more than 100 ppm in the rocks define most of the mineral belt. Rocks containing as much as 100 ppm arsenic directly overlie the Atlas pluton, and weak isolated arsenic anomalies are associated with the Bunker Hill mine and some of the ore deposits north of the Osburn fault (pl. 7*C, D*). The distribution of arsenic by formation is given in table 9. A cumulative frequency plot is shown in figure 9.

There is not much conformity between the distribution of arsenic in soils and rocks. Although arsenic dispersion patterns in the rocks define the Moe-Reindeer Queen mineral belt and the eastern part of the Page-Galena mineral belt, there is very little definition of these mineral belts by the arsenic in the soils.

Anomalously high arsenic, which cannot be accounted for with any certainty, occurs in the Prichard Formation east of Kellogg and north of the Osburn fault. It is possible that these anomalies are the result of contamination derived from smelter fumes. The arsenic, however, is more highly concentrated in the rocks than it is in the soils, suggesting that the smelter may not be the source of the arsenic.

BARIUM

According to Fryklund (1964), barite occurs as a minor constituent in some of the productive veins and

TABLE 9.—*Percentile distribution (in parts per million) of arsenic in soils and rocks in the Coeur d'Alene district, by formation*

[Leaders, (---), no data]

Formation	Sample medium	Percentile distribution				Valid observation
		25th	50th	75th	90th	
Monzonite	Soil	---	---	11	21	192
	Rock	---	---	---	---	---
Wallace	Soil	---	---	10	20	2,178
	Rock	---	---	17	27	993
St. Regis	Soil	---	---	9.8	20	1,544
	Rock	---	---	---	18	832
Revett	Soil	---	---	10	20	693
	Rock	---	---	---	20	455
Burke	Soil	---	8.6	11	22	565
	Rock	---	---	---	19	393
Prichard	Soil	---	10	21	28	1,441
	Rock	---	---	21	40	726
All formations	Soil	---	---	10	22	8,265
	Rock	---	---	9	24	3,969

as a major constituent in barren veins that are south of the Osburn fault. The barium concentrations in 3,312 rock samples range from 20 to 5,000 ppm and have a median concentration of 383 ppm (table 10). The cumulative frequencies plotted in figure 10 indicate that the threshold between anomalous and background populations is about 1,500 ppm barium. Barite probably accounts for most of the barium found within the district, but some barium is normally incorporated into rock-forming minerals.

Estimates by Parker (1967) and by Lee and Yao (1970) indicate that the average concentration of barium in the Earth's crust ranges from 300 to 500 ppm. According to Brobst (1973), granite generally contains 700–800 ppm, syenite and some of the more potassic igneous rocks contain 3,000–5,000 ppm, shale contains 500–1,000 ppm, and limestone contains <200 ppm barium. The bivalent barium ion has an ionic radius of 1.43 A (angstroms), which is similar to the radius of bivalent strontium (Sr^{+2}, 1.27 A) and the monovalent ion of potassium (K^{+}, 1.33 A). This similarity in size of ionic radius permits the substitution of barium for strontium and potassium resulting in an enrichment of barium in potassium-rich rocks, such as potassium feldspars and the micas. Barium likewise substitutes for strontium in the strontium minerals and vice versa.

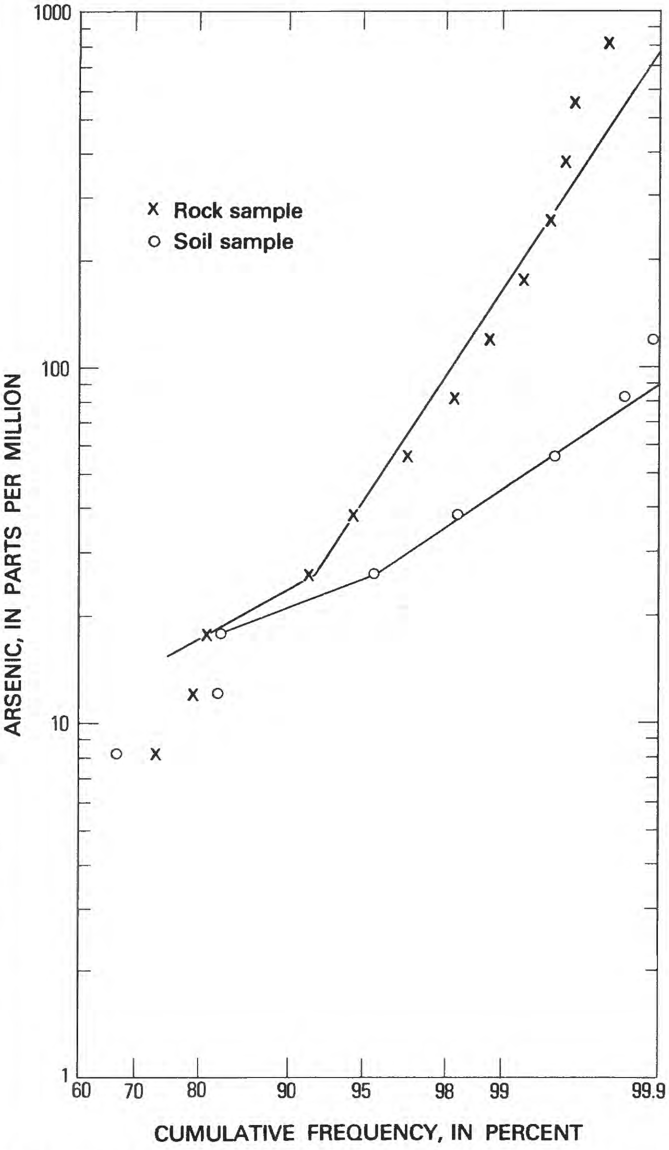

FIGURE 9.—Cumulative frequency plot for arsenic, from 3,969 rock samples and 8,265 soil samples.

Within the Coeur d'Alene district, barium in the soils poorly defines the mineral belts but barium-dispersion patterns in the rocks occur in the Moe-Reindeer Queen mineral belt and over the eastern parts of the Gem-Gold Hunter and Rex-Snowstorm mineral belts (pl. 7*E*, *F*). Some definition is given to the northwestern extension of the Gem-Gold Hunter mineral belt in an area parallel to the Blackcloud fault and extending northwestward beyond the Dago Peak stocks. Elsewhere, the distribution of barium does not form coherent dispersion patterns. It can be concluded, therefore, that the occurrence of barium within the district has limited significance as an indicator of sulfide deposits.

TABLE 10.—*Percentile distribution (in parts per million) of barium in soils and rocks in the Coeur d'Alene district, by formation*

[Leaders, (...), no data]

Formation	Sample medium	Percentile distribution 25th	50th	75th	90th	Valid observation
Monzonite ...	Soil	350	527	705	838	192
	Rock ...	478	675	923	1,661	106
Wallace	Soil	416	586	756	996	2,175
	Rock ...	171	378	694	1,088	993
St. Regis	Soil	486	684	979	1,431	1,544
	Rock ...	289	543	924	1,780	839
Revett	Soil	454	616	812	1,125	693
	Rock ...	110	235	575	1,030	455
Burke	Soil	475	647	822	1,065	565
	Rock ...	161	360	642	903	402
Prichard	Soil	473	647	828	1,090	1,441
	Rock ...	193	343	512	708	727
All formations ...	Soil	446	628	824	1,109	8,248
	Rock ...	182	383	677	1,085	3,979

TABLE 11.—*Percentile distribution (in parts per million) of boron in soils and rocks in the Coeur d'Alene district, by formation*

[Leaders, (—), no data]

Formation	Sample medium	Percentile distribution 25th	50th	75th	90th	Valid observation
Monzonite ...	Soil	10	15	21	25	192
	Rock ...	—	—	—	—	106
Wallace	Soil	22	37	66	109	2,175
	Rock ...	17	47	109	221	993
St. Regis	Soil	19	31	55	145	1,544
	Rock ...	17	47	116	236	839
Revett	Soil	20	30	48	79	693
	Rock ...	16	38	85	131	455
Burke	Soil	19	29	44	74	565
	Rock ...	11	33	68	110	402
Prichard	Soil	20	28	41	62	1,441
	Rock ...	18	35	66	105	727
All formations ...	Soil	19	30	50	90	8,247
	Rock ...	13	38	84	166	3,979

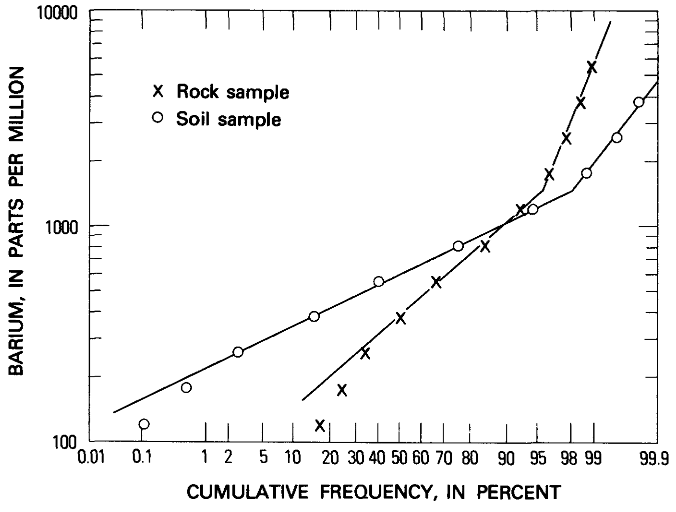

FIGURE 10.—Cumulative frequency plot for barium, from 3,979 rock samples and 8,248 soil samples.

BORON

The crustal abundance of boron was estimated by Goldschmidt (1954) to be about 10 ppm. The data in table 11 show that the median concentration of boron in soils and rocks of the Coeur d'Alene district is 30 ppm and 38 ppm, respectively; 10 percent of the samples contain 90 ppm and 166 ppm in soils and rocks, respectively. The highest boron concentrations roughly conform with the distribution of many of the known ore deposits (pl. 7*G*, *H*). The cumulative frequencies are plotted in figure 11.

Tourmaline, having 9-11.5 percent B_2O_3, is the most abundant of the boron minerals. It is a widespread mineral characteristic of pegmatite, granite, and many metamorphic rocks. It is resistant to the processes of erosion and weathering and is, therefore, concentrated in residual sediments. Ransome and Calkins (1908, p. 101) found that tourmaline is widely disseminated as a microscopic constituent throughout the rocks of the Belt Supergroup. They regarded it, however, as an introduced mineral closely associated with the ore minerals.

The distribution of boron in soils and rocks leads to a similar conclusion. Boron in concentrations of 50 ppm and greater forms a dispersion pattern that coincides with the eastern part of the Page-Galena mineral belt (pl. 7*G*, *H*). Similar concentrations of boron in the rocks form dispersion patterns coextensive with part of the Gem-Gold Hunter mineral belt as well as with the eastern limb of the Gem-Dago Peak halo. Northwest of the Dobson Pass fault extensions of the Rex-Snowstorm and Gem-Gold Hunter mineral belts ap-

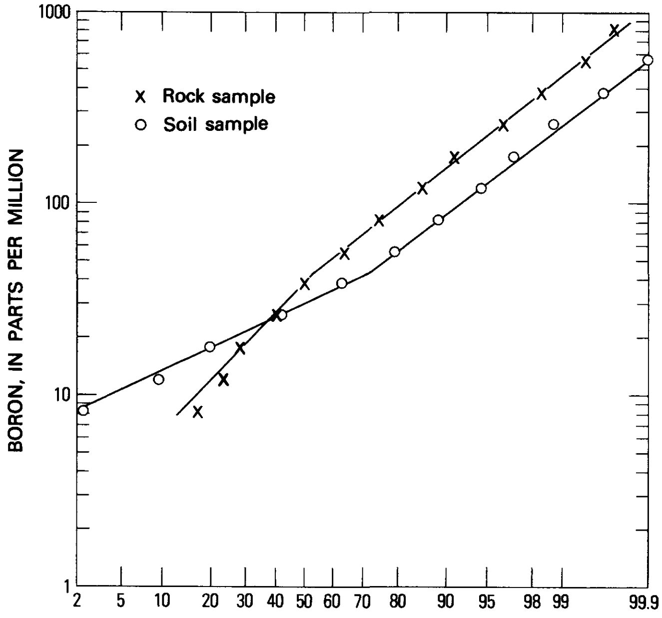

FIGURE 11.—Cumulative frequency plot for boron, from 3,979 rock samples and 8,247 soil samples.

parently are also defined by boron dispersion patterns in the rocks. Some anomalous boron in concentrations of 100-200 ppm in the soils east of Kellogg and north of the Osburn fault occurs where ore deposits are not known or suspected. Inasmuch as the rocks do not contain similar boron concentrations, it seems likely that this anomalous boron resulted from emissions from the Kellogg smelter.

COPPER

Copper is widespread throughout the Coeur d'Alene district, though it is not as abundant as lead and zinc. The district produced 139,850 t of copper through 1978; but during the same time it produced 49 times as much lead and 19 times as much zinc. The principal copper minerals within the district are tetrahedrite ($(Cu,Fe,ZnAg)_{12}(Sb,As)_4S_{13}$) and chalcopyrite ($CuFeS_2$).

The cumulative frequency plot shown in figure 12 indicates that the threshold of anomalous copper is about 60 ppm. In soils and rocks the median concentrations of 28 ppm and 12 ppm copper, respectively (table 12), indicate that the unmineralized rocks of the Belt Supergroup are impoverished in copper as compared to estimates of the 70-ppm crustal abundance of this metal (table 2).

The highest concentrations of copper appear to vary by formation. For example, the 90th-percentile levels in rock samples from the Wallace, St. Regis, and Prichard Formations are, respectively, 76, 70, and 69 ppm; whereas the 90th-percentile levels in the Revett and Burke Formations are 45 ppm (table 12).

The highest concentrations of copper are confined to a few areas within the district (pl. 7*I*, *J*). The eastern part of the Page-Galena mineral belt, where the most important ore mineral is tetrahedrite, is defined by a few discontinuous anomalies of copper in the rocks. A copper dispersion pattern containing as much as 3,000 ppm is present in the vicinity of the Snowstorm copper mine at the southeast end of the Rex-Snowstorm mineral belt. The trend of the mineral belt to the northwest, however, is not well indicated by the copper distribution. That part of the Moe-Reindeer Queen mineral belt that is underlain by the buried Atlas pluton is well defined by a copper dispersion pattern for a distance of about 6 mi (9.6 km) in an east-west direction (fig. 13). The other copper-dispersion patterns occur south of the Moe-Reindeer Queen belt. They are, in part, associated with the Placer Creek fault and in part with the Wishards sill. Several chalcopyrite-siderite veins have been observed in this area. North and northeast of Kellogg, copper anomalies in the soil probably were derived from the Kellogg smelter. Elsewhere, only isolated copper anomalies occur.

LEAD

Lead is the most abundant ore-forming metal in the Coeur d'Alene district. Through 1978, the mines within the district had produced 7,563,000 t of lead. Galena is the overwhelmingly dominant lead mineral in the ore deposits, and cerussite and anglesite are the most common oxidation products of galena. Other lead-bearing minerals that have been identified from

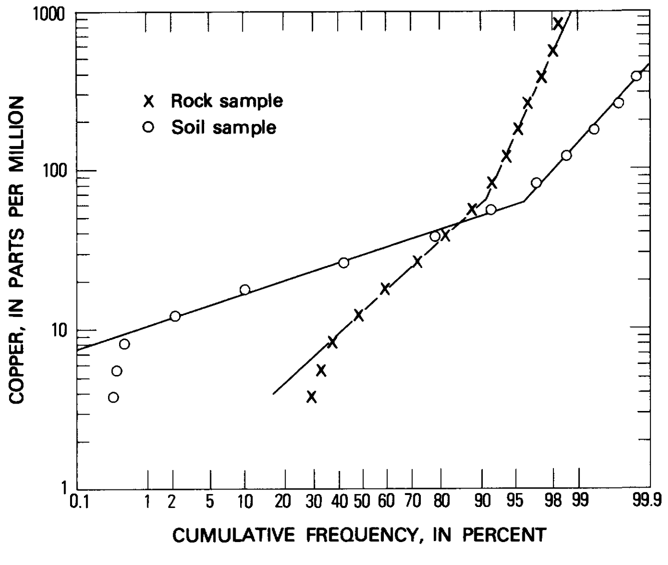

FIGURE 12.—Cumulative frequency plot for copper, from 3,950 rock samples and 8,695 soil samples.

TABLE 12.—*Percentile distribution (in parts per million) of copper in soils and rocks in the Coeur d'Alene district, by formation*

[Leaders, (---), no data]

Formation	Sample medium	Percentile distribution 25th	50th	75th	90th	Valid observation
Monzonite ...	Soil	14	21	34	65	177
	Rock ...	---	18	36	69	105
Wallace	Soil	22	29	35	47	2,293
	Rock ...	---	11	26	76	980
St. Regis	Soil	22	30	42	60	1,584
	Rock ...	---	9	25	70	834
Revett	Soil	21	29	38	53	698
	Rock ...	---	8	20	45	449
Burke	Soil	15	20	24	31	476
	Rock ...	---	6.2	18	45	401
Prichard	Soil	17	21	28	37	1,586
	Rock ...	12	22	38	69	726
All formations ...	Soil	21	28	37	53	8,695
	Rock ...	---	12	29	69	3,950

TABLE 13.—*Percentile distribution (in parts per million) of lead in soils and rocks in the Coeur d'Alene district, by formation*

[Leaders, (---), no data]

Formation	Sample medium	Percentile distribution 25th	50th	75th	90th	Valid observation
Monzonite ...	Soil	22	34	51	139	192
	Rock ...	18	24	34	51	106
Wallace	Soil	29	45	75	149	2,296
	Rock ...	10	23	52	188	933
St. Regis	Soil	24	39	71	195	1,584
	Rock ...	---	11	26	111	839
Revett	Soil	25	39	68	149	431
	Rock ...	---	10	28	301	455
Burke	Soil	27	41	76	218	698
	Rock ...	---	14	41	216	402
Prichard	Soil	35	54	107	237	1,642
	Rock ...	20	34	55	125	727
All formations ...	Soil	28	43	75	171	8,514
	Rock ...	8	19	43	140	3,979

the district are bouronite ($PbCuSbS_2$), menghinite ($PbSb_7S_{22}$), boulangerite ($Pb_5Sb_4S_{14}$) and jamesonite ($Pb_4FeSb_6S_{14}$) (Fryklund, 1964).

Galena is probably present to some extent in all the ore deposits; and dispersion patterns of anomalous lead derived from galena-bearing deposits are present in the soils and surficial rocks within many of the mineral belts. Despite its widespread distribution, the enrichment of lead in most rocks of the district is not great. The median concentration level of lead in 3,979 rock samples is only 19 ppm (table 13)—not a significant enrichment above the 16-ppm lead that Goldschmidt (1954) estimated is present in the Earth's crust. As shown by figure 14, the soils and rocks having more than about 60 ppm are anomalously high in lead; this population of anomalous lead shows geochemical trends that define many of the mineral belts.

The oxidized lead minerals, anglesite and cerussite, are sparingly soluble minerals. As a result of the low solubility of these minerals, lead has a low mobility within the oxidized zone. In spite of this low mobility, several hundred samples of needles and twigs collected by the authors from conifer trees, principally Douglas-fir and western white pine, show that lead is taken up by these trees and concentrated in the needles and twigs in surprisingly high concentrations. After death and decay of the tree, this lead is incorporated into the soils. As a result, lead is enriched in the soils relative to the rocks. The enrichment is shown by the median lead concentration of 43 ppm in 8,514 soil samples as compared to a median lead concentration of 19 ppm in 3,979 rock samples (table 13).

The mineralogical relation of silver to galena in the Coeur d'Alene district has not been determined; silver may be present as exsolution blebs in galena or as a mixture of galena and tetrahedrite. Several heavy-mineral separates were obtained by A. P. Pierce of the U.S. Geological Survey (written commun., 1970) by hand picking minerals from crushed ore samples from the Galena and Lucky Friday mines. Spectrographic analyses of these minerals are tabulated in table 14. The galena samples contain surprisingly high concentrations of manganese, silver, bismuth, copper, antimony, and zinc. Many galenas in ore deposits throughout the world have been found to contain concentrations of antimony, silver, and bismuth as high as those shown in table 14, but such high concentrations of zinc, copper, and manganese do not normally occur in galena. It is probable that fragments of other minerals, such as sphalerite, tetrahedrite, and a manganese mineral, were mixed with the galena. The proportions of copper, antimony, and silver, however, are not the same as would be expected if these metals were all derived from argentian tetrahedrite inclusions in the galena. Argentian tetrahedrite from the Coeur d'Alene district generally contains Cu>Sb>Ag in about the proportions 30:25:6 (table 7). However, the proportion of these metals in many of the galena separates is the reverse with Ag>Sb>Cu. From this it

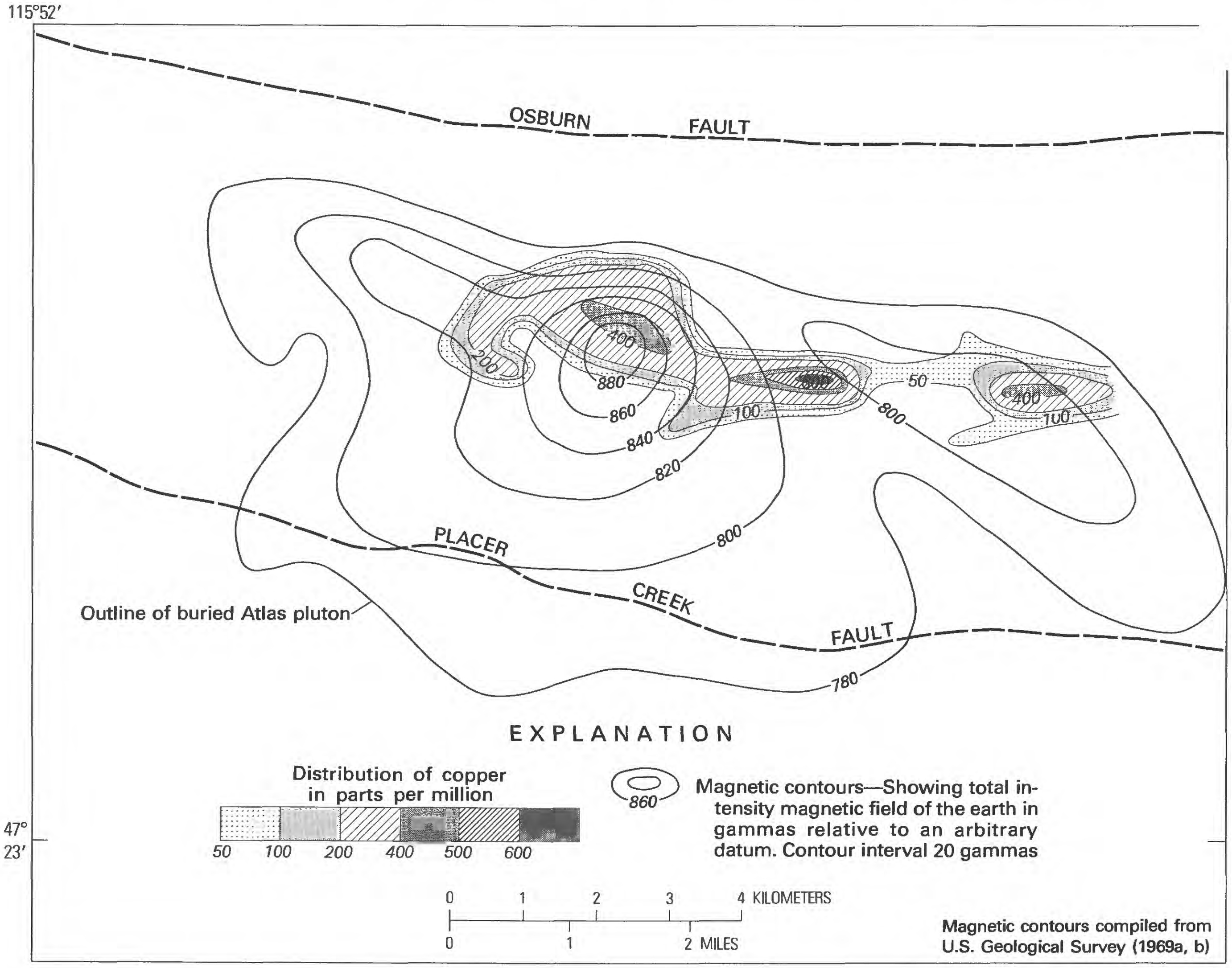

Magnetic contours compiled from U.S. Geological Survey (1969a, b)

FIGURE 13.—Magnetic map and distribution of copper, Atlas pluton area, Coeur d'Alene district.

appears likely that, in addition to possible contamination, the galenas contain appreciable amounts of antimony and silver in some form other than tetrahedrite, as well as bismuth in some unknown combination.

Studies of many silver-bearing lead deposits have resulted in the conclusion by many that silver is contained as minute inclusions in argentiferous galena. These inclusions, generally disseminated evenly throughout the galena, are thought to have resulted from the unmixing of silver originally held in solid solution (Van Hook, 1960). At least some of the silver in the Coeur d'Alene galenas may be held in a similar manner.

The analytical data presented in table 14 also indicate that antimony occurs in the range of 3,000–10,000 ppm in the Coeur d'Alene galenas. This concentration of antimony appears to be similar to the antimony content of some Russian galenas described by Malakhov (1969). He tabulated the results of chemical determinations of the bismuth and antimony content of 204 galena samples from 84 deposits representing a depth range of 984–16,400 ft (300–5,000 m) and concluded that the ratio antimony to bismuth is indicative of the temperature of formation. Low ratios (Sb:Bi <0.06) are characteristic of galena that formed at high temperatures, and high ratios (Sb:Bi >6.0–13) are characteristic of galena formed at low temperatures. By analogy with the antimony-bismuth content of the Russian galenas, most of the Coeur d'Alene galenas were formed at relatively low temperatures.

The distribution of lead in the soils and oxidized rock is generally similar (pl. 3; pl. 7*K*, *L*). Lead in both soils and rocks well defines the Gem–Gold Hunter mineral

TABLE 14.—*Semiquantitative spectrographic analyses of some sulfides and siderite from the Coeur d'Alene district*

[Samples collected by A. P. Pierce, U. S. Geological Survey. N, not detected. Values in parts per million, except iron, in percent. >, greater than]

Lab No.	Field No.	Fe	Mn	Ag	As	Bi	Cd	Co	Cu	Mg	Ni	Pb	Sb	Zn
Tetrahedrite														
D132826	G5T	5	300	70,000	5,000	3,000	300	30	>100,000	13.9	10	30,000	>100,000	70,000
D132828	G6L	7	150	70,000	30,000	5,000	200	30	>100,000	12.3	10	1,500	>100,000	70,000
D132821	G2T	7	1,500	50,000	7,000	3,000	150	30	>100,000	10.4	15	7,000	>100,000	50,000
D132822	G2L	5	15	50,000	5,000	3,000	200	70	>100,000	14.0	15	2,000	>100,000	70,000
D132824	G4T	5	150	70,000	3,000	2,000	200	20	>100,000	10.7	10	5,000	>100,000	70,000
D132829	G6T	10	1,500	70,000	50,000	3,000	300	50	>100,000	10.9	50	1,000	>100,000	50,000
D132895	G8T	10	30	70,000	50,000	3,000	200	20	>100,000	11.3	15	300	>100,000	30,000
D132838	G9T	7	300	50,000	15,000	3,000	200	20	>100,000	11.4	N	150	>100,000	30,000
D132841	G11T	10	1,500	>20,000	7,000	3,000	150	30	>100,000	10.7	10	5,000	>100,000	30,000
D132850	G16T	10	1,000	50,000	7,000	3,000	200	30	>100,000	11.3	N	10,000	>100,000	50,000
D132852	G17T	7	150	>100,000	10,000	3,000	200	7	>100,000	14.0	10	7,000	>100,000	30,000
D132855	G19L	7	150	100,000	7,000	3,000	100	7	>100,000	12.4	10	1,000	>100,000	15,000
D132868	G24T	7	700	70,000	15,000	7,000	70	20	>100,000	11.5	10	1,500	>100,000	70,000
D132869	G25T	7	700	70,000	20,000	1,000	70	70	>100,000	12.0	15	150	>100,000	30,000
D132880	LF8A	3	300	70,000	5,000	N	700	50	>100,000	13.0	20	15,000	>100,000	7,000
Galena														
D132824	G5G	0.15	20	10,000	N	15,000	N	N	5,000	1.0	N	>100,000	7,000	N
D132823	G3G	.7	300	7,000	N	30	50	N	1,500	6.0	N	>100,000	7,000	N
D132840	G10G	.5	200	5,000	N	N	N	T	700	2.0	5	>100,000	3,000	2,000
D132845	G13G	.2	150	2,000	N	70	50	N	2,000	2.3	N	>100,000	3,000	1,000
D132853	G18G	3	2,000	10,000	N	150	N	N	5,000	0.6	N	>100,000	7,000	1,000
D132856	G20G	1	500	2,000	N	20	N	N	1,500	.34	N	>100,000	3,000	N
D132857	G21G	.015	10	10,000	N	1,500	N	N	300	2.0	15	>100,000	5,000	N
D132864	G23G	2	2,000	3,000	N	20	N	N	1,500	.32	10	>100,000	3,000	N
D132874	G27G	7	700	1,500	N	700	N	N	10,000	2.5	N	>100,000	7,000	7,000
D132876	LF1G	.7	700	3,000	N	150	N	N	2,000	3	10	>100,000	5,000	2,000
D132879	LF8G	.2	300	1,500	N	N	50	N	5,000	6.5	10	>100,000	10,000	7,000
D132883	LF9G	3	3,000	5,000	2,000	70	50	N	100	1.2	N	>100,000	3,000	2,000
D132884	LF11G	.2	100	5,000	N	N	50	N	1,500	.23	N	>100,000	7,000	1,500
Sphalerite														
D132847	G14H	5	300	50	N	N	5,000	30	700	5.0	N	5,000	300	>100,000
D132873	G27H	5	200	300	N	N	1,500	15	1,500	5.0	N	3,000	1,000	>100,000
D132885	LF11H	3	1,500	700	N	N	3,000	30	1,500	6.1	10	15,000	1,000	>100,000
D132887	C1H	10	1,000	30	N	20	3,000	70	150	2.7	20	30,000	N	>100,000
Chalcopyrite														
D132839	G9C	>10	150	700	N	30	50	10	>100,000	6.7	5	100	5,000	2,000
D132833	G7C	>10	100	1,500	N	300	N	15	>100,000	9.3	15	5,000	7,000	700
D132836	G8C	>10	10	700	N	70	N	50	>100,000	8.2	N	200	3,000	500
D132844	G12C	>10	300	100	N	N	N	N	>100,000	4.3	5	150	1,000	700
D132870	G25C	>10	700	500	20,000	30	N	150	>100,000	2.6	30	100	2,000	N
Pyrite														
D132819	G1Y	>10	200	1,000	3,000	700	N	50	50,000	8.7	100	20,000	15,000	3,000
D132848	G14Y	>10	500	700	3,000	N	50	N	5,000	3.0	10	50,000	3,000	3,000
D132859	G21Y	>10	700	15,000	2,000	50	N	30	30,000	7.3	500	50,000	30,000	7,000
D132864	G23Y	>10	700	70	7,000	20	N	700	1,500	1.2	700	7,000	2,000	N
D132872	G25Y	>10	300	500	N	20	50	500	20,000	5.0	15	150	1,500	N
D132885	R1Y	>10	150	7	N	N	N	150	1,500	.36	200	700	N	3,000
Arsenopyrite														
D132882	LF9A	>10	150	100	>100,000	N	N	70	1,000	5.6	30	300	1,500	N
Siderite														
D132820	G1S	>10	30,000	70	N	N	N	N	5,000	0.15	10	300	N	N
D132827	G6S	>10	50,000	150	N	20	N	N	1,000	.38	10	300	1,500	N
D132831	G7S	>10	30,000	200	N	20	N	N	2,000	.13	N	150	1,500	N
D132837	G9S	>10	30,000	30	N	N	N	70	700	.36	N	100	N	500
D132842	G11S	>10	30,000	100	N	N	N	N	3,000	.17	N	500	700	N
D132849	G15S	>10	70,000	7	N	N	N	N	200	.12	5	300	N	N
D132851	G16S	>10	30,000	70	N	20	N	N	1,000	.18	10	100	700	N
D132845	G18S	>10	30,000	100	N	10	N	N	500	.14	N	5,000	150	500
D132860	G21S	>10	30,000	100	N	N	N	N	1,500	.54	N	300	700	500
D132864	G23S	>10	70,000	7	N	N	N	N	150	.16	100	2,000	N	N
D132867	G24S	>10	70,000	50	N	20	N	N	700	.25	10	200	N	N
D132871	G25S	>10	70,000	30	N	N	N	N	1,500	.11	300	70	150	N
D132875	G27S	>10	50,000	3	N	N	N	N	150	.03	5	700	N	N
D132878	LF2S	>10	50,000	5	N	N	N	15	100	.09	20	200	N	N

belt and also forms a lead-rich halo around the eastern side of the Gem stocks. The Rex-Snowstorm, Carlisle-Hercules, and Sunset mineral belts are partly defined by lead. Two lead anomalies, north and northwest of the Dago Peak stocks, probably represent the extensions of the Gem-Gold Hunter and Carlisle-Hercules belts. The distribution of lead south of the Osburn fault poorly defines the mineral belts. Anomalous lead in the soil north and northeast of Kellogg (pl. 7*L*) probably is contamination from the Kellogg smelter. The lead content of the rocks in this area is low relative to the lead content of the soils, indicating that the rocks are only slightly if at all affected by smelter contamination.

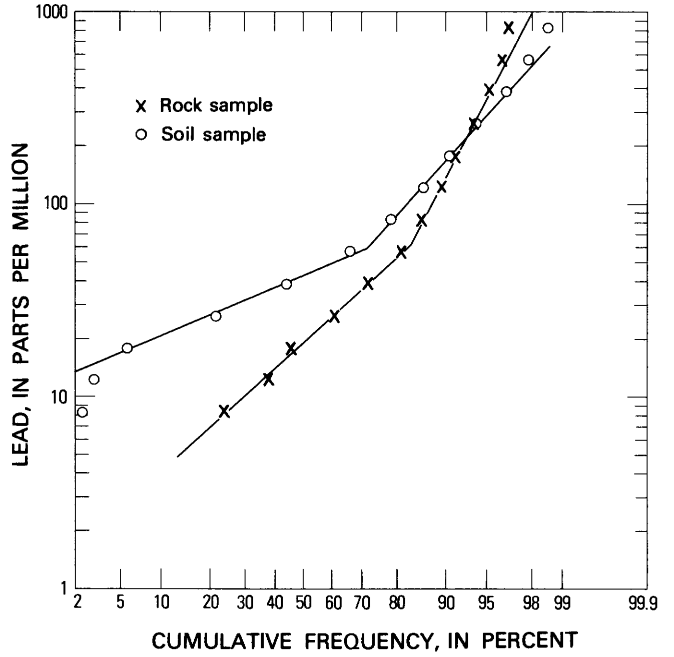

FIGURE 14.—Cumulative frequency plot for lead, from 3,979 rock samples and 8,514 soil samples.

MANGANESE

The ionic radius of bivalent manganese is 0.80 A, closely comparing to a radius of 0.74 A of bivalent iron. This similarity permits a substitution of iron by bivalent manganese in ferrous minerals. Apparently, the substitution of manganese for iron in siderite occurred to a considerable degree in the Coeur d'Alene district. As shown by table 14, siderite collected from mines within the district contain from 3-7 percent manganese presumably in diadochic substitution for iron. Ankerite also contains appreciable amounts of manganese (Fryklund, 1964, p. 21, table 13).

Manganese is relatively soluble in the bivalent state but is very insoluble in higher stages of oxidation. Thus, as siderite and ankerite are oxidized, the manganese that these minerals contain is changed to the immobile quadrivalent form and becomes increasingly concentrated in the soils. In the Coeur d'Alene district the median level of concentration of manganese in the soils is 1,333 ppm as compared to a median level of concentration of only 366 ppm in the rocks (table 15; fig. 15).

TABLE 15.—*Percentile distribution (in parts per million) of manganese in soils and rocks in the Coeur d'Alene district, by formation*

[Leaders, (—), no data]

Formation	Sample medium	Percentile distribution 25th	50th	75th	90th	Valid observation
Monzonite	Soil	473	781	1,340	1,946	192
	Rock	344	610	833	1,130	106
Wallace	Soil	795	1,377	2,308	3,675	2,175
	Rock	168	360	819	1,883	993
St. Regis	Soil	993	1,809	3,241	5,198	1,544
	Rock	212	600	1,715	4,760	839
Revett	Soil	961	1,730	2,504	3,829	693
	Rock	97	381	1,329	4,723	455
Burke	Soil	829	1,373	2,249	3,313	565
	Rock	119	386	978	2,086	402
Prichard	Soil	766	1,285	2,034	3,010	1,441
	Rock	121	224	475	1,083	727
All formations	Soil	777	1,333	2,242	3,597	8,248
	Rock	147	366	938	2,508	3,979

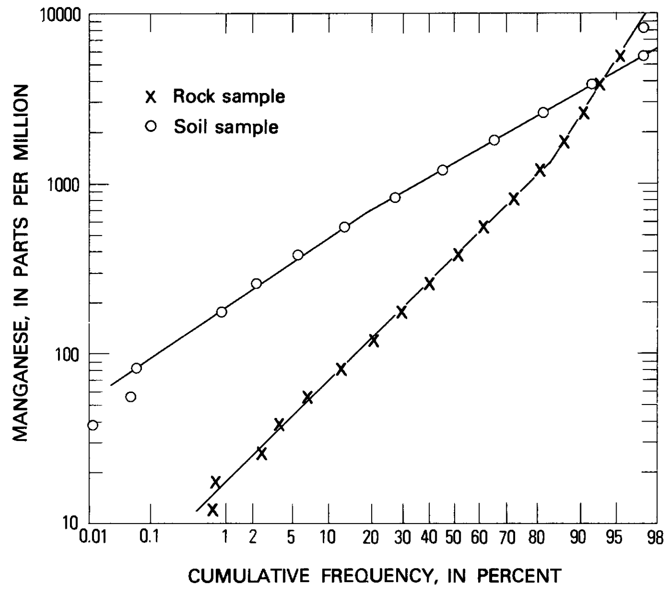

FIGURE 15.—Cumulative frequency plot for manganese, from 3,979 rock samples and 8,248 soil samples.

The region between the Osburn and Placer Creek faults and between Wallace and Pine Creek may be an area where the immobilized manganese oxidized near the surface is coextensive with unoxidized siderite at depth (fig. 16; pl. 7*M*, *N*). The manganese-dispersion patterns closely conform to the dispersion patterns of silver and antimony (fig. 16). The high manganese content of siderite and the close spatial relationship of siderite to the ore minerals suggest that the conformity among manganese, silver, and antimony is controlled by the distribution of siderite and tetrahedrite.

Anomalously high concentrations of manganese also form a dispersion pattern in the oxidized bedrock that fits the shape and orientation of the Atlas pluton, as shown by figure 17. The distribution of manganese in this area is also similar to the distribution of antimony, silver, and copper—the components of tetrahedrite. This can be interpreted to mean that tetrahedrite and siderite also have similar distributions in this area.

The mineral belts north of the Osburn fault are erratically overlain by high amounts of manganese in the soils as well as in the rocks. The manganese in this area, however, is not arranged in well-defined dispersion patterns that are clearly related to the mineral belts.

MERCURY

Mercury tends to concentrate in sulfide minerals, but in the Coeur d'Alene district, mercury is not abundant; its median value being 0.03 ppm in all of the rocks that were analyzed. Mercury amounts greater than 0.25 ppm in both soils and rocks appear to be anomalous for the district (fig. 18). As shown by table 14, it is concentrated in the range of about 2.5–14 ppm in tetrahedrite, sphalerite, chalcopyrite, and arsenopyrite from the district. The dispersion patterns of mercury in the rocks (pl. 7*O*) delineate parts of the Gem–Gold Hunter, Moe–Reindeer Queen, and Page-Galena mineral belts. Anomalous mercury is present in the soils in the vicinity of the Kellogg smelter (pl. 7*P*).

NICKEL

The soils and rocks of the Coeur d'Alene district have a median nickel value of 23 and 9 ppm, respectively (table 16; fig. 19). Weak nickel anomalies occur in the rocks and soils as a discontinuous halo around the Gem stocks, as spotty dispersion patterns in the Moe–Reindeer Queen, Page-Galena, and Pine Creek mineral belts, and as anomalous concentrations associated with the eastern part of the Placer Creek fault (pl. 7*Q*, *R*). Fryklund (1964) found that 10 samples of pyrrhotite from the Pine Creek area contain an average of 100 ppm nickel and that gersdorffite, (Ni,Fe,Co)AsS, is present as a minor constituent in most of the siderite-tetrahedrite veins, particularly in the Silver Summit mine. As shown in table 14, the nickel content of six pyrite samples from mines within the district range from 10 to 700 ppm.

The nickel-bearing pyrrhotite probably accounts for the anomalous nickel in the soils of part of the Pine Creek area and in rocks and soils (pl. 7*Q*, *R*) in some areas peripheral to the Gem stocks where pyrrhotite is known to occur as a major gangue mineral (Hobbs and Fryklund, 1968, p. 1428). The nickel-dispersion pattern in soils defining that part of the Page-Galena mineral belt from the Sunshine mine eastward to the Galena mine probably reflects the distribution of gersdorffite. The anomalous nickel partly enclosing the Dago Peak stocks west of the Dobson Pass fault appears to be a nickel halo overlying the position that the Gem stocks occupied before they were faulted eastward to their present position. This is a similar pattern to that shown by lead and the cadmium to zinc ratio.

The nickel anomalies in soils northeast of Kellogg apparently have been derived from the Kellogg smelter. This source is suggested by the absence of any known ore deposits in that area and by the conformity of the nickel anomalies to the topography, the highest concentration of nickel being on the windward side of the ridges.

SILVER

The Coeur d'Alene district is the leading silver-producing district in the United States and is one of the few mining districts in the world where silver is a principal product of a large proportion of its ores. Through 1978 the district had produced approximately 907,064,000 ounces (28.2×10^9 g) of silver.

Tetrahedrite and silver-rich galena ores are the source of almost all the silver produced from the district. Argentite (Ag_2S), pyrargyrite (Ag_3SbS_3) and polybasite ($(Ag,Cu)_{16}Sb_2S_{11}$) have been identified from a few of the tetrahedrite-rich mines. The silver content of galena has not been studied in detail, and, as discussed in the section on "Lead," there is some uncertainty as to whether silver substitutes for lead in the crystal lattice of galena or whether small amounts of tetrahedrite or other silver minerals are mixed with the galena ores.

The cumulative frequency plot (fig. 20) indicates that concentrations of 2 ppm or more of silver is anomalous. The median silver value in all formations is 0.6 ppm in the soils and 0.2 ppm in the rocks (table 17). At the 90th percentile level, the silver concentration is about the same in soils and rocks although the silver-dispersion patterns in the rocks more clearly define the mineral belts. Segments of the Page-Galena, Gem–Gold Hunter, Rex-Snowstorm, Carlisle-Hercules, and Moe–Reindeer Queen mineral belts are defined by subdued silver-dispersion patterns (pl. 7*S*, *T*). Likewise, the eastern segment of the Gem–Dago Peak halo is well defined by silver. Where the halo coalesces with the northwest-trending mineral belts, the dispersion patterns are indistinguishable. Silver largely defines that part of the Moe–Reindeer Queen mineral belt that overlies the buried Atlas pluton (fig. 21). Although the ore that has been produced from this belt is characterized by an abundance of galena, the geochemical evidence shows that silver, antimony, and copper form remarkably coextensive dispersion patterns. The similarity of the dispersion patterns of these elements suggests that the source of the silver as well as the source of antimony and copper may be tetrahedrite.

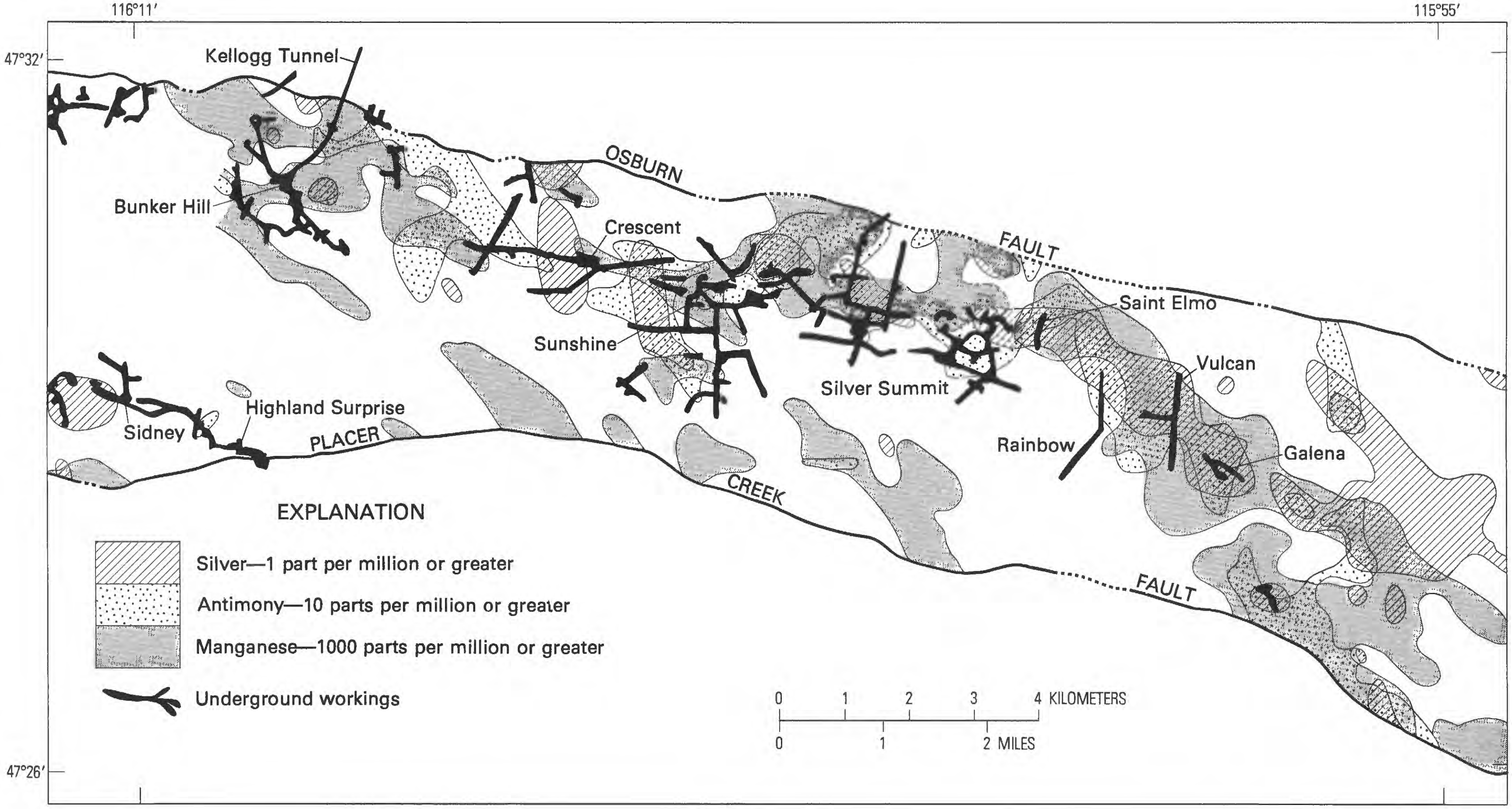

FIGURE 16.—Distribution of anomalous silver, antimony, and manganese in rocks and some underground workings in the Page-Galena mineral belt, Coeur d'Alene district. Underground workings from, and faults modified from Hobbs, Griggs, Wallace, and Campbell (1965, pls. 1-3).

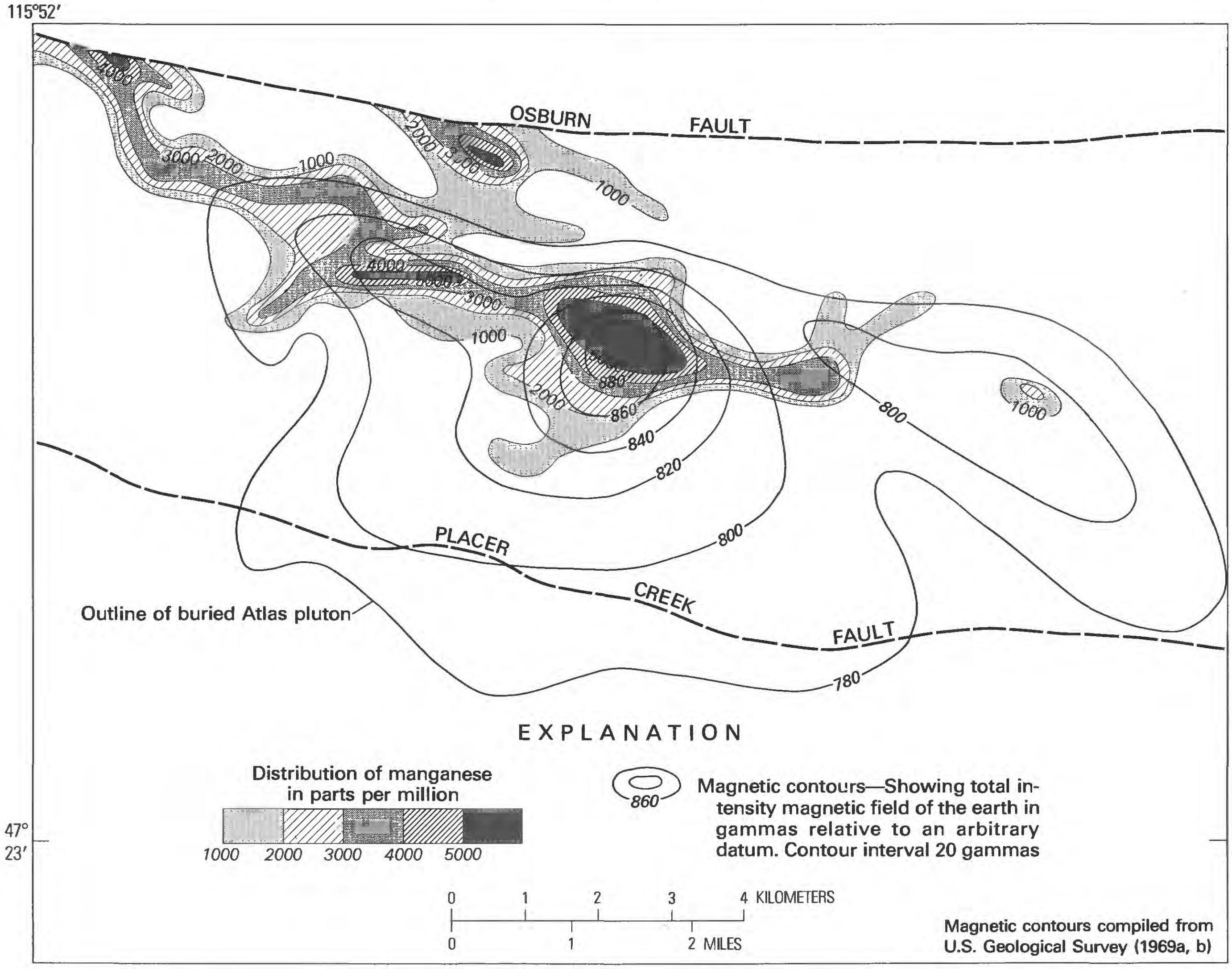

FIGURE 17.—Magnetic map and distribution of manganese in rocks in the Atlas pluton area, Coeur d'Alene district.

SULFUR

A large amount of sulfur was involved in the mineralizing processes that resulted in the formation of the sulfide minerals throughout the district. Under oxidizing conditions, sulfide is converted to sulfate; and in the process of soil formation some of the soluble sulfate becomes available to the plants, and some of it is removed in solution. sulfur is, therefore, present in soils in both organic and inorganic forms, and in a temperate climate, such as exists in the Coeur d'Alene district, it tends to concentrate in the organic material. The buildup of the concentration level of sulfur in soils as compared with that in rocks is illustrated in table 18, which shows that the sulfur concentration in the soils is nearly six times greater than it is in the surficial rocks; the median value of sulfur in the soils is 0.047 percent and in the rocks only 0.008 percent. The cumulative-frequency plot (fig. 22) indicates that anomalous sulfur in rocks and soils starts at about 0.015 percent. The dispersion patterns are more extensive in the soils than they are in the rocks (pl. 7*U*, *V*).

With the exception of the Moe–Reindeer Queen belt, sulfur does not form dispersion patterns that coincide well with the mineral belts, but in both soils and rocks it forms a halo around the original position of the Gem stocks (pl. 5*B*). A strong sulfur-dispersion pattern in rocks in an area about 10 mi (16 km) long conforms remarkably well to the magnetic anomaly that presumably shows the position of the buried Atlas pluton (fig. 23). Formation of these dispersion halos that are so closely associated with intrusive rocks apparently

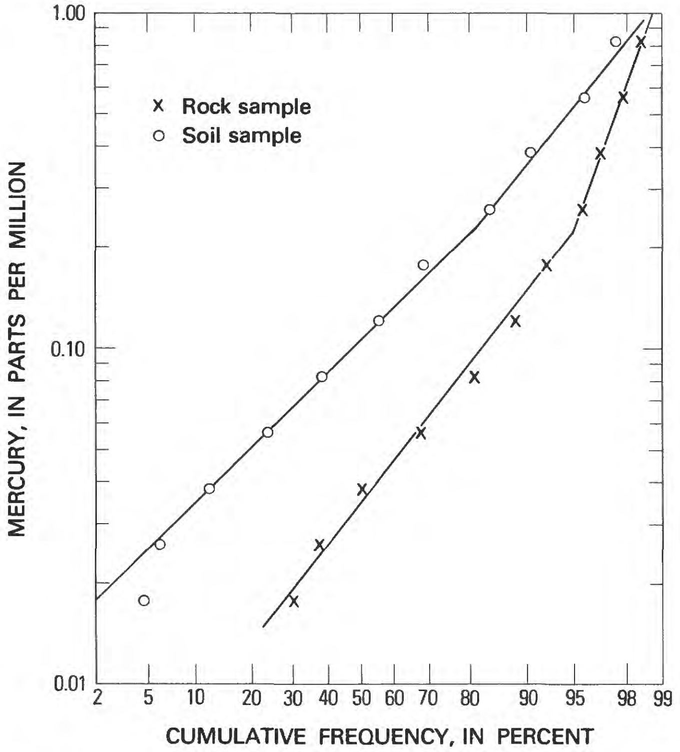

FIGURE 18.—Cumulative frequency plot for mercury, from 3,922 rock samples and 8,124 soil samples.

TABLE 16.—*Percentile distribution (in parts per million) of nickel in soils and rocks in the Coeur d'Alene district, by formation*

[Leaders, (---), no data]

Formation	Sample medium	Percentile distribution				Valid observation
		25th	50th	75th	90th	
Monzonite ...	Soil	13	16	21	27	192
	Rock...	---	---	4.8	9.6	106
Wallace	Soil	17	24	32	43	2,175
	Rock...	5.9	11	21	29	993
St. Regis	Soil	15	21	29	35	1,544
	Rock...	5	10	20	25	839
Revett	Soil	15	20	25	33	693
	Rock...	---	4.2	9.4	15	455
Burke........	Soil	15	21	29	35	565
	Rock...	---	5.5	13	21	402
Prichard	Soil	20	29	38	51	1,441
	Rock...	---	10	17	29	727
All formations ...	Soil	16	23	31	38	8,249
	Rock...	---	9	17	25	3,979

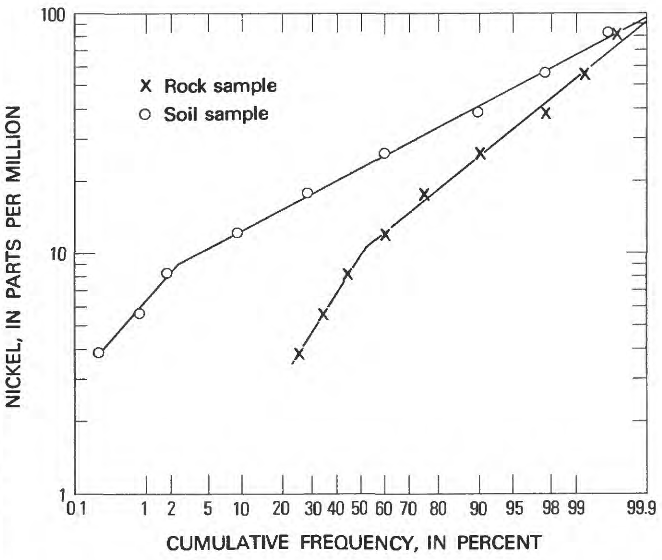

FIGURE 19.—Cumulative frequency plot for nickel, from 3,979 rock samples and 8,249 soil samples.

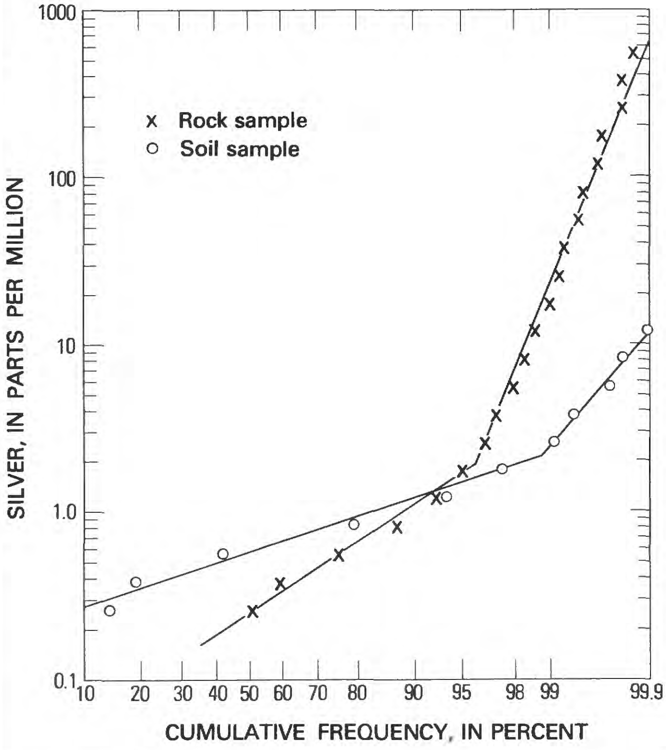

FIGURE 20.—Cumulative frequency plot for silver, from 3,961 rock samples and 8,611 soil samples.

TABLE 17.—*Percentile distribution (in parts per million) of silver in soils and rocks in the Coeur d'Alene district, by formation*

[Leaders, (---), no data]

Formation	Sample medium	Percentile distribution 25th	50th	75th	90th	Valid observation
Monzonite	Soil	0.4	0.6	0.8	1.1	192
	Rock	---	.2	.5	.9	106
Wallace	Soil	.5	.6	.8	1.1	2,292
	Rock	---	.3	.6	1.1	990
St. Regis	Soil	.4	.6	.8	1.1	1,583
	Rock	---	.2	.46	1.0	831
Revett	Soil	.4	.6	.7	1.0	697
	Rock	---	.2	.5	.9	452
Burke	Soil	.4	.6	.8	1.1	567
	Rock	.17	.36	.67	1.2	401
Prichard	Soil	.4	.5	.7	1.1	1,632
	Rock	.2	.4	.6	1.0	725
All formations	Soil	.4	.6	.7	1.1	8,611
	Rock	---	.2	.5	1	3,961

resulted from the remobilization of existing sulfur in the Belt formations or from the proximity of the invading magma from which sulfur and other volatile elements escaped.

Coextensive and north-trending sulfur anomalies are present 2–3 mi (3.2–4.8 km) east of Kellogg where the concentrations of sulfur are as much as 0.05 percent in soils and 0.5 percent in the bedrock below. The anomalies are over a magnetic low which would seem to indicate that the anomalous sulfur is not in the form of a halo above an igneous intrusive, although it is possible that magnetite in an intrusive mass was destroyed by hydrothermal solutions, thereby changing the magnetic properties of the intrusive. It is possible that the sulfur is part of the Gem–Dago Peak halo surrounding the original position of the Gem stocks.

An east-trending elongate sulfur anomaly occurs in the soils south of the Placer Creek fault in the western half of the map area. This anomaly is not known to be associated with sulfide deposits, and its significance, if any, is unknown.

ZINC AND CADMIUM

Although 2,980,933 t of zinc have been produced from the Coeur d'Alene district through 1978, the distribution of zinc and its close associate, cadmium, in the soils and surficial rocks does not closely define the mineral belts or ore deposits. Zinc, particularly, has a random distribution and low concentration and this suggests that it may have been partly removed by leaching and redistributed in secondary dispersion patterns. The low level of zinc and cadmium concentrations as compared to crustal abundance, tabulated below, would tend to support this suggestion. Zinc readily goes into solution as a sulfate or chloride during weathering, and these compounds are transported in oxidizing ground waters.

	Soil		Rock		
	Number of samples	Median concentration level (parts per million)	Number of samples	Median concentration level (parts per million)	Crustal abundance (Goldschmidt, 1954) (parts per million)
Zinc	8.684	95	3,963	36	80
Cadmium	7,167	.8	3,959	.4	.18

Cadmium is a strongly chalcophile element that occurs with zinc in sulfide deposits much more closely than it does lead and copper, and it is contained chiefly in sphalerite. There is a fractionation of the two elements, however, depending on the geochemical environment that exists. Cadmium has a stronger affinity for sulfur than does zinc, resulting in a proportionately larger concentration of cadmium in sulfide minerals. Conversely, there is a proportionately lower concentration of cadmium, as compared to zinc, in some silicate rocks where zinc replaces ferrous iron and magnesium in mineral structures.

These variations in the proportions of zinc and cadmium result in an average zinc to cadmium ratio of nearly 500 in all magmatic rocks of the Earth's crust (Goldschmidt, 1954, p. 268) where important amounts of zinc are held in nonsulfide minerals. In contrast, the mean zinc to cadmium ratio is 90 in rocks of the Coeur d'Alene district, where both zinc and cadmium are largely held in sphalerite, the second most abundant ore mineral in the district.

The zinc and cadmium concentration in the soils is 2–2.5 times their concentration in the parent-rock material in the Belt Supergroup (tables 19, 20). This enrichment in the soils relative to the rocks is apparently the result of the constant addition of decaying plant material to the soil. About 600 conifers, mostly Douglas-fir and western white pine, were samples by the authors for needles, twigs, and mull along traverse lines normal to the mineral belts (unpub. data, 1973). Zinc and cadmium are concentrated at unusually high levels in the ash of those samples that grew on the mineral belts. The ash of such samples commonly ranged from 5,000–10,000 ppm zinc and 100–500 ppm

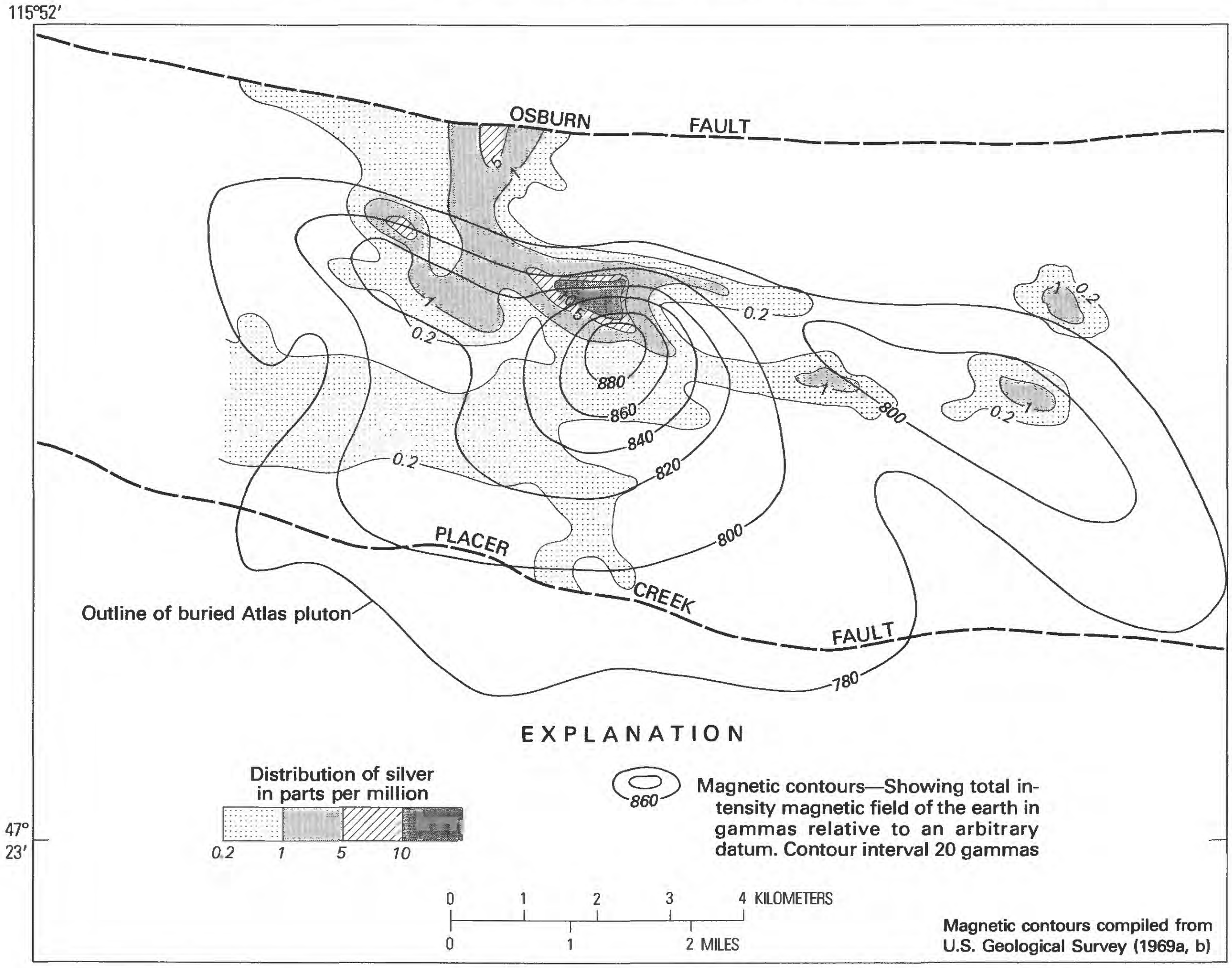

FIGURE 21.—Magnetic map and distribution of silver in rocks in the Atlas pluton area, Coeur d'Alene district.

cadmium. The zinc and cadmium contents of the soils are anomalously high in the same areas.

According to the cumulative frequency plot in figure 24, the zinc threshold is about 250 ppm in both rocks and soils; whereas the threshold of cadmium is about 2 ppm (fig. 25). The distributions of zinc and cadmium, as shown on plate 7*W*, 7*X*, 7*Y*, and 7*Z*, do not closely define the mineral belts.

Relative to the other ore metals, zinc decreases from northwest to southeast. Zinc also increases in the ore deposits of the Prichard Formation, such as those in the Pine Creek area and in several of the ore deposits west of the Gem stocks. As the Prichard Formation is generally exposed in the northwestern part of the district and toward the southeast is generally overlain by successively younger formations, the decrease in zinc from northwest to southeast may result from a stratigraphic control.

There is a strong tendency for zinc and cadmium to fractionate under higher temperatures of formation of sphalerite. According to Goldschmidt (1954, p. 271), sphalerite that forms at high temperatures will accept less cadmium in its structure than will sphalerite that forms at low temperatures. The correlation between the cadmium content of sphalerite and the temperature of formation of the sphalerite seems to be good in the temperature range of 100–600 °C (Goldschmidt, 1954).

Such fractionation between the two metals explains the cadmium-rich halo around the original position of the Gem–Dago Peak stocks (pl. 6), which implies that the halo was localized as a consequence of the heat

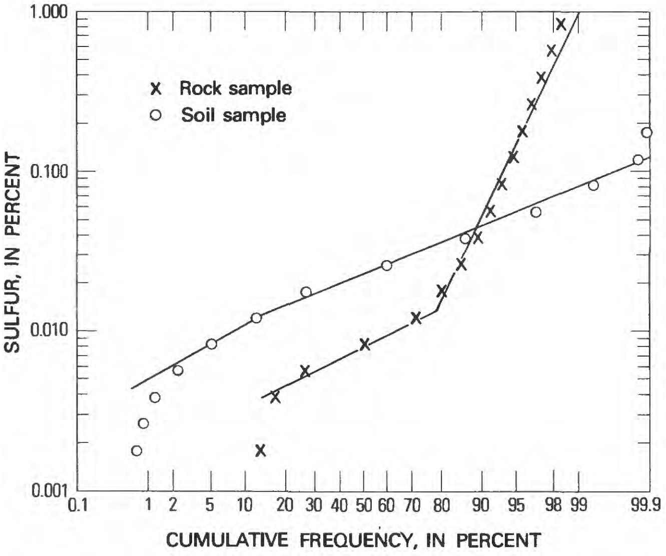

FIGURE 22.—Cumulative frequency plot for sulfur, from 3,735 rock samples and 759 soil samples.

TABLE 18.—*Percentile distribution (in parts per million) of sulfur in soils and rocks in the Coeur d'Alene district, by formation*

[Leaders, (—), no data]

Formation	Sample medium	Percentile distribution 25th	50th	75th	90th	Valid observation
Monzonite	Soil	0.019	0.029	---	---	31
	Rock	.002	.006	0.008	0.01	12
Wallace	Soil	.038	.046	.055	.070	395
	Rock	.006	.009	.01	.03	971
St. Regis	Soil	.039	.049	.063	.078	155
	Rock	.003	.007	.01	.025	795
Revett	Soil	.044	.053	.071	.095	55
	Rock	.004	.006	.009	.01	423
Burke	Soil	.023	.035	.051	.07	143
	Rock	.007	.01	.01	.04	394
Prichard	Soil	.019	.029	.044	.060	421
	Rock	.007	.01	.02	.1	720
All formations	Soil	.039	.047	.057	.073	759
	Rock	.005	.008	.01	.04	3,735

TABLE 19.—*Percentile distribution (in parts per million) of zinc in soils and rocks in the Coeur d'Alene district, by formation*

[Leaders, (—), no data]

Formation	Sample medium	Percentile distribution 25th	50th	75th	90th	Valid observation
Monzonite	Soil	74	107	181	452	192
	Rock	33	50	72	108	106
Wallace	Soil	70	115	203	365	2,295
	Rock	16	41	83	209	933
St. Regis	Soil	57	86	141	250	1,584
	Rock	10	20	50	90	832
Revett	Soil	50	77	117	218	697
	Rock	5	15	40	70	452
Burke	Soil	63	89	125	176	566
	Rock	12	31	55	118	400
Prichard	Soil	89	140	220	339	1,697
	Rock	40	60	90	138	724
All formations	Soil	61	95	161	280	8,684
	Rock	12	36	68	130	3,963

from the intrusion. The cadmium was apparently fractionated from the zinc near the intrusive where the temperature was highest; then, as the distance from the intrusive increased, the decreasing temperature of formation of sphalerite permitted an increasing amount of cadmium to be incorporated in the sphalerite.

A similar halo is present above and around the margins of the Atlas pluton. It is assumed that the magnetic anomaly, as shown by figure 26, is centered directly above the pluton. The relation between the cadmium:zinc dispersion pattern and the magnetic anomaly appears to indicate that the pluton intruded the Moe-Reindeer Queen mineral belt and that the fractionation of the cadmium and zinc resulted in the formation of a cadmium-rich halo in the cooler rock beyond the pluton.

Similar fractionation between cadmium and zinc apparently took place in vein material and wallrock in the Lucky Friday mine. Figure 27 shows the sample distribution and the cadmium to zinc ratio of samples supplied to the authors by Merle Hutchinson of the Hecla Mining Co. Samples were collected from the Lucky Friday mine, where accessible, from all levels down to the 3,650-ft (1,113-m) level. Both vein material and wallrock were samples. Where possible, wallrock was collected at distances of 50, 100, and 150 ft (15, 30, and 46 m) on each side of the vein. There is a decided enrichment of cadmium in the wallrock as compared to the vein material.

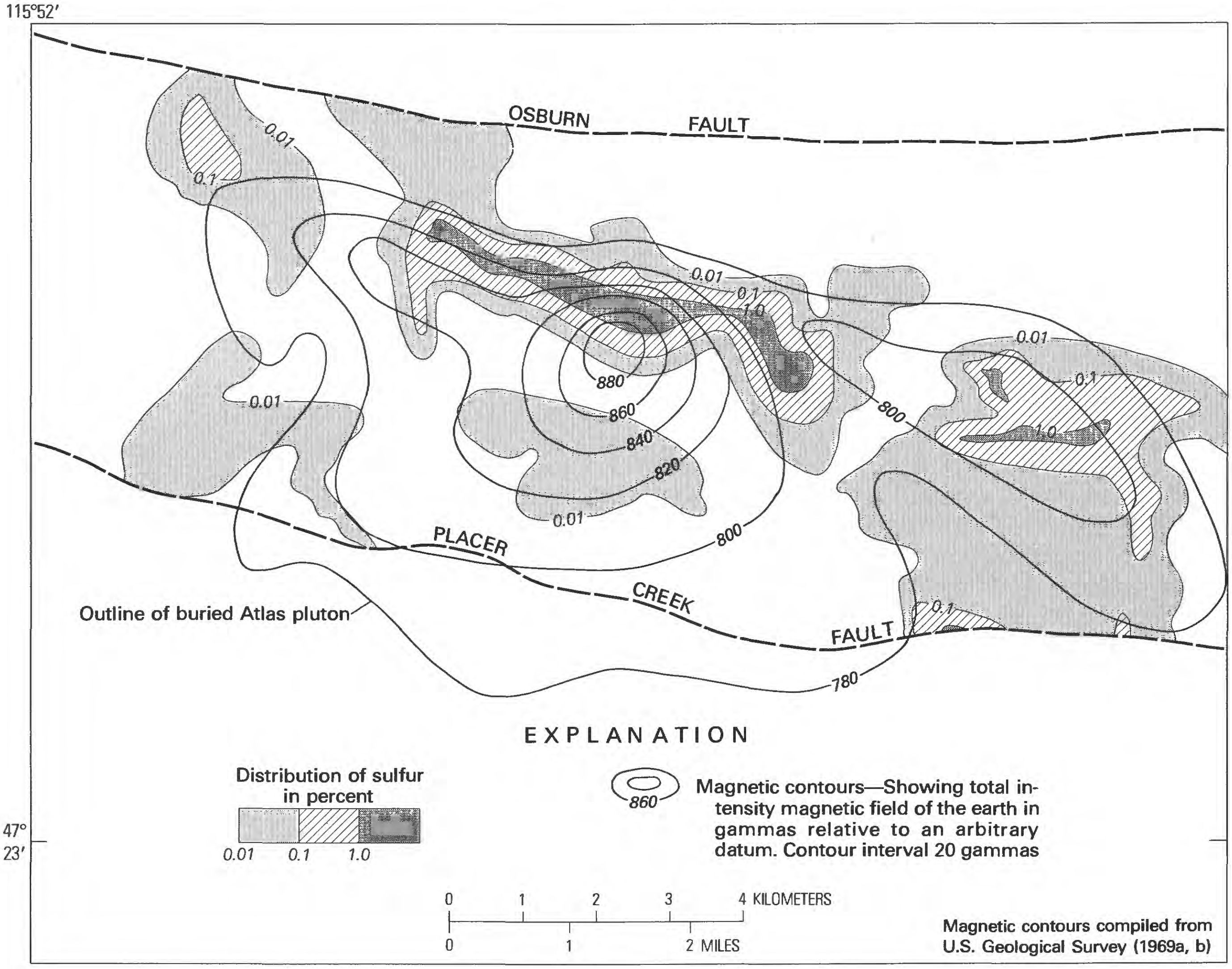

FIGURE 23.—Magnetic map and distribution of sulfur in rocks in the Atlas pluton area, Coeur d'Alene district.

MINERAL BELTS

The major productive veins of the Coeur d'Alene district have been delineated by Fryklund (1964, pl. 2) and by Hobbs and Fryklund (1968, p. 1421) as restricted to 12 mineral belts and subbelts (fig. 6). The boundaries of these mineral belts were drawn to include the known ore deposits and mineralized structures. The Success, Dayrock, and Douglas subbelts, however, are not geochemically defined by this study, and no discussion pertaining to them is given here.

Geochemical dispersion patterns associated with the mineral belts probably show the overall primary dispersion patterns of ore-forming elements. Secondary redistribution at the time of weathering and oxidation has probably made only minor modifications to the original patterns. The concentration of these elements in both soils and rocks is variable and depends on their original concentration in the rocks, the depth to the primary sulfide deposits, and the solubility and mobility of the elements in the zone of weathering. The geochemical data indicate that zinc and copper have been leached from the surficial materials to a greater extent than have the other elements. Zinc particularly appears to be an element that has been dispersed by weathering processes.

The trend, shape, and location of many of the mineral belts is indicated by the underground workings and by the geochemical dispersion patterns of several elements. Most of the mineral belts are defined particularly well by the combined enrichment of several elements in amounts above the district median (pl. 7*AA*, *BB*, *CC*).

TABLE 20.—*Percentile distribution (in parts per million) of cadmium in soils and rocks in the Coeur d'Alene district, by formation*

[Leaders, (—), no data]

Formation	Sample medium	Percentile distribution				Valid observation
		25th	50th	75th	90th	
Monzonite	Soil	0.6	0.8	1.1	2.2	192
	Rock	—	.42	.67	.96	106
Wallace	Soil	—	.5	1	1.7	2,142
	Rock	—	.5	.8	1.3	987
St. Regis	Soil	.4	.7	1.1	2.8	1,480
	Rock	—	.4	.6	.9	834
Revett	Soil	.4	.7	1.1	2.3	654
	Rock	—	.3	.5	.7	453
Burke	Soil	.5	.7	1.1	1.9	559
	Rock	—	.3	.6	.8	399
Prichard	Soil	.8	1.3	2.8	5.7	1,440
	Rock	.3	.5	.8	1.5	724
All formations	Soil	.5	.8	1.3	2.7	7,167
	Rock	—	.4	.7	1.1	3,959

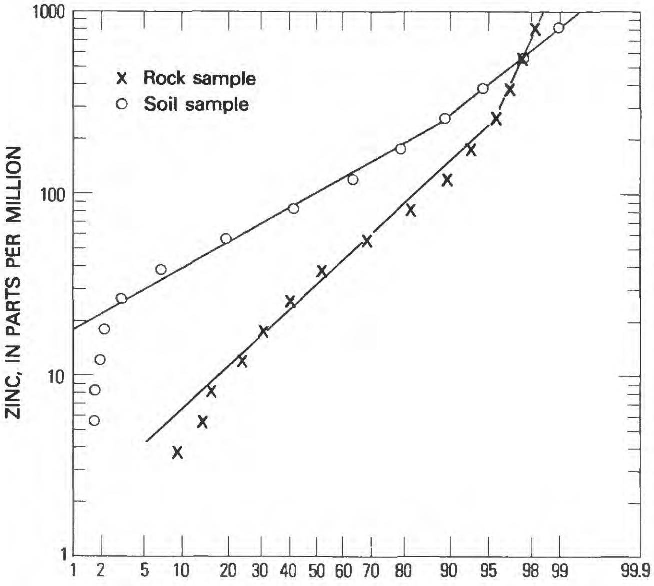

FIGURE 24.—Cumulative frequency plot for zinc, from 3,963 rock samples and 8,684 soil samples.

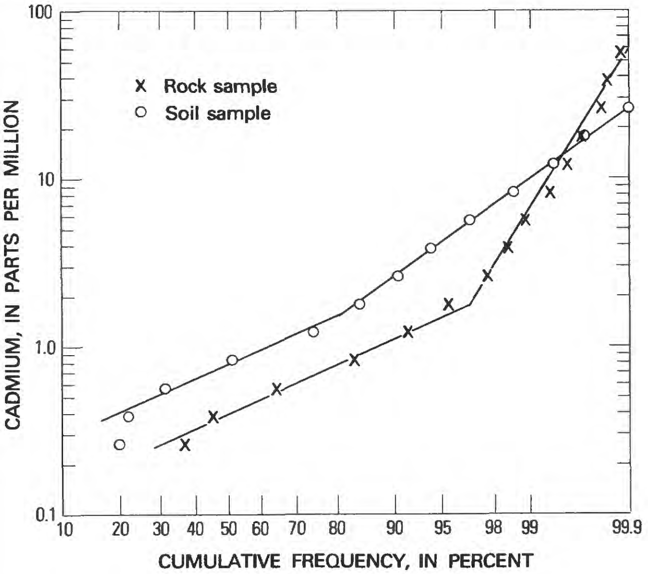

FIGURE 25.—Cumulative frequency plot for cadmium, from 3,959 rock samples and 7,167 soil samples.

The continuity of the northwest-trending belts has been interrupted by postore faulting whereby the northern part of the district has been shifted eastward relative to the southern part of the district, along the Osburn fault. The Gem stocks and those mineral belts in the vicinity of the stocks have been shifted relatively eastward to their present positions by normal faulting along the Dobson Pass fault. The geochemical dispersion patterns, reflecting the mineral belts, have likewise been offset by this postore faulting (pls. 2–6).

Postore faulting and subsequent erosion has left some of the ore deposits within the mineral belts at or near the surface; whereas the sulfide deposits in other mineral belts are hundreds or even thousands of feet deep. In general, those deposits in the northern and western part of the district are relatively shallow or were exposed at the surface at the time of their discovery. Those deposits east of the Bunker Hill mine in the Page-Galena mineral belt are generally deeper than 1,000 ft (305 m).

Dispersion patterns of lead best characterize the mineral belts containing shallow deposits, although dispersion patterns of antimony, silver, cadmium, and copper are also present over some of the shallow deposits. The deeply buried deposits in the southern part of the district are best characterized by antimony, silver, cadmium, and manganese dispersion patterns. The dominant elements in the geochemical halos surrounding the intrusive rocks are antimony, sulfur, cadmium, arsenic, silver, and lead, and dispersion patterns formed by the cadmium to zinc ratio also form a prominent halo around the original position of the Gem stocks.

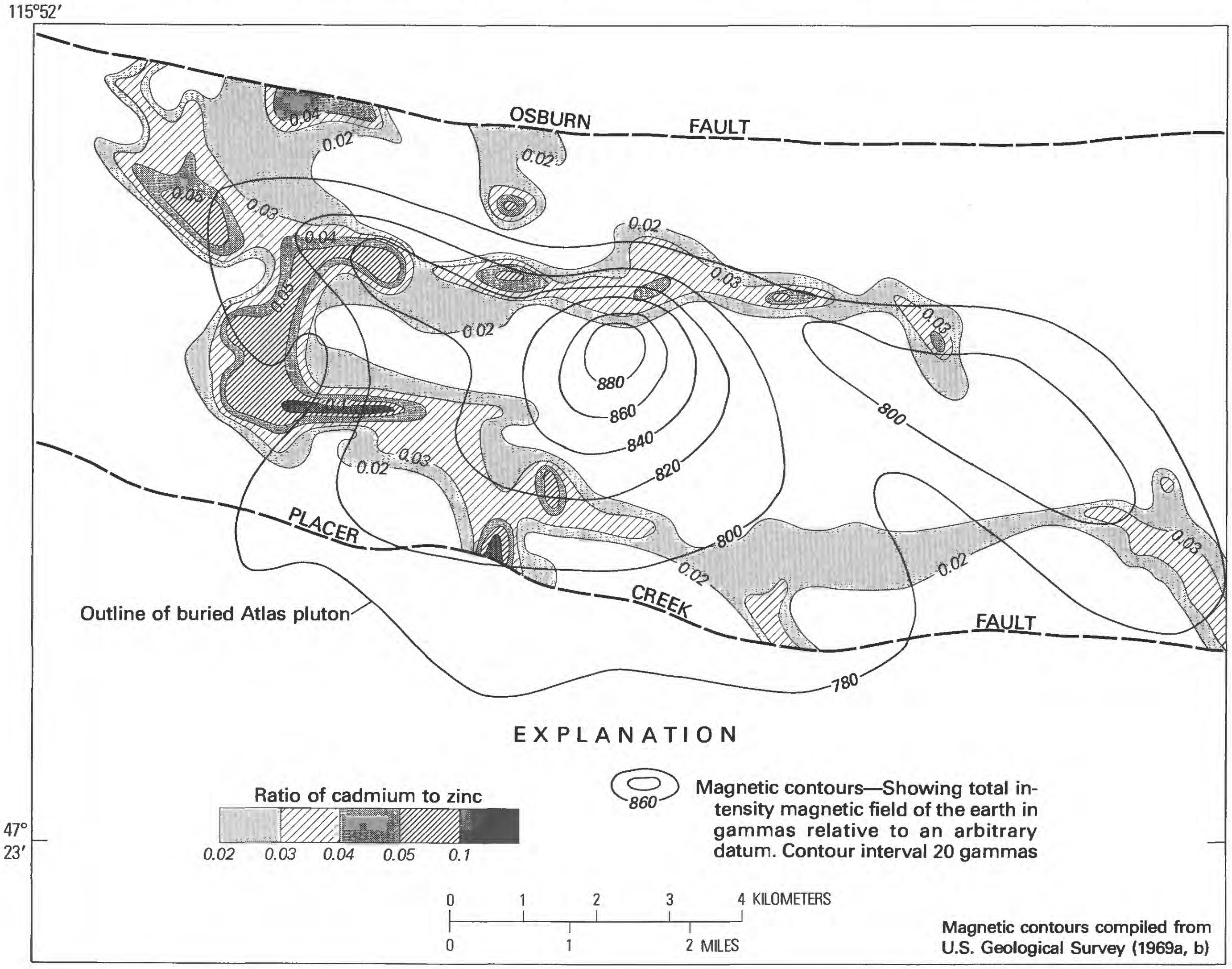

FIGURE 26.—Magnetic map and dispersion patterns formed by the cadmium to zinc ratio in rocks in the Atlas pluton area, Coeur d'Alene district.

GEM-GOLD HUNTER BELT

The Gem-Gold Hunter belt coalesces with the Gem-Dago Peak halo and terminates to the southeast either against the Paymaster fault or the Osburn fault. On the basis of the geochemical dispersion patterns, the belt appears to terminate against the Paymaster fault. This would suggest appreciable strike-slip movement along that fault, but Hobbs, Griggs, Wallace, and Campbell (1965, p. 103) believed that the fault has reverse movement and that there has been no strike-slip movement. If this is the case, the mineral belt must terminate against the Osburn fault. The structural restoration shown on plates 2-6, however, requires some strike-slip movement along the Paymaster fault in order to make the most reasonable restoration.

The Gem-Gold Hunter belt is best defined by the lead dispersion pattern in rocks (pl. 3*A*), but dispersion patterns of antimony, silver, and cadmium in rocks also, in part, define this belt (pl. 7*A*, *S*, *Y*). Crosby (1969, p. 172) gave the total tonnage of ore mined from this belt through 1967 as 28,510,271 short tons (25,864,083 t).

REX-SNOWSTORM BELT

The Rex-Snowstorm belt decreases in zinc and lead and increases in copper from northwest to southeast. The mineral belt is in part delineated by antimony, lead, silver, and sulfur in rocks (pl. 7*A*, *K*, *S*, *U*). Toward the Gem stocks the belt coalesces with the dispersion patterns contained within the halo that surrounds the

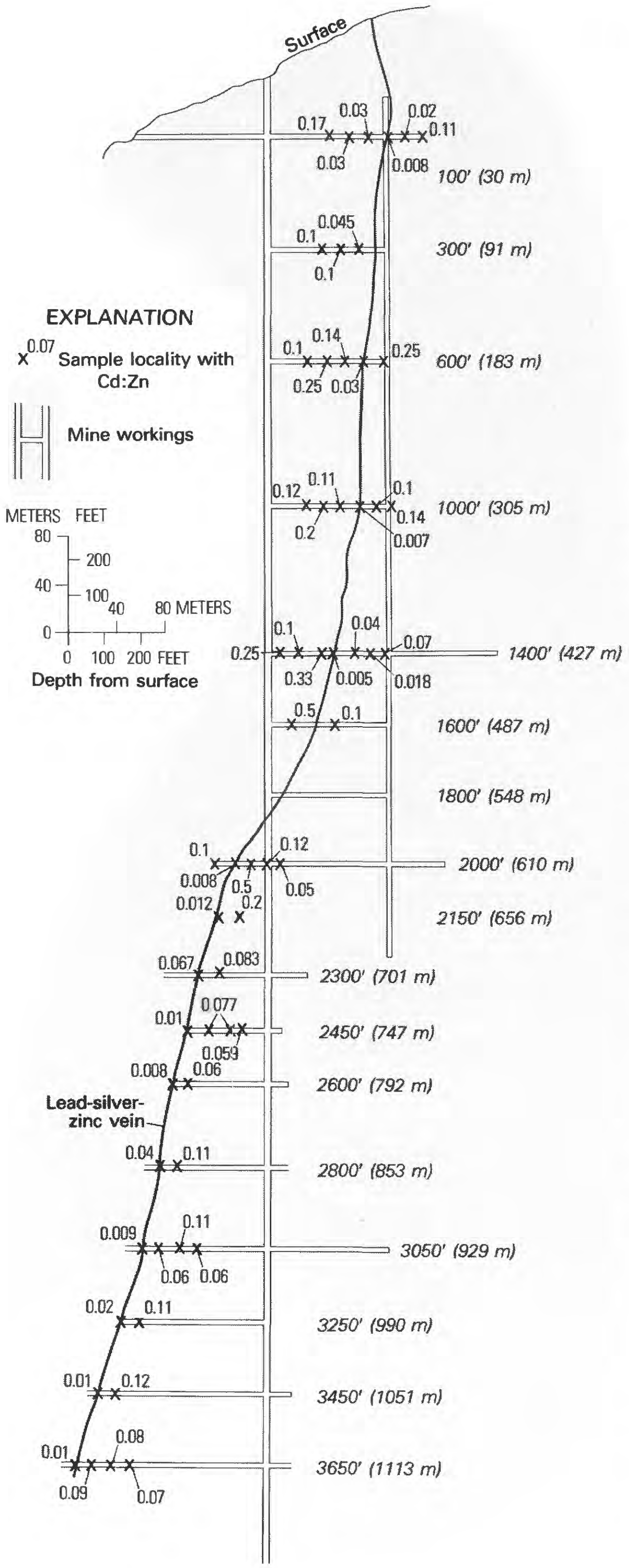

FIGURE 27.—Cross section in Lucky Friday mine along lead-silver-zinc vein showing cadmium to zinc ratios, Coeur d'Alene district.

stocks. Copper is the dominant metal in the southeastern part of the belt where the Snowstorm and National deposits consist largely of disseminated bornite, chalocite, and chalcopyrite in quartzite of the Revett Formation. The antimony dispersion patterns in rocks on plates 2*A* and 2*B* indicate that the Rex-Snowstorm belt was originally continuous with the Moe-Reindeer Queen belt.

CARLISLE-HERCULES AND SUNSET BELTS

The Carlisle-Hercules and Sunset belts are apparently interrupted by the geochemical halos surrounding the Gem stocks, and in this area of overlap the dispersion patterns related to the mineral belts and the dispersion patterns that are part of the halos surrounding the stocks are indistinguishable. Spotty anomalies of antimony, sulfur, zinc, and copper, however, occur southeastward from the Gem stocks and may be indicative of the Carlisle-Hercules and Sunset belts.

GOLCONDA-LUCKY FRIDAY BELT

There are anomalous concentrations of silver, lead, antimony, zinc, and sulfur within the Golconda-Lucky Friday belt, but they are so erratic that the belt is poorly defined. The belt is confined to a zone of intensely deformed rocks where there are many faults that have sliced the Burke, Revett, and St. Regis Formations into many tabular plates further complicated by many isoclinal folds. Mineral deposits that might be present in such structurally deformed rocks are unlikely to be indicated by coherent dispersion patterns at the surface. The structural restoration shown by plates 2-6 indicates that this mineral belt was offset eastward from mineral belts that occur to the west on the south side of the Osburn fault. The mineralized structures in the Golconda-Lucky Friday belt may not, therefore, have significant lateral continuity such as appears to exist in some of the other mineral belts.

MOE-REINDEER QUEEN BELT

Production from the Moe-Reindeer Queen mineral belt has been restricted to the Moe and Atlas mines. According to Fryklund (1964), production from the Moe mine consisted largely of galena from massive siderite veins, and ore from the Atlas mine contained barite, magnetite, pyrite, sphalerite, chalcopyrite, galena, ankerite, and massive siderite.

The belt is geochemically delineated by the distribution of antimony, barium, copper, manganese, silver, and sulfur (figs. 17, 21, 23, 28; pl. 7*A*, *E*, *I*). That part of the magnetic map that is also shown in figures

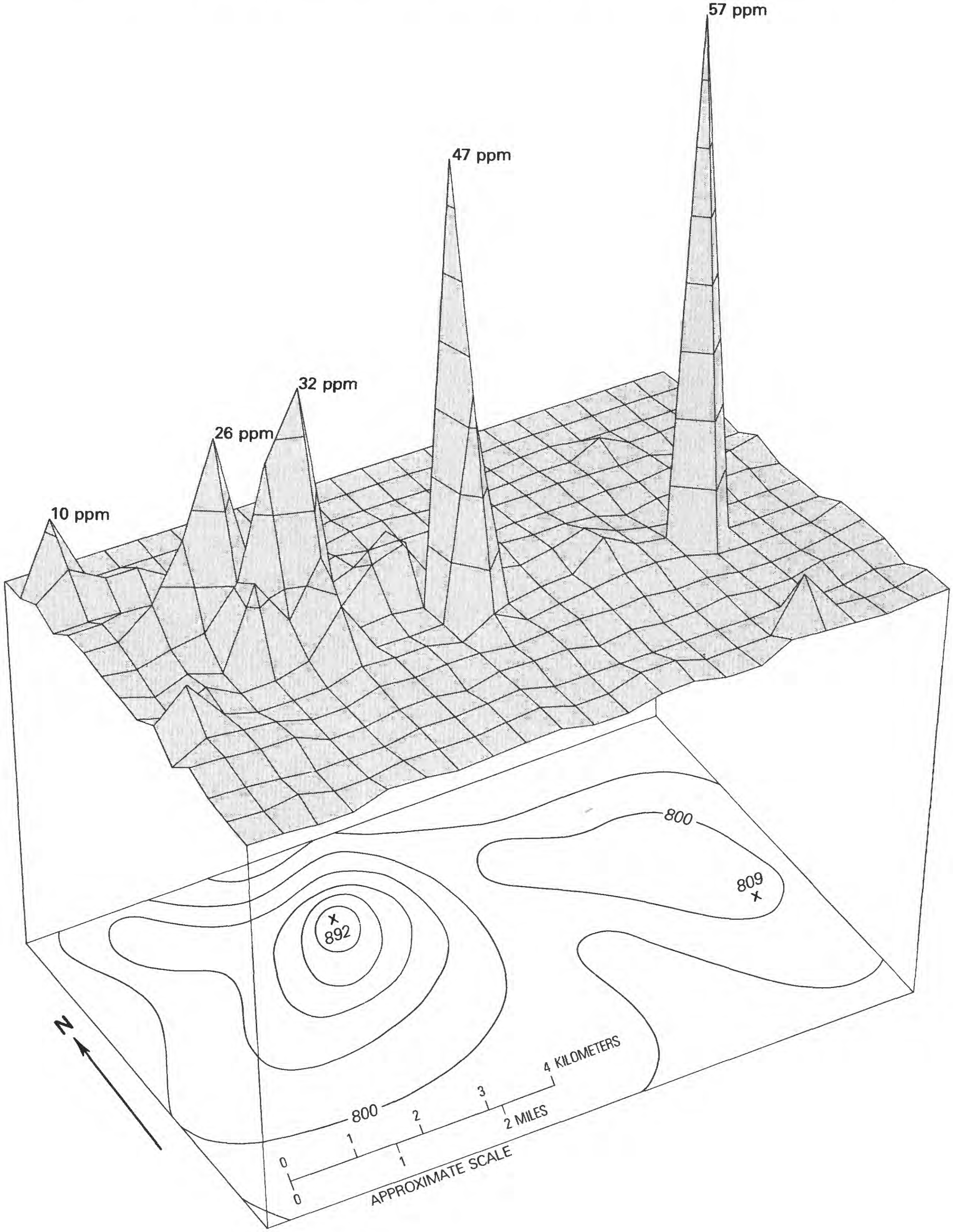

FIGURE 28.—Comparison of the distribution of antimony in rocks, shown in perspective with the aeromagnetic map in the Atlas pluton area, Coeur d'Alene district, viewed from S. 30° W. and 30° above horizontal. Range in perspective view is 0.5–57 ppm. Magnetic contours modified from U.S. Geological Survey (1969a, b). Contour interval 20 gammas.

17, 21, 23, and 28 include a magnetic anomaly that is interpreted to indicate the presence of a buried pluton, here referred to as the Atlas pluton. The crest of the pluton was estimated by Lennart A. Anderson of the U.S. Geological Survey to be about 3,500 ft (1,067 m) deep. The anomalous metals form a geochemical halo directly above the pluton. The coextensive distribution of antimony, copper, and silver (figs. 8, 13, 21) suggest that tetrahedrite may be the source of these elements. The data given in table 14 show that unoxidized siderite from mines within the Coeur d'Alene district contains about 5 percent manganese. As the distribution of manganese in this area is similar to that of copper, antimony, silver, and sulfur, the dispersion patterns formed by these elements may possibly be indicative of the presence of both tetrahedrite and siderite. This possibility is reinforced by the sum of the enrichment above the median district value for these elements as shown by plate 7*AA*, 7*BB*, and 7*CC*. Within the anomalous area, the total enrichment ranges from 5–2,900 times the district median value.

The spatial relation of the geochemical dispersion patterns to the buried stock are similar to the dispersion patterns of these elements around the Gem stocks. It is conceivable that the difference is mostly the result of erosional levels, relative to the two stocks. The dispersion patterns that probably were originally present directly above the south Gem stock have been removed by erosion; whereas the dispersion patterns present in the rocks directly above the Atlas pluton are still intact. Dispersion patterns, prior to any erosion, were probably in the shape of hemispheres as illustrated by figure 29.

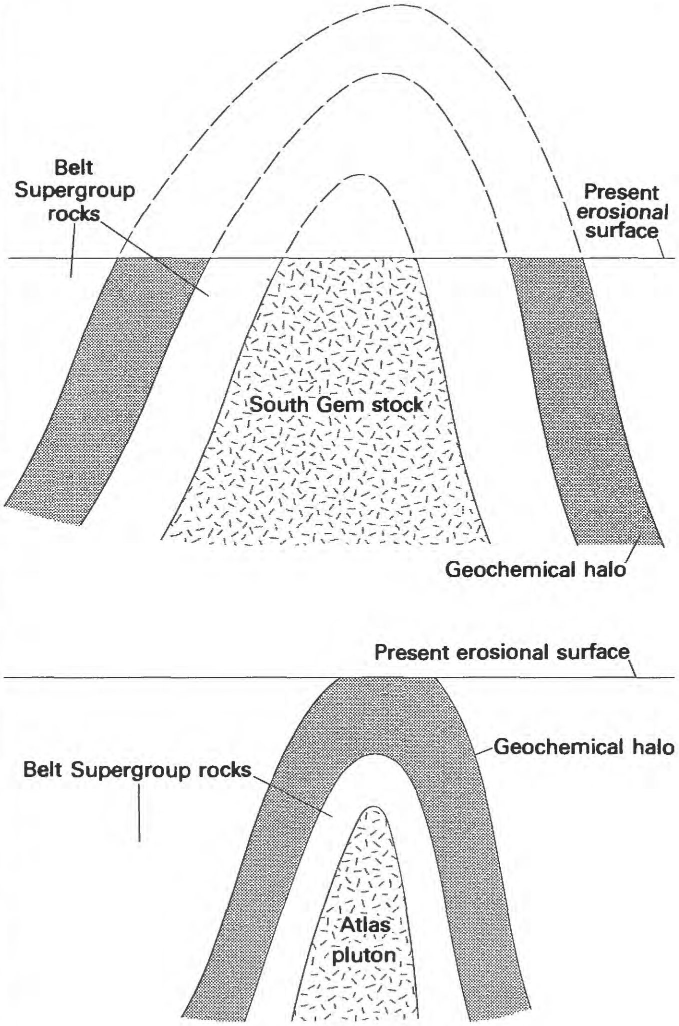

FIGURE 29.—Probable relation of geochemical halos to south Gem stock and Atlas pluton, Coeur d'Alene district.

PAGE-GALENA MINERAL BELT

The Page-Galena mineral belt extends eastward from the Page mine on the west side of the district to the Galena mine, about 5 mi (8 km) west of Wallace. The mineral belt is well defined by the distribution of antimony as shown in perspective by figure 30. The Bunker Hill and Page mines on the west end of this belt produce lead-dominant ores—sphalerite being the second most abundant ore mineral. Tetrahedrite occurs as irregularly shaped blebs and as veinlets along with the galena in the Bunker Hill mine. Chalcopyrite is less abundant than is tetrahedrite. Massive to disseminated siderite is the chief gangue mineral and quartz is abundant in places (Fryklund, 1964).

The remaining part of the mineral belt to the east produces a relatively high-grade silver ore and is often referred to as the "Silver Belt." The principal mines are the Sunshine, Silver Syndicate, Polaris, Silver Summit, Coeur d'Alene, American Silver, St. Elmo, Rainbow, Vulcan, and Galena and the main orebodies are generally 1,000 ft (305 m) or more below the surface. The only indications of these orebodies at the surface are tetrahedrite-siderite-quartz veins, ranging in width from an inch (2.5 cm) or less to a maximum of a few feet (1 m) (Ransome and Calkins, 1908). Most of these ore deposits in the eastern part of the mineral belt contain argentiferous tetrahedrite as the most important ore mineral and siderite as the most important gangue mineral. The deposits have generally formed as replacement veins along fractures and faults of small displacement. The veins intersect steeply dipping beds in the Belt formations on the north limb of the Big Creek anticline.

Early silver production from the eastern part of this belt was restricted to near-surface workings that produced very little ore. The discovery of high-grade silver ore in 1930 on the 1,700-ft (518-m) level of the Sunshine

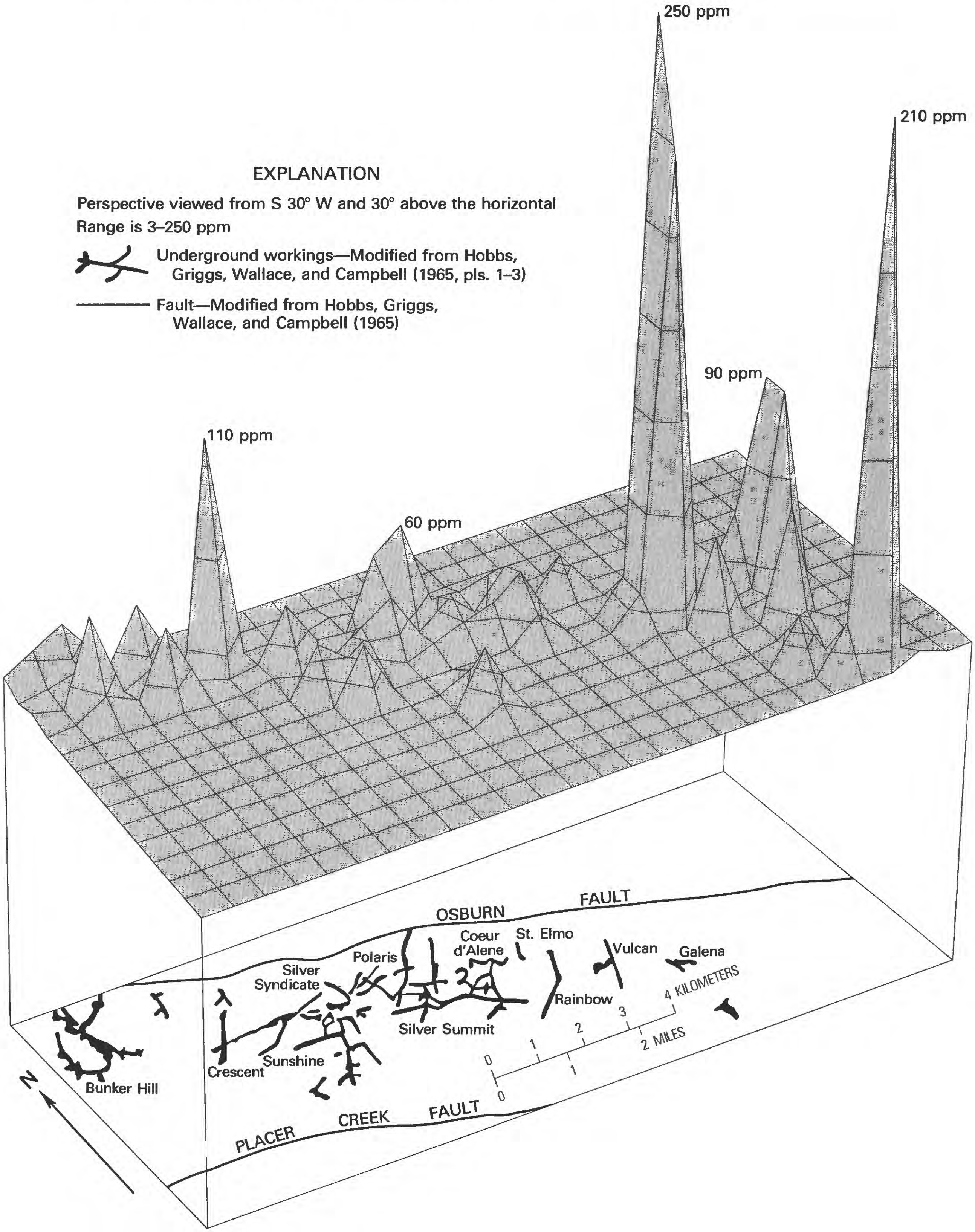

FIGURE 30.—Perspective of antimony showing the trend of the Page-Galena mineral belt, Coeur d'Alene district.

mine, however, stimulated much exploration throughout the eastern part of the Page-Galena belt (Shenon and McConnel, 1939). This exploration led to the discovery of many tetrahedrite deposits, all of which were found at considerable depth.

The mineral belt is traversed by many faults that are parallel or subparallel to the Osburn and Big Creek faults. The most important of these faults are the Polaris, Alhambra, Mineral Point, St. Elmo, Argentine, Killbuck, Fort Wayne, Silver Standard, and Silver Summit. This complex fault system, which has cut the Belt rocks into a series of blocks and slices, has provided numerous conduits along which the mobile elements could migrate from deeply buried sources to the surface.

Some of the mine workings that have explored the Page-Galena belt together with the distribution of silver, antimony, and manganese in rocks are shown in figure 16. The distribution of these three elements is clearly related to the known tetrahedrite ores. Inasmuch as the most important metals in the silver-rich tetrahedrite ores are, respectively, copper, antimony, and silver, it is not surprising that antimony and silver correlate closely with the tetrahedrite ores. Apparently much of the copper has been leached near the surface. Of 14 siderite samples collected from mines within the Coeur d'Alene district, the manganese content ranges from 3 to 7 percent and seems to be characteristic of the siderite. This large amount of manganese suggests that the distribution of manganese shown in figure 16 is largely influenced by the distribution of siderite, the most abundant gangue mineral within the district.

As discussed elsewhere, the Page-Galena mineral belt may consist of segments of several belts. Plates 2-6 suggest that the southern part of the halo surrounding the original position of the Gem–Dago Peak stocks is superimposed on or constitutes the middle segment of the Page-Galena belt.

PINE CREEK BELT

The Pine Creek belt is along the East Fork of Pine Creek at the western end of the district. Sphalerite is the most abundant ore mineral, galena is the second most abundant, chalcopyrite is sparse, and tetrahedrite is rare. Several stibnite veins have been mined, mostly at the west end of the belt.

The ore deposits are restricted to the Prichard Formation and perhaps for this reason are very similar to some ore deposits such as the Interstate-Callahan deposit in the northern part of the district, which is also restricted to the Prichard Formation.

The Pine Creek belt is not as well defined geochemically as some other belts of the district. The belt is partly delineated by dispersion patterns within the soils that contain as much as 500 ppm zinc, 600 ppm lead, 80 ppm copper, and 70 ppm arsenic. It is also somewhat better defined by a dispersion pattern of antimony in the rocks.

CONCLUSIONS AND POSSIBLE EXPLORATION TARGETS SUGGESTED BY GEOCHEMICAL DISPERSION PATTERNS

As previously described, strong geologic evidence indicates extensive postore movement along several of the major faults within the Coeur d'Alene mining district. This movement includes large right-lateral displacement along the Osburn, Kellogg, and Paymaster faults, and several miles of dip-slip displacement on the low-angle Dobson Pass fault. Such faulting has resulted in the apparent offset of some of the mineral belts by as much as 16 mi (26 km). Significantly, the geochemical dispersion patterns that are coextensive with the mineral belts, and the huge dispersion halos of antimony, lead, sulfur, arsenic, and the cadmium to zinc ratio (pls. 2-6) that were concentric to the original position of the Gem–Dago Peak stocks, are likewise offset in direction and distances compatible with the geologic evidence.

The distribution of the more volatile elements in concentric halos surrounding the Gem–Dago Peak stocks was apparently caused by an event that was independent of and subsequent to the implacement of the productive veins in the linear mineral belts. Two mineralizing events that affected the distribution and shape of the geochemical anomalies are thus suggested in the Coeur d'Alene district—an early event that emplaced the major deposits in the mineral belts, and a later event, related to the intrusion of the Cretaceous monzonite stocks, that remobilized and redistributed certain elements from the older deposits to form the halos. These halos intercept and modify the dispersion patterns related to the northwest-trending linear mineral belts. Although these mineral belts are best developed southeastward from the Gem stocks, they appear on the basis of the geochemical evidence, also to continue further northwest beyond the boundary of the superimposed geochemical patterns that are concentric to the stocks.

Where the redistributed metals in the halo related to the Gem–Dago Peak stocks overlaps the earlier mineral belts, the older sulfide deposits were reconstituted and possibly enriched by the remobilized and redistributed elements. Production statistics show that about 85 percent of all the ore mined from the Coeur d'Alene district to date (1974) has been derived from mines overlapped by the halos of secondary geochemical dispersion. This fact strongly suggests that enrichment during remobilization may have influenced the location of major ore shoots. Consequently, favorable host rocks within mineral belts that have been enveloped by the secondary dispersion halos should be considered to be important exploration targets.

The possibility of the extension of the known mineral belts northwest from the Dobson Pass fault is particularly significant with respect to future exploration and is based both on geochemical studies and on geologic deduction. Geochemical data based on the analyses of soil samples led Gott and Botbol (1975) to conclude that the known mineral belts extend northwest beyond the Dobson Pass fault and Dago Peak stocks, and additional geochemical data based on the analyses of rock samples and presented in plates 2, 3, and 7 support this conclusion. When the geochemical patterns are restored to their original positions around the Gem–Dago Peak stocks, dispersion patterns of lead, antimony, and the cadmium to zinc ratio can reasonably be interpreted to represent the extensions of the Gem–Gold Hunter and the Rex-Snowstorm mineral belts. Furthermore, well-documented dip-slip movement along the Dobson Pass fault has almost certainly offset many lead-zinc-silver veins whose footwall segments were displaced eastward and which have been exploited in the many mines in the northern part of the district and east of the fault trace. The upward extensions of these veins in the hanging-wall block to the west, however, have been but slightly explored and more work in this area seems well justified.

Strong dispersion patterns of antimony, copper, silver, and sulfur in the surficial rocks above the postulated Atlas pluton (figs. 8, 13, 21, 23) suggest that ore-forming minerals may be present in significant concentrations near the pluton at depth. By analogy with the Gem–Dago stocks, these crudely concentric element-distribution patterns possibly represent the upper parts of a halo remobilized and redistributed from deeply-buried vein deposits that may also have been enriched by the same processes that are thought to have enhanced the Gem–Dago Peak deposits.

A southeastward extension .of the Page-Galena mineral belt from the Galena mine to the Placer Creek fault is indicated by the dispersion patterns of antimony, copper, silver, manganese, arsenic, and boron. Several similar southeast-trending patterns of ore-forming metals occur to the west in the area between the Page-Galena mineral belt and the Placer Creek fault and are best delineated by the distribution of antimony, copper, manganese, and silver in both soils and rocks.

Dispersion patterns in the southeast part of the district that appear to be associated with the Placer Creek fault may indicate mineralized veins in that area.

The foregoing conclusions and potential exploration targets are based on the prevailing concept of a primary epigenetic origin for the veins in the Coeur d'Alene district. In recent years, many strata-bound deposits and minor mineral occurrences have been observed within the Belt Supergroup. Clark (1971) described strata-bound copper deposits in the Revett Formation which are overlain by a lead-rich zone in the Idaho-Montana area north of the Coeur d'Alene district. According to Harrison (1972), strata-bound copper in concentrations as high as ore grade occurs locally throughout most of the formations of the Belt Supergroup over a wide geographic area. Consequently, the possibility may exist that the presence of strata-bound metals in favorable units of the stratigraphic section may contribute to the geochemical dispersion patterns. Confusion could exist in an area such as that northwest of the Dago Peak stocks where the strike of the formations that might contain strata-bound metals is nearly parallel to the projection of several mineral belts. However, the distribution patterns, concentrations, and great variety of metals in soils and rocks throughout the Coeur d'Alene district, including the anomalies northwest of Dago Peak, are considered strong evidence for a source of metals in veins associated with the recognized mineral belts, and having little if any direct contribution from strata-bound occurrences.

REFERENCES CITED

Brobst, D. A., 1973, Barite, *in* D. A. Brobst, and W. A. Pratt, eds., United States Mineral Resources: U.S. Geological Survey Professional Paper 820, p. 75–84.

Canney, F. C., 1959, Geochemical study of soil contamination in the Coeur d'Alene district, Shoshone County, Idaho: Mining Engineering, v. 11, no. 2, p. 205–210.

Cannon, R. S., Jr., Pierce, A. P., Antweiler, J. C., and Buck, K. L., 1962, Lead isotope studies in the northern Rockies, U.S.A., *in* A. E. J. Engel, H. L. James, and B. F. Leonard, eds., Petrologic studies—A volume in honor of A. F. Buddington: New York, Geological Society of America, p. 115-131.

Clark, A. L., 1971, Strata-bound copper sulfides in the Precambrian Belt Supergroup, northern Idaho and northwestern Montana, *in* Y. Takeuchi, ed., International Association of the Genesis of Ore Deposits, Papers and Proceedings of the Tokyo-Kyoto meetings, 1970: Society of Mining Geologists of Japan Special Issue 3, p. 261-267.

Crosby, G. M., 1969, A preliminary examination of trace mercury in rocks, Coeur d'Alene district, Idaho: International Geochemical Exploration Symposium, 2nd, Golden, Colo. 1968, Proceedings: Quarterly of the Colorado School of Mines, v. 64, no. 1, p. 169-194.

Fryklund, V. C., Jr., 1964, Ore deposits of the Coeur d'Alene district, Shoshone County, Idaho: U.S. Geological Survey Professional Paper 445, 103 p.

Goldschmidt, V. M., 1954, Geochemistry (edited by Alex Muir): Oxford, Clarendon Press, 730 p.

Gott, G. B., and Botbol, J. M., 1973, Zoning of major and minor metals in the Coeur d'Alene mining district, Idaho, U.S.A., *in* M. J. Jones, ed., Geochemical exploration 1972: International Geochemical Exploration Symposium, 4th, London, 1972, Proceedings, no. 4, p. 1-12.

______1975, Possible extension of mineral belts, northern part of Coeur d'Alene district, Idaho: U.S. Geological Survey Journal of Research, v. 3, no. 1, p. 1-7.

Grimes, D. J., and Marranzino, A. P., 1968, Direct-current arc and alternating-current spark emission spectrographic field methods for the semiquantitative analysis of geologic materials: U.S. Geological Survey Circular 591, 6 p.

Harrison, J. E., 1972, Precambrian Belt Basin of northwestern United States; its geometry, sedimentation, and copper occurrences: Geological Society of America Bulletin, v. 83, no. 5, p. 1215-1240.

Hershey, O. H., 1916, Origin and distribution of the ore in the Coeur d'Alenes: San Francisco, private publication, 32 p.; Mining and Scientific Press, v. 112, p. 734 [summ.].

Hobbs, S. W., and Fryklund, V. C., Jr., 1968, The Coeur d'Alene district, Idaho, *in* J. D. Ridge, ed., Ore Deposits of the United States, 1933-1967, (Graton-Sales Volume), v. 2: New York, American Institute of Mining, Metallurgical, and Petroleum Engineers, Inc., p. 1417-1435.

Hobbs, S. W., Griggs, A. B., Wallace, R. E., and Campbell, A. B., 1965, Geology of the Coeur d'Alene district, Shoshone County, Idaho: U.S. Geological Survey Professional Paper 478, 139 p.

Lee, Tan, and Yao, Chi-lung, 1970, Abundance of chemical elements in the earth's crust and its major tectonic units: International Geology Review, v. 12, no. 7, p. 778-786.

Long, Austin, Silverman, A. J., and Kulp, J. L., 1960, Isotopic composition of lead and Precambrian mineralization of the Coeur d'Alene district, Idaho: Economic Geology, v. 55, no. 4, p. 645-658.

Malakhov, A. A., 1969, Bismuth and antimony in galenas as indicators of some conditions of ore formation: Translated from Geokhimiya, no. 11, p. 1055-1068, 1969. [Translation published in Geochemistry International, p. 1055].

Mitcham, T. W., 1952, Indicator minerals, Coeur d'Alene silver belt [Idaho]: Economic Geology, v. 47, no. 4, p. 414-450.

Parker, R. L., 1967, Composition of the earth's crust: U.S. Geological Survey Professional Paper 440-D, p. D1-D19.

Ransome, F. L., and Calkins, F. C., 1908, The geology and ore deposits of the Coeur d'Alene district, Idaho: U.S. Geological Survey Professional Paper 62, 203 p.

Rasor, C. A., 1934, Silver mineralization at the Sunshine mine, Coeur d'Alene, Idaho: Moscow, Idaho University M.S. Thesis.

Shannon, E. V., 1926, The minerals of Idaho: U.S. National Museum Bulletin 131, 483 p.

Shenon, P. J., and McConnel, R. H., 1939, The silver belt of the Coeur d'Alene district, Idaho: Idaho Bureau of Mines and Geology Pamphlet 50, 8 p.

Umpleby, J. B., 1924, The Osburn fault, Idaho: Journal of Geology, v. 32, no. 7, p. 601-614.

Umpleby, J. B., and Jones, E. L., Jr., 1923, Geology and ore deposits of Shoshone County, Idaho: U.S. Geological Survey Bulletin 732, 156 p.

U.S. Geological Survey, 1969a, Aeromagnetic map of the Trout Creek quadrangle, Sanders and Lincoln Counties, Montana, and Shoshone County, Idaho: U.S. Geological Survey Geophysical Investigations Map GP-685.

______1969b, Aeromagnetic map of part of the Avery quadrangle, Shoshone County, Idaho, and Mineral and Sanders Counties, Montana: U.S. Geological Survey Geophysical Investigations Map GP-689.

Van Hook, H. J., 1960, The ternary system Ag_2S-Bi_2S-PbS: Economic Geology, v. 55, no. 4, p. 759-788.

Vaughn, W. W., and McCarthy, J. H., Jr., 1964, An instrumental technique for the determination of submicrogram concentrations of mercury in soils, rocks, and gas, *in* Geological Survey Research 1964: U.S. Geological Survey Professional Paper 501-D, p. D123-D127 [1965].

Wallace, R. E., and Hosterman, J. W., 1956, Reconnaissance geology of western Mineral County, Montana: U.S. Geological Survey Bulletin 1027-M, p. 575-612.

Ward, F. N., Lakin, H. W., Canney, F. C., and others, 1963, Analytical methods used in geochemical exploration by the U.S. Geological Survey: U.S. Geological Survey Bulletin 1152, 100 p.

Ward, F. N., Nakagawa, H. M., Harms, T. F., and Von Sickle, G. H., 1969, Atomic-absorption methods of analysis useful in geochemical exploration: U.S. Geological Survey Bulletin 1289, 45 p.

Warren, H. V., 1934, Silver-tetrahedrite relationship in the Coeur d'Alene district, Idaho: Economic Geology, v. 29, no. 7, p. 691-696.

Zartman, R. E., and Stacey, J. S., 1971, Lead isotopes and mineralization ages in Belt Supergroup rocks, northwestern Montana and northern Idaho: Economic Geology, v. 66, no. 6, p. 849-860.

TABLES 3–6

TABLE 3.—*Correlation coefficients of selected elements in rocks in the Coeur d'Alene district, by formation*

[All analyses are spectrographic except as indicated]

Key to table:

Correlation coefficients × 100

Number of valid pairs of observations

	Monzonite (106 samples)																								
	Fe	Mg	Ca	Ti	Mn	B	Ba	Be	Co	Cr	La	Ni	Sc	Sr	V	Y	Zr	[1]Hg	[2]Cu	[2]Pb	[2]Zn	[2]Ag	[2]Cd	[3]As	[3]Sb	[4]S	
Fe		43	39	65	50	−1	48	11	58	32	54	25	45	34	74	55	21	0	23	−20	21	0	12	−7	0	52	Fe
Mg	106		52	36	28	−17	16	−11	17	7	7	9	41	17	16	23	21	2	−5	−7	12	−9	−11	−5	−55	−33	Mg
Ca	102	102		23	27	−55	43	−11	25	−27	6	−22	21	56	18	10	−16	−14	10	−33	4	−19	−7	−28	−68	15	Ca
Ti	106	106	102		34	55	41	15	59	47	51	37	61	27	64	29	33	−10	38	−6	8	3	10	−15	−2	66	Ti
Mn	106	106	102	106		2	20	36	13	8	26	8	19	20	51	27	25	4	−8	−6	2	−20	4	25	−32	54	Mn
B	18	18	17	18	18		−50	17	−1	84	25	11	40	−72	−24	51	72	18	−2	−20	−34	−25	−7	−15	7	−4	B
Ba	105	105	101	105	105	18		−3	33	−12	31	−6	16	76	53	9	−23	5	27	−25	16	8	0	−44	−19	71	Ba
Be	84	84	82	84	84	13	84		21	16	25	32	38	−7	27	24	8	9	12	16	2	0	−1	−35	39	0	Be
Co	68	68	67	68	68	6	67	55		36	36	38	55	35	52	53	−1	−4	46	−27	−14	19	25	0	0	83	Co
Cr	75	75	73	75	75	14	75	60	54		31	59	58	−24	38	65	43	−21	39	19	3	−5	24	−15	21	−33	Cr
La	82	82	80	82	82	11	81	66	58	63		34	20	20	48	49	3	13	15	−15	13	−10	6	−42	10	58	La
Ni	77	77	74	77	77	16	76	61	55	60	63		49	−4	39	55	10	−22	17	27	−2	15	18	9	48	−32	Ni
Sc	67	67	65	67	67	12	66	55	55	57	61	55		18	48	75	22	−26	14	4	10	14	26	−29	11	−31	Sc
Sr	99	99	97	99	99	13	98	79	63	69	77	70	61		38	9	−29	14	28	−33	11	0	4	−42	−44	10	Sr
V	105	105	102	105	105	18	104	84	67	75	82	76	67	99		56	18	−18	35	−17	10	12	16	−12	22	34	V
Y	96	96	93	96	96	16	95	78	67	71	79	71	66	89	95		24	−21	32	−11	−2	−3	16	−34	16	14	Y
Zr	104	104	100	104	104	17	103	84	68	74	81	75	66	97	103	94		0	−15	17	3	3	7	29	30	−23	Zr
[1]Hg	97	97	93	97	97	14	96	77	66	71	76	70	63	90	96	89	95		−26	−16	6	−3	13	−20	15	38	Hg
[2]Cu	48	48	47	48	48	10	47	33	36	38	42	35	37	44	48	45	47	44		−15	8	1	−22	14	−39	−2	Cu
[2]Pb	91	91	88	91	91	13	90	71	61	65	74	65	59	84	90	85	89	87	42		7	−2	23	61	33	31	Pb
[2]Zn	104	104	100	104	104	18	103	82	68	74	80	76	66	97	103	94	102	96	48	90		−2	48	17	19	34	Zn
[2]Ag	89	89	87	89	89	13	88	71	63	65	72	67	58	84	88	85	87	85	39	80	88		−15	27	33	99	Ag
[2]Cd	81	81	77	81	81	13	81	66	48	57	60	58	47	77	80	73	79	74	34	68	80	68		21	54	66	Cd
[3]As	22	22	21	22	22	7	22	19	10	14	16	14	13	19	22	20	21	21	11	18	21	17	19		20	0	As
[3]Sb	40	40	37	40	40	11	40	30	27	32	30	28	29	35	39	38	39	39	28	38	40	32	32	9		72	Sb
[4]S	9	9	9	9	9	3	9	4	6	6	8	5	8	7	9	8	9	6	7	7	8	3	6	0	5		S

Wallace Formation (933 samples)

	Fe	Mg	Ca	Ti	Mn	B	Ba	Be	Co	Cr	La	Ni	Sc	Sr	V	Y	Zr	[1]Hg	[2]Cu	[2]Pb	[2]Zn	[2]Ag	[2]Cd	[3]As	[3]Sb	[4]S	
Fe		48	17	35	35	43	22	18	38	44	18	58	45	9	50	32	13	8	25	19	29	25	33	18	19	24	Fe
Mg	962		41	56	8	27	38	25	7	55	18	37	42	41	56	25	12	−6	−10	−4	22	−5	23	−5	−21	11	Mg
Ca	639	641		−1	37	0	−3	−9	10	0	−11	7	4	23	14	−3	−17	4	2	12	18	31	39	−1	4	22	Ca
Ti	996	965	635		12	35	56	31	−4	62	23	32	47	17	64	27	59	−8	−6	−10	9	−21	−3	−12	−15	−3	Ti
Mn	938	934	622	941		5	−2	−19	16	4	7	27	11	11	9	20	14	10	8	19	13	15	28	2	19	6	Mn
B	857	865	578	865	835		31	35	9	52	9	41	48	4	52	27	19	2	7	2	3	−1	−1	15	16	1	B
Ba	937	941	631	945	913	856		40	−10	40	25	26	29	8	38	27	49	6	−16	1	16	−9	−4	−4	−2	7	Ba
Be	668	673	478	674	651	653	667		9	40	8	31	47	42	39	30	12	5	9	−2	0	−4	−5	8	2	3	Be
Co	611	615	445	612	590	567	604	484		14	6	52	32	16	26	23	−2	18	50	23	12	30	23	33	24	30	Co
Cr	853	858	595	856	833	800	848	646	573		22	49	62	3	71	37	24	−5	−5	−3	6	−11	3	6	−2	4	Cr
La	752	746	521	751	742	689	740	567	499	692		15	20	−34	12	45	26	11	6	2	6	0	0	3	−2	1	La
Ni	907	913	620	914	880	830	894	665	611	828	705		49	4	57	37	17	11	37	13	21	6	20	29	16	21	Ni
Sc	818	824	583	820	798	757	811	640	579	771	674	799		25	70	46	13	−6	14	5	10	−3	3	6	−4	1	Sc
Sr	173	173	129	169	168	136	164	89	105	153	127	168	14		25	7	−36	−12	−31	−12	1	0	11	2	18	5	Sr
V	898	904	621	907	878	837	896	665	592	840	713	874	791	161		37	22	−9	9	−3	14	−13	1	3	−7	5	V
Y	881	886	615	889	856	818	882	663	592	822	719	853	804	144	860		29	18	6	7	13	−3	13	9	−5	−2	Y
Zr	930	932	631	935	905	849	924	668	602	847	740	885	806	163	888	873		5	−14	14	16	−17	−7	−15	−1	−6	Zr
[1]Hg	827	829	565	833	806	737	804	575	535	737	642	788	701	167	777	758	795		32	27	40	42	32	31	36	23	Hg
[2]Cu	452	447	303	453	440	382	437	295	291	373	376	418	372	82	408	411	434	416		18	9	67	25	61	50	40	Cu
[2]Pb	742	738	516	745	726	646	724	509	487	652	596	699	633	147	687	684	719	685	419		53	35	32	15	29	22	Pb
[2]Zn	892	893	608	899	867	802	875	637	587	803	689	858	767	161	852	834	866	773	418	709		25	43	8	16	18	Zn
[2]Ag	665	671	467	672	644	622	656	490	440	618	494	654	575	139	649	622	650	587	233	494	651		35	53	54	44	Ag
[2]Cd	715	723	496	725	695	672	706	520	469	662	532	692	612	138	703	666	700	628	268	539	696	637		23	22	28	Cd
[3]As	562	566	384	564	542	526	553	401	386	515	414	547	483	99	538	521	549	494	222	413	525	465	475		48	35	As
[3]Sb	792	792	522	799	767	724	775	580	537	707	613	763	690	130	759	742	768	688	380	606	755	581	614	484		36	Sb
[4]S	870	872	575	876	844	782	853	615	568	780	666	836	754	162	818	809	842	762	408	676	810	618	641	533	719		S

See footnotes at the end of table.

TABLE 3.—*Correlation coefficients of selected elements in rocks in the Coeur d'Alene district, by formation*—Continued

	St. Regis Formation (839 samples)																										
	Fe	Mg	Ca	Ti	Mn	B	Ba	Be	Co	Cr	La	Ni	Sc	Sr	V	Y	Zr	^{1}Hg	^{2}Cu	^{2}Pb	^{2}Zn	^{2}Ag	^{2}Cd	^{3}As	^{3}Sb	^{4}S	
Fe		41	11	48	26	49	42	20	15	39	17	56	43	22	45	32	27	10	8	2	28	19	34	23	29	29	Fe
Mg	786		19	44	−8	13	15	14	−4	47	11	38	35	31	51	26	5	−9	4	−4	30	9	20	−5	−15	13	Mg
Ca	305	311		−19	24	1	−2	−24	−6	−7	−8	−4	−2	7	−3	−6	−15	12	11	19	12	21	36	1	14	20	Ca
Ti	817	798	310		5	38	54	24	−25	61	33	33	42	29	61	33	62	−20	−19	−21	−5	−28	−17	−25	−20	9	Ti
Mn	760	733	294	767		11	21	−2	5	−3	−8	9	−6	−18	3	3	15	8	17	13	12	10	21	3	17	8	Mn
B	742	743	277	756	692		24	29	−5	44	18	42	38	9	47	24	33	5	−10	−9	−3	0	−6	5	22	−1	B
Ba	773	757	294	787	728	720		26	12	30	26	27	25	16	39	27	43	−10	−11	−13	−2	−13	−5	−15	2	19	Ba
Be	577	581	227	585	537	576	566		10	38	21	26	33	35	40	34	2	−9	−3	6	8	8	−3	−2	10	10	Be
Co	435	444	213	448	393	424	432	376		0	4	26	8	15	0	5	−18	27	33	18	22	33	23	20	26	22	Co
Cr	686	690	290	694	642	654	668	534	412		32	52	61	30	71	34	20	−11	−11	−11	7	−4	−4	−7	5	1	Cr
La	635	623	260	642	602	595	617	484	364	567		21	37	24	25	39	19	0	−1	−9	10	8	4	−17	1	−1	La
Ni	712	715	295	728	664	687	691	559	438	643	559		49	23	50	32	11	2	5	−10	19	14	20	9	13	14	Ni
Sc	618	624	275	628	575	605	605	516	400	583	525	602		38	63	49	17	4	−27	−5	15	12	7	8	14	3	Sc
Sr	92	88	48	94	90	79	67	49	41	68	71	78	66		40	56	−29	14	−47	5	−29	−9	33	8	−3	34	Sr
V	748	752	298	763	700	725	734	580	443	675	610	697	617	83		45	25	−13	−19	−19	4	−8	−4	−8	0	0	V
Y	747	750	299	761	699	720	733	569	437	672	615	687	620	80	736		13	5	−7	−8	10	0	5	−3	4	3	Y
Zr	768	761	302	780	722	721	748	569	432	672	619	694	610	84	734	732		−12	−12	−8	−10	−19	−15	−9	4	−9	Zr
^{1}Hg	629	611	247	645	596	578	604	437	341	526	482	551	468	81	582	582	594		27	34	34	48	36	44	49	30	Hg
^{2}Cu	276	260	117	282	270	241	266	169	152	224	220	230	188	40	243	247	266	248		32	26	60	24	17	47	31	Cu
^{2}Pb	443	427	210	449	428	392	425	304	275	382	356	387	336	49	403	410	426	397	227		35	54	22	26	36	27	Pb
^{2}Zn	749	738	303	764	701	696	721	549	429	653	584	690	594	93	710	705	716	597	259	428		43	50	25	22	17	Zn
^{2}Ag	513	511	186	528	473	490	495	384	302	445	400	471	407	63	500	496	491	404	152	281	498		49	42	58	44	Ag
^{2}Cd	663	651	245	677	617	621	641	505	381	572	523	604	526	69	641	632	638	511	204	351	632	485		45	39	30	Cd
^{3}As	223	225	81	235	210	221	213	168	141	193	161	214	172	40	218	213	219	190	67	122	213	198	206		45	30	As
^{3}Sb	717	701	265	731	672	679	698	534	402	624	563	651	559	75	688	683	689	563	253	402	686	487	612	211		25	Sb
^{4}S	613	605	214	623	569	576	587	449	338	521	473	550	478	70	571	577	582	473	185	331	572	435	497	204	563		S

Revett Formation (455 samples)																									
	Fe	Mg	Ca	Ti	Mn	B	Ba	Be	Co	Cr	La	Ni	Sc	Sr	V	Y	Zr	^{1}Hg	^{2}Cu	^{2}Pb	^{2}Zn	^{2}Ag	^{2}Cd	^{3}As	^{3}Sb	^{4}S	
Fe		49	43	37	48	49	19	22	18	39	4	35	38	0	49	28	17	1	26	30	42	15	50	38	29	61	Fe
Mg	413		51	58	11	26	26	20	8	62	5	45	38	27	66	35	11	−11	−3	1	5	0	23	3	0	24	Mg
Ca	62	62		26	44	15	27	11	−5	−4	−2	2	0	−3	21	−5	−25	−8	48	23	9	20	11	8	23	26	Ca
Ti	439	416	60		9	52	47	2	0	63	21	29	38	9	67	50	63	−15	−28	−4	3	−17	3	−14	−11	2	Ti
Mn	407	384	55	411		20	25	7	22	14	−4	−17	12	−25	19	16	2	15	20	29	4	4	15	15	21	26	Mn
B	408	388	55	413	380		30	26	15	36	13	18	29	−3	49	28	34	4	25	−5	14	−17	14	0	8	18	B
Ba	418	396	58	424	392	55		29	16	36	17	38	33	−6	37	38	39	2	17	20	−16	7	2	−1	11	6	Ba
Be	231	230	48	235	215	232	228		36	18	9	23	30	59	27	29	10	−12	−8	25	−9	−5	11	1	−4	23	Be
Co	118	115	32	123	100	118	115	94		−5	3	28	29	21	5	10	3	−8	0	6	19	11	6	3	11	11	Co
Cr	294	289	45	299	273	281	292	189	102		21	50	53	13	68	36	8	0	3	−11	5	−2	20	0	3	19	Cr
La	318	298	54	321	306	307	311	191	90	231		0	−24	−20	15	29	17	6	−8	−7	9	−1	−8	7	−12	−4	La
Ni	318	312	51	322	291	301	302	195	117	233	217		36	−4	41	34	10	4	11	6	4	−13	13	7	14	6	Ni
Sc	235	232	49	240	222	229	231	194	100	202	192	196		12	48	40	16	−4	−9	9	18	1	18	−5	4	22	Sc
Sr	62	61	19	62	54	58	53	29	14	35	42	52	30		40	13	−14	15	−51	−65	−26	−27	52	7	−24	24	Sr
V	376	373	52	381	384	365	366	222	117	292	273	294	221	49		41	16	−9	−7	−4	7	−5	22	1	0	26	V
Y	385	376	58	391	358	373	377	232	120	282	290	293	235	48	358		36	−10	−7	0	−4	1	−1	−16	0	0	Y
Zr	396	373	59	401	370	376	386	214	114	264	292	289	217	52	342	352		−11	−19	7	−1	−7	−8	−16	−11	−8	Zr
^{1}Hg	345	320	45	349	324	323	332	173	101	228	253	250	179	60	291	298	315		45	21	26	43	29	30	45	30	Hg
^{2}Cu	141	121	30	139	139	127	135	64	44	82	112	90	81	27	102	114	131	134		47	37	78	43	60	75	47	Cu
^{2}Pb	209	193	45	212	206	189	204	106	76	152	163	152	122	24	171	181	193	192	113		56	50	45	60	47	61	Pb
^{2}Zn	351	339	59	356	325	329	335	201	114	235	247	289	203	58	308	316	316	289	116	183		54	57	35	33	44	Zn
^{2}Ag	269	267	41	273	240	256	256	150	87	191	175	226	147	52	254	246	242	223	70	115	234		39	49	62	44	Ag
^{2}Cd	338	332	50	341	309	319	324	190	96	239	235	264	184	53	315	308	301	262	76	145	292	245		45	41	57	Cd
^{3}As	183	178	20	184	165	167	173	97	69	130	120	146	101	45	159	156	166	149	47	74	152	147	157		53	53	As
^{3}Sb	349	330	44	353	323	334	333	192	108	241	251	270	196	50	312	313	310	286	123	176	304	233	284	148		44	Sb
^{4}S	344	328	45	348	328	318	329	188	96	226	239	264	200	59	292	306	312	277	109	169	287	235	260	164	280		S

See footnotes at the end of table.

TABLE 3.—*Correlation coefficients of selected elements in rocks in the Coeur d'Alene district, by formation*—Continued

Burke Formation (402 samples)																										
	Fe	Mg	Ca	Ti	Mn	B	Ba	Be	Co	Cr	La	Ni	Sc	Sr	V	Y	Zr	^{1}Hg	^{2}Cu	^{2}Pb	^{2}Zn	^{2}Ag	^{2}Cd	^{3}As	^{3}Sb	^{4}S	
Fe		59	16	53	39	47	51	19	25	39	9	60	53	23	53	35	31	6	31	29	37	14	27	25	22	36	Fe
Mg	373		19	57	9	36	51	27	−13	53	1	52	44	53	69	31	13	−21	4	−3	18	−7	2	13	−4	26	Mg
Ca	114	115		−13	41	9	−4	−8	15	−12	2	2	−3	62	0	11	−9	−7	−3	−13	7	0	3	−18	−13	19	Ca
Ti	393	371	115		1	49	64	23	−13	63	25	37	46	18	69	39	60	−27	−25	−31	−7	−28	−14	−2	−20	3	Ti
Mn	387	364	110	384		16	13	−6	27	−14	−1	11	2	23	−1	7	9	3	27	16	22	14	23	−9	5	9	Mn
B	341	334	98	339	334		37	29	15	45	23	41	47	−20	49	30	25	−2	2	18	17	−1	−5	21	13	10	B
Ba	386	368	113	384	376	337		22	−9	47	18	42	36	25	50	27	38	−23	−5	−27	−8	−29	−16	1	−17	9	Ba
Be	264	263	91	263	256	250	264		1	26	10	16	33	44	23	33	−14	−8	23	−2	6	−3	−1	27	7	8	Be
Co	161	161	75	160	152	151	159	141		−5	−2	27	13	−18	−6	3	−6	8	35	17	34	10	22	17	11	26	Co
Cr	306	305	105	305	298	283	302	245	153		27	53	70	−3	80	47	16	−6	−10	−22	−6	−10	−9	18	3	10	Cr
La	304	291	97	301	299	281	300	230	138	261		−5	29	−46	25	33	32	−14	−10	8	2	11	−18	20	−3	−5	La
Ni	293	293	105	293	285	270	289	223	154	258	231		48	−1	51	42	10	−7	25	10	13	6	23	20	21	29	Ni
Sc	249	250	96	247	242	241	250	216	140	238	228	217		−32	59	53	−4	2	9	−2	22	0	12	42	20	15	Sc
Sr	57	57	16	56	57	50	53	32	18	45	38	54	27		13	4	−27	−12	25	−33	−11	−3	11	−13	12	31	Sr
V	344	341	109	342	337	319	343	258	156	295	285	273	246	47		45	24	−12	−4	−6	11	−1	−4	6	−3	18	V
Y	333	331	111	332	325	304	331	255	159	290	280	267	250	39	320		20	−3	8	5	16	10	1	17	10	19	Y
Zr	365	250	111	365	358	322	362	253	154	291	288	279	238	50	327	316		−15	−21	−16	−8	−22	−23	−18	−17	−3	Zr
^{1}Hg	294	274	72	292	288	244	286	189	109	220	217	202	170	51	247	241	271		10	41	27	40	34	12	41	8	Hg
^{2}Cu	116	110	28	115	112	97	113	83	49	96	86	82	69	17	102	99	107	104		60	49	48	48	23	41	51	Cu
^{2}Pb	202	188	60	203	199	159	197	139	76	153	149	133	120	22	168	170	192	177	100		69	79	61	27	68	42	Pb
^{2}Zn	353	340	109	354	347	307	348	248	156	279	269	267	233	43	314	307	327	260	110	188		56	53	24	32	30	Zn
^{2}Ag	327	311	106	327	319	280	318	228	151	264	245	257	217	47	289	283	302	239	102	169	298		51	25	52	36	Ag
^{2}Cd	304	290	92	305	296	264	297	209	136	242	229	236	201	42	269	259	282	233	86	154	277	258		19	41	35	Cd
^{3}As	144	140	28	144	141	132	142	94	52	116	105	111	89	41	127	120	135	123	55	84	132	128	115		28	30	As
^{3}Sb	310	297	86	309	301	273	301	214	138	251	241	240	203	43	276	268	287	237	103	157	276	264	247	116		32	Sb
^{4}S	326	312	96	326	320	279	318	226	140	257	239	249	217	50	284	281	298	242	99	163	299	287	250	133	256		S

Prichard Formation (729 samples)

	Fe	Mg	Ca	Ti	Mn	B	Ba	Be	Co	Cr	La	Ni	Sc	Sr	V	Y	Zr	[1]Hg	[2]Cu	[2]Pb	[2]Zn	[2]Ag	[2]Cd	[3]As	[3]Sb	[4]S	
Fe		57	6	45	32	32	42	19	22	43	11	51	27	19	51	26	11	9	39	25	43	15	23	22	22	38	
Mg	700		8	65	7	53	56	25	−11	68	23	26	56	22	71	33	17	−11	3	−3	24	−3	0	−7	−15	27	Mg
Ca	267	268		−19	43	−4	−12	−10	17	−33	−3	−1	−10	41	−18	−19	−13	16	13	14	19	14	22	−5	9	30	Ca
Ti	716	704	269		−3	60	73	36	−16	71	38	22	61	17	67	45	57	−16	−19	−23	−1	−24	−16	−4	−23	−1	Ti
Mn	708	690	263	707		0	3	0	28	−10	−4	28	−4	28	−1	6	3	2	5	17	23	9	16	−2	11	23	Mn
B	637	641	244	641	629		45	38	−10	54	37	18	61	1	51	51	23	−4	−5	2	15	2	−16	−7	−1	11	B
Ba	696	689	269	701	687	630		34	−6	67	26	17	52	25	61	34	32	−16	−23	−25	−3	−19	−12	−10	−14	−3	Ba
Be	576	578	238	579	567	556	578		2	41	20	14	42	2	33	42	8	−7	16	6	−2	4	0	7	−2	−3	Be
Co	447	450	211	452	440	423	451	413		−6	−6	51	−6	−16	3	6	−3	13	43	26	27	23	33	18	29	27	Co
Cr	656	653	253	660	647	615	654	568	441		31	23	74	3	82	45	15	−14	14	−11	2	−10	−4	−6	−7	7	Cr
La	586	586	235	586	577	565	583	537	400	575		7	42	−31	31	49	21	−19	2	10	10	11	−15	0	−6	5	La
Ni	625	623	255	631	616	581	615	530	438	598	528		12	−7	25	22	14	−6	30	10	36	8	21	4	11	27	Ni
Sc	588	590	247	592	581	569	589	544	425	585	546	546		−20	69	58	11	−12	−12	−6	3	2	−15	−8	5	3	Sc
Sr	103	103	45	102	102	94	90	72	55	91	77	99	78		20	−29	−29	5	−10	−22	−10	−30	13	−21	−9	4	Sr
V	673	674	261	678	663	628	665	575	443	641	585	604	589	96		47	15	−18	0	3	15	−1	5	−3	−6	16	V
Y	653	655	262	660	644	617	659	574	446	637	579	589	587	87	648		24	−11	−3	4	5	7	−8	4	0	2	Y
Zr	678	674	262	681	669	625	674	572	441	647	583	601	587	91	660	649		−9	−18	−16	−6	−11	−21	−18	−20	−14	Zr
[1]Hg	547	537	200	551	540	481	533	430	345	494	433	476	441	84	513	497	516		19	31	21	28	24	10	31	19	Hg
[2]Cu	491	486	188	495	485	450	482	426	330	460	422	448	431	77	473	465	468	394		49	43	42	38	26	45	47	Cu
[2]Pb	642	631	244	645	635	576	630	537	424	596	534	566	541	91	608	596	611	507	467		56	63	38	19	47	42	Pb
[2]Zn	708	694	266	711	699	633	692	573	448	652	576	628	585	103	667	650	669	544	494	640		46	58	8	24	50	Zn
[2]Ag	616	607	239	619	607	551	606	509	404	572	496	555	513	89	581	572	586	476	426	556	618		36	19	47	38	Ag
[2]Cd	648	637	240	651	639	586	636	532	423	604	534	574	544	91	616	601	617	493	456	590	648	575		17	31	33	Cd
[3]As	485	478	181	487	477	455	469	398	318	452	403	440	416	81	462	450	460	346	336	425	482	434	452		32	16	As
[3]Sb	622	618	232	627	613	575	614	519	406	584	520	556	537	88	597	584	595	483	452	576	622	543	577	427		23	Sb
[4]S	687	673	259	690	679	613	670	557	435	630	557	610	565	101	647	630	648	532	477	619	686	606	626	471	601		S

See footnotes at the end of table.

TABLE 3.—*Correlation coefficients of selected elements in rocks in the Coeur d'Alene district, by formation*—Continued

Belt (446 samples)																										
	Fe	Mg	Ca	Ti	Mn	B	Ba	Be	Co	Cr	La	Ni	Sc	Sr	V	Y	Zr	^{1}Hg	^{2}Cu	^{2}Pb	^{2}Zn	^{2}Ag	^{2}Cd	^{3}As	^{3}Sb	^{4}S	
Fe		58	35	29	25	42	17	28	40	46	12	57	46	24	50	40	−6	21	43	20	46	28	28	19	13	36	Fe
Mg	422		41	50	6	33	33	10	8	51	−9	45	48	−11	60	27	11	10	10	5	37	17	22	−3	−17	31	Mg
Ca	255	254		−21	45	−10	−3	−18	27	2	−10	12	11	−23	11	17	−31	9	25	68	17	32	33	11	27	40	Ca
Ti	425	422	248		2	28	60	29	6	61	21	20	51	−25	64	6	56	−9	−18	−1	16	−28	−15	−6	−4	−5	Ti
Mn	420	409	249	415		−7	20	12	25	0	12	13	14	11	7	36	6	5	24	4	4	5	15	13	14	15	Mn
B	382	381	219	378	370		13	35	2	48	23	30	30	−9	40	29	7	10	6	2	19	1	19	4	13	6	B
Ba	425	423	250	426	415	382		24	0	30	16	18	26	50	37	19	42	1	−22	0	4	−27	−17	−8	8	16	Ba
Be	271	270	173	271	268	249	270		10	34	25	22	37	33	38	27	4	3	3	3	3	−14	−8	−2	16	0	Be
Co	287	292	200	287	280	262	290	209		13	12	50	53	16	37	35	−3	8	35	10	13	0	−14	21	15	12	Co
Cr	354	353	231	349	348	329	355	250	264		16	61	57	−33	66	42	17	6	2	7	20	−1	7	7	18	17	Cr
La	370	366	218	368	361	340	366	256	255	320		7	15	38	12	27	15	2	13	−5	−4	−21	−16	0	26	0	La
Ni	365	367	235	366	354	330	368	246	288	321	316		55	−25	57	45	14	16	30	14	34	8	16	16	12	19	Ni
Sc	348	350	221	346	342	318	349	255	269	319	316	323		14	80	42	16	5	19	17	24	−12	7	5	11	−1	Sc
Sr	43	42	39	38	42	22	41	24	31	35	33	36	36		15	−30	−49	−7	−4	−4	37	−19	−4	−38	−20	63	Sr
V	401	400	250	398	390	361	401	266	285	351	352	362	343	42		36	17	1	14	8	33	−17	3	−1	3	3	V
Y	406	410	250	407	395	370	408	268	293	350	356	363	348	41	392		20	13	42	7	7	21	1	28	3	19	Y
Zr	413	409	249	410	402	373	413	267	284	348	362	357	342	41	390	395		−17	−22	−3	−15	−28	−22	−9	1	−13	Zr
^{1}Hg	379	377	227	381	367	333	379	235	263	306	320	324	303	37	352	363	363		38	17	34	45	44	4	16	31	Hg
^{2}Cu	291	295	180	296	282	257	296	174	215	243	253	267	239	32	278	285	286	288		20	24	73	47	32	1	30	Cu
^{2}Pb	385	385	235	388	376	342	388	248	272	323	330	340	317	41	367	371	372	349	283		44	34	40	8	26	17	Pb
^{2}Zn	386	388	240	388	377	344	389	253	281	334	333	355	330	43	377	375	374	349	278	361		35	52	−1	4	18	Zn
^{2}Ag	127	130	96	129	124	105	131	98	95	113	107	119	110	22	127	126	124	101	61	119	131		55	26	5	38	Ag
^{2}Cd	166	166	101	163	162	144	167	116	111	142	150	137	138	25	161	160	161	136	86	146	160	104		4	16	32	Cd
^{3}As	134	134	91	136	132	124	134	95	110	120	122	123	114	12	132	132	133	112	80	117	133	71	76		3	8	As
^{3}Sb	343	343	202	344	336	309	343	213	246	286	294	302	290	33	323	332	331	308	246	322	321	107	142	109		7	Sb
^{4}S	320	321	203	323	312	297	321	195	238	271	270	295	276	23	298	313	309	285	231	293	297	88	103	121	266		S

All Formations (3,979 samples)

	Fe	Mg	Ca	Ti	Mn	B	Ba	Be	Co	Cr	La	Ni	Sc	Sr	V	Y	Zr	[1]Hg	[2]Cu	[2]Pb	[2]Zn	[2]Ag	[2]Cd	[3]As	[3]Sb	[4]S	
Fe		50	18	44	30	41	31	33	37	49	26	56	48	1	52	34	14	9	28	16	37	17	35	28	20	34	Fe
Mg	3,659		33	49	1	23	29	13	−2	51	10	35	39	−27	57	29	1	−4	4	−4	30	6	20	−5	−18	23	Mg
Ca	1,509	1,511		−11	38	9	0	−4	16	−2	−2	10	4	3	10	−5	−20	11	9	9	15	19	26	1	9	19	Ca
Ti	3,868	3,677	1,501		3	36	53	26	−9	60	32	26	52	−1	62	35	54	−16	−8	−15	8	−21	−7	13	−17	1	Ti
Mn	3,730	3,524	1,466	3,734		9	17	5	23	−6	3	18	2	−6	2	9	8	9	14	11	7	7	15	−2	15	10	Mn
B	3,272	3,205	1,234	3,295	3,143		29	41	10	43	30	35	40	39	40	27	22	11	2	6	9	−1	5	13	17	3	B
Ba	3,729	3,596	1,481	3,756	3,602	3,238		32	2	32	29	24	28	53	38	24	34	0	−4	−8	3	−13	−6	−8	1	9	Ba
Be	2,038	2,038	942	2,049	1,985	1,931	2,022		19	39	27	28	46	29	36	33	12	13	10	13	13	7	5	18	22	10	Be
Co	1,778	1,783	950	1,794	1,685	1,611	1,775	1,255		13	13	48	30	−6	23	20	−1	21	40	23	21	24	25	32	28	29	Co
Cr	2,815	2,812	1,259	2,820	2,726	2,636	2,795	1,860	1,571		33	44	69	4	73	43	11	−4	6	2	22	−3	9	4	2	14	Cr
La	2,665	2,589	1,145	2,665	2,609	2,387	2,616	1,705	1,381	2,187		20	37	50	31	43	26	6	11	6	17	4	0	14	10	6	La
Ni	2,909	2,882	1,314	2,934	2,787	2,670	2,879	1,814	1,714	2,480	2,079		43	−12	44	34	15	11	28	7	28	11	20	19	14	23	Ni
Sc	2,613	2,615	1,238	2,619	2,532	2,430	2,587	1,856	1,575	2,386	2,091	2,341		5	69	52	18	3	15	9	23	5	5	16	10	11	Sc
Sr	326	316	266	320	321	158	301	165	161	196	238	203	226		21	−16	−23	7	2	−8	13	−18	−16	−2	9	1	Sr
V	3,406	3,390	1,446	3,430	3,289	3,073	3,375	2,011	1,740	2,775	2,475	2,790	2,555	310		42	11	−9	8	−1	23	−3	7	−1	−3	14	V
Y	3,490	3,443	1,457	3,522	3,360	3,127	3,463	2,022	1,769	2,771	2,538	2,811	2,600	312	3,304		23	7	15	−1	13	5	6	10	−1	10	Y
Zr	3,658	3,534	1,480	3,677	3,530	3,192	3,603	2,023	1,747	2,761	2,589	2,845	2,571	321	3,331	3,397		−2	−11	0	0	−13	−11	−11	−2	−7	Zr
[1]Hg	2,675	2,537	1,142	2,705	2,583	2,238	2,605	1,452	1,343	1,929	1,855	2,022	1,797	267	2,335	2,436	2,536		34	34	36	45	35	34	45	23	Hg
[2]Cu	2,753	2,652	1,146	2,778	2,652	2,348	2,689	1,602	1,506	2,145	1,991	2,238	1,986	238	2,498	2,564	2,639	2,069		24	24	48	31	37	42	36	Cu
[2]Pb	3,039	2,931	1,334	3,066	2,941	2,562	2,959	1,688	1,585	2,315	2,146	2,390	2,169	302	2,745	2,833	2,906	2,286	2,396		50	51	39	24	43	30	Pb
[2]Zn	3,528	3,376	1,462	3,558	3,402	3,005	3,424	1,922	1,747	2,632	2,394	2,785	2,469	317	3,177	3,248	3,352	2,489	2,601	2,916		40	56	19	22	30	Zn
[2]Ag	2,598	2,480	998	2,626	2,484	2,216	2,521	1,337	1,209	1,888	1,623	1,999	1,731	220	2,355	2,407	2,466	1,749	1,839	2,156	2,493		43	38	53	39	Ag
[2]Cd	2,595	2,499	1,010	2,620	2,483	2,245	2,525	1,412	1,250	1,972	1,739	2,023	1,805	218	2,384	2,396	2,475	1,779	1,923	2,148	2,471	2,088		26	30	35	Cd
[3]As	1,035	1,002	433	1,049	997	946	1,004	631	606	841	730	882	796	44	932	968	1,000	781	874	924	998	828	802		43	26	As
[3]Sb	2,908	2,791	1,082	2,935	2,785	2,618	2,826	1,620	1,476	2,257	2,009	2,366	2,096	187	2,649	2,712	2,764	2,103	2,252	2,386	2,738	2,007	2,064	890		26	Sb
[4]S	3,177	3,032	1,180	3,201	3,067	2,766	3,072	1,703	1,520	2,362	2,117	2,510	2,233	192	2,797	2,914	3,002	2,193	2,270	2,536	2,947	2,266	2,085	971	2,460		S

[1] Mercury-vapor detector analysis.
[2] Atomic-absorbtion analysis.
[3] Colorimetric analysis.
[4] Leco combustion analysis.

TABLE 4.—*Correlation coefficients of selected elements in soils in the Coeur d'Alene district, by formation*

[All analyses are spectrographic except as indicated. ×, number of valid pairs insufficient to calculate correlation coefficients]

Key to table:

	Correlation coefficients × 100
Number of valid pairs of observations	

Monzonite (192 samples)																											
	Fe	Mg	Ca	Ti	Mn	B	Ba	Be	Co	Cr	La	Nb	Ni	Sc	Sr	V	Y	Zr	^{1}Hg	^{2}Cu	^{2}Pb	^{2}Zn	^{2}Ag	^{2}Cd	^{3}As	^{3}Sb	^{4}S	
Fe		53	34	58	28	19	55	22	24	60	44	0	35	52	53	60	46	24	−25	35	−16	−14	−1	−23	−38	−3	−6	Fe
Mg	192		43	44	35	21	55	13	20	56	25	0	57	53	35	47	40	18	−25	8	−14	1	−2	−13	−18	−15	−11	Mg
Ca	192	192		32	9	−12	28	26	35	24	21	0	18	36	46	7	17	33	0	−18	−7	6	0	0	−54	−10	4	Ca
Ti	192	192	192		41	28	52	32	37	49	34	0	29	51	25	44	56	36	−20	17	−2	−12	9	−16	−35	12	−19	Ti
Mn	192	192	192	192		42	58	25	1	30	4	0	36	24	11	44	37	7	−25	8	10	9	8	3	−25	17	−50	Mn
B	178	178	178	178	178		45	16	−7	38	0	0	37	32	−16	30	42	15	−18	33	20	−2	31	−6	14	29	−8	B
Ba	192	192	192	192	192	178		40	−2	60	29	0	44	48	42	62	55	24	−37	27	−5	−14	3	−25	−32	11	−35	Ba
Be	186	186	186	186	186	177	186		2	23	37	0	−3	30	31	27	35	35	−22	17	−4	−20	3	−13	−32	16	−49	Be
Co	191	191	191	191	191	178	191	185		13	35	0	14	28	3	20	20	27	32	6	8	3	6	5	−25	11	7	Co
Cr	192	192	192	192	192	178	192	186	191		36	0	60	58	35	57	46	27	−25	24	−4	−15	1	−19	−13	13	−35	Cr
La	170	170	170	170	170	162	170	169	170	170		0	0	42	42	33	57	36	3	43	−1	−16	2	−11	−8	5	−60	La
Nb	71	71	71	71	71	71	71	71	71	71	70		0	0	0	0	0	0	0	0	0	0	0	0	0	0	0	Nb
Ni	192	192	192	192	192	178	192	186	191	192	170	71		37	6	35	28	2	−13	3	7	14	14	1	−9	1	12	Ni
Sc	191	191	191	191	191	178	191	185	190	191	169	71	191		34	41	52	31	−9	28	−5	0	4	−6	−14	0	−44	Sc
Sr	191	191	191	191	191	178	191	186	190	191	170	71	191	190		38	24	16	−14	18	−10	−5	−9	−10	−45	−10	−44	Sr
V	192	192	192	192	192	178	192	186	191	192	170	71	192	191	191		41	14	−48	42	−12	−19	−2	−18	−13	5	−64	V
Y	191	191	191	191	191	178	191	186	190	191	170	71	191	190	191	191		21	−8	42	12	−4	24	−14	−11	13	−32	Y
Zr	192	192	192	192	192	178	192	186	191	192	170	71	192	191	191	192	191		−8	2	13	−25	4	−4	−20	31	−62	Zr
^{1}Hg	191	191	191	191	191	177	191	185	190	191	169	70	191	190	190	191	190	191		11	57	50	41	54	−12	25	47	Hg
^{2}Cu	164	164	164	164	164	150	164	159	163	164	146	54	164	163	163	164	163	164	163		26	10	31	0	14	22	−10	Cu
^{2}Pb	151	151	151	151	151	139	151	145	150	151	129	46	151	151	150	151	150	151	150	137		56	64	63	0	64	0	Pb
^{2}Zn	180	180	180	180	180	166	180	174	179	180	158	59	180	179	179	180	179	180	179	164	151		39	73	−17	17	36	Zn
^{2}Ag	175	175	175	175	175	162	175	169	174	175	153	59	175	174	174	175	174	175	174	159	146	175		34	−9	49	−11	Ag
^{2}Cd	190	190	190	190	190	176	190	184	189	190	168	70	190	189	189	190	189	190	189	162	149	178	173		−17	34	−46	Cd
^{3}As	85	85	85	85	85	80	85	83	84	85	75	40	85	85	84	85	84	185	185	67	57	73	71	84		0	0	As
^{3}Sb	155	155	155	155	155	143	155	150	155	155	136	48	155	154	154	155	154	155	154	139	131	149	145	153	61		−57	Sb
^{4}S	31	31	31	31	31	23	31	26	31	31	26	14	31	31	31	31	31	31	30	30	24	31	31	30	7	28		S

Wallace Formation (2,298 samples)																											
	Fe	Mg	Ca	Ti	Mn	B	Ba	Be	Co	Cr	La	Nb	Ni	Sc	Sr	V	Y	Zr	^{1}Hg	^{2}Cu	^{2}Pb	^{2}Zn	^{2}Ag	^{2}Cd	^{3}As	^{3}Sb	^{4}S	
Fe		48	41	59	23	17	29	4	10	21	10	26	46	31	25	39	8	14	15	34	1	6	−8	1	−1	−2	−17	Fe
Mg	2,175		28	43	10	23	42	11	29	49	18	25	43	48	31	33	37	27	2	19	8	7	4	3	8	−6	−18	Mg
Ca	2,173	2,173		42	42	−2	25	−5	16	−5	−6	16	32	24	45	25	6	8	19	22	−1	19	4	19	−15	0	9	Ca
Ti	2,112	2,112	2,110		19	13	38	18	7	24	18	21	33	34	20	26	19	30	16	24	−2	0	−3	−2	−5	−8	−10	Ti
Mn	2,105	2,105	2,103	2,048		13	27	−5	21	0	−13	9	31	14	22	11	11	7	34	22	14	28	10	25	2	22	10	Mn
B	2.104	2,104	2,138	2,077	2,070		27	23	17	25	28	33	44	27	8	12	43	36	11	15	30	20	19	12	19	43	−6	B
Ba	2,174	2,174	2,172	2,111	2,104	2,139		17	20	45	19	16	35	36	35	20	33	32	5	6	24	23	8	7	18	15	−16	Ba
Be	1,676	1,676	1,674	1,650	1,616	1,668	1,676		12	25	31	21	16	21	15	8	26	21	−13	8	24	1	13	24	0	11	−11	Be
Co	1,256	1,256	1,255	1,233	1,210	1,249	1,256	1,162		41	12	13	28	46	24	17	30	16	17	20	17	17	19	16	21	17	−9	Co
Cr	2,168	2,168	2,166	2,105	2,098	2,134	2,167	1,671	1,256		16	14	28	44	20	33	39	38	−18	10	19	−6	10	−3	21	1	−13	Cr
La	1,586	1,586	1,584	1,543	1,522	1,576	1,585	1,408	1.162	1,586		35	21	30	7	13	40	20	2	11	8	9	6	2	12	16	−10	La
Nb	1,005	1,005	1,003	1,003	957	1,004	1,005	938	803	1,003	942		33	39	24	33	34	17	9	8	6	15	11	5	14	0	−35	Nb
Ni	2,173	2,173	2,174	2,110	2,103	2,139	2,172	1,676	1,256	2,167	1,586	1,005		42	23	30	41	20	15	31	12	27	12	17	10	24	−9	Ni
Sc	2,131	2,131	2,129	2,068	2,062	2,104	2,130	1,669	1,254	2,126	1,581	1,005	2,131		38	35	57	35	10	25	7	12	13	3	14	6	−12	Sc
Sr	1,837	1,837	1,837	1,775	1,770	1,812	1,836	1,497	1,129	1,832	1,407	920	1,837	1,817		14	19	22	−5	8	3	23	13	12	−5	8	−12	Sr
V	2,170	2,170	2,168	2,107	2,100	2,135	2,169	1,672	1,256	2,163	1,583	1,004	2,168	2,126	1,832		24	19	−9	22	3	−2	−3	0	2	−5	3	V
Y	2,064	2,064	2,062	2,011	1,995	2,049	2,063	1,662	1,248	2,059	1,569	1,004	2,064	2,043	1,763	2,060		40	11	19	13	08	16	1	19	17	−17	Y
Zr	2,173	2,173	2,171	2,110	2,104	2,138	2,172	1,674	1,254	2,166	1,584	1,003	2,171	2,129	1,835	2,168	2,062		−10	15	10	−6	16	3	4	12	−6	Zr
^{1}Hg	2,089	2,089	2,087	2.047	2,023	2,054	2,088	1,651	1,243	2,082	1,533	1,003	2,087	2,046	1,762	2,084	1,995	2,087		10	0	28	−1	16	10	25	0	Hg
^{2}Cu	2,174	2,174	2,172	2,111	2,104	2,140	2,173	1,676	1,256	2,168	1,586	1,005	2,173	2,131	1,837	2,169	2,064	2,172	2,089		2	1	10	7	5	13	−2	Cu
^{2}Pb	2,154	2,154	2,152	2,091	2,085	2,119	2,154	1,668	1,251	2,147	1,570	997	2,152	2,110	1,820	2,149	2,044	2,152	2,073	2,271		41	30	42	7	36	0	Pb
^{2}Zn	2,142	2,142	2,140	2,079	2,073	2,107	2,141	1,645	1.233	2,135	1,556	999	2,140	2,098	1,818	2,137	2,031	2,140	2,061	2,259	2,242		12	50	0	33	−3	Zn
^{2}Ag	2,139	2,139	2,138	2,076	2,069	2,104	2,138	1,646	1,235	2,132	1,556	984	2,137	2,095	1,818	2,134	2,029	2,137	2,057	2,256	2,238	2,228		18	16	28	9	Ag
^{2}Cd	1,329	1,329	1,328	1,273	1,308	1,295	1,328	878	582	1,327	809	378	1,328	1,288	1,032	1,324	1,225	1,329	1,261	1,328	1,311	1,311	1,303		−3	36	7	Cd
^{3}As	957	957	956	955	928	944	956	718	521	956	657	494	956	934	763	952	921	956	945	957	938	949	943	608		14	13	As
^{3}Sb	1,832	1,832	1,830	1,775	1,764	1,809	1,831	1,461	1,123	1,828	1,405	890	1,831	1,798	1,551	1,828	1,750	1,830	1,758	1,834	1,819	1,804	1,806	1,059	774		4	Sb
^{4}S	394	394	394	357	383	384	394	240	125	393	228	91	394	371	325	389	347	394	379	394	395	393	384	384	353	334		S

See footnotes at the end of table.

TABLE 4.—*Correlation coefficients of selected elements in soils in the Coeur d'Alene district, by formation*—Continued

St. Regis Formation (1,586 samples)																											
	Fe	Mg	Ca	Ti	Mn	B	Ba	Be	Co	Cr	La	Nb	Ni	Sc	Sr	V	Y	Zr	^{1}Hg	^{2}Cu	^{2}Pb	^{2}Zn	^{2}Ag	^{2}Cd	^{3}As	^{3}Sb	^{4}S	
Fe		62	46	52	28	31	37	2	35	37	11	12	47	41	42	42	17	26	−17	24	11	0	15	−7	12	0	4	Fe
Mg	1,543		45	47	14	17	33	−8	29	43	−2	0	41	38	40	38	15	26	−16	17	4	0	11	−6	−14	−17	−8	Mg
Ca	1,542	1,543		47	34	5	22	−4	22	10	−15	−1	36	25	55	30	−4	10	−2	23	2	7	14	5	−24	−13	4	Ca
Ti	1,454	1,455	1,454		19	20	35	11	15	38	8	20	39	33	31	33	21	44	−7	23	4	−1	0	3	−12	−8	−10	Ti
Mn	1,426	1,426	1,425	1,352		34	33	12	26	13	−5	4	38	20	24	21	9	12	18	23	24	40	13	36	7	28	38	Mn
B	1,505	1,506	1,505	1,417	1,388		27	24	15	27	38	44	43	25	9	7	34	36	−2	1	16	15	13	8	7	47	6	B
Ba	1,542	1,542	1,541	1,453	1,425	1,504		22	20	43	8	7	43	31	19	27	37	34	6	36	27	17	12	28	11	24	9	Ba
Be	1,112	1,112	1,111	1,095	1,062	1,093	1,112		1	6	26	14	15	9	9	−3	21	31	−3	13	15	5	7	14	−9	24	32	Be
Co	913	914	914	894	878	902	912	844		36	10	6	28	38	23	22	22	12	19	18	4	9	10	6	7	13	−1	Co
Cr	1,523	1,524	1,523	1,435	1,406	1,488	1,522	1,094	909		18	20	40	44	8	47	36	41	2	16	10	7	4	11	4	11	−8	Cr
La	1,119	1,120	1,119	1,077	1,033	1,104	1,118	932	839	1,110		38	7	22	−8	6	45	30	−21	0	−1	−21	0	−19	10	21	−2	La
Nb	597	597	596	596	572	586	597	584	526	596	546		22	32	1	29	40	11	15	0	9	1	5	11	11	11	−10	Nb
Ni	1,537	1,538	1,537	1,449	1,420	1,502	1,536	1,109	914	1,521	1,117	597		39	28	28	33	22	7	30	20	31	12	29	3	16	1	Ni
Sc	1,520	1,521	1,520	1,435	1,408	1,487	1,519	1,106	914	1,502	1,114	597	1,519		32	39	41	32	4	14	4	10	4	3	0	3	−4	Sc
Sr	1,356	1,356	1,356	1,269	1,249	1,324	1,355	996	844	1,338	1,007	542	1,354	1,346		11	−1	18	−20	14	2	12	13	2	−14	0	11	Sr
V	1,538	1,539	1,538	1,450	1,421	1,501	1,537	1,107	912	1,519	1,115	595	1,533	1,516	1,351		15	24	−6	17	8	−1	5	−4	−11	−6	21	V
Y	1,442	1,443	1,442	1,378	1,332	1,418	1,441	1,102	910	1,426	1,095	597	1,443	1,430	1,274	1,438		35	17	23	6	−2	2	14	24	18	−20	Y
Zr	1,540	1,541	1,540	1,452	1,425	1,503	1,539	1,111	914	1,521	1,117	596	1,535	1,518	1,355	1,536	1,440		−14	18	4	−4	4	0	0	19	−3	Zr
^{1}Hg	1,331	1,331	1,330	1,278	1,242	1,293	1,331	1,006	805	1,311	966	595	1,326	1,311	1,157	1,326	1,267	1,329		13	26	45	3	51	40	21	21	Hg
^{2}Cu	1,541	1,542	1,541	1,453	1,424	1,504	1,540	1,112	914	1,522	1,119	597	1,537	1,520	1,356	1,537	1,442	1,539	1,332		33	−20	31	31	22	19	4	Cu
^{2}Pb	1,520	1,521	1,521	1,435	1,407	1,483	1,519	1,095	906	1,501	1,112	583	1,515	1,502	1,336	1,516	1,422	1,518	1,312	1,558		47	47	53	22	39	23	Pb
^{2}Zn	1,537	1,538	1,537	1,449	1,420	1,500	1,536	1,106	910	1,518	1,115	595	1,532	1,515	1,351	1,533	1,437	1,535	1,327	1,576	1,554		17	68	30	30	24	Zn
^{2}Ag	1,499	1,500	1,500	1,411	1,384	1,463	1,498	1,075	883	1,480	1,085	566	1,494	1,477	1,327	1,495	1,402	1,497	1,291	1,538	1,516	1,534		18	13	30	−1	Ag
^{2}Cd	1,202	1,203	1,202	1,132	1.136	1,166	1,201	843	670	1,184	824	374	1,197	1,181	1,039	1,198	1,109	1,201	1,007	1,203	1,183	1,199	1,168		33	37	36	Cd
^{3}As	535	536	536	529	510	526	534	399	290	536	340	233	535	528	448	534	518	535	478	536	519	534	529	441		26	0	As
^{3}Sb	1,364	1,365	1,364	1,279	1,248	1,345	1,363	1,003	829	1,350	1,037	543	1,360	1,344	1,196	1,361	1,282	1,362	1,170	1,364	1,345	1,360	1,325	1,057	455		17	Sb
^{4}S	155	155	155	121	144	150	155	75	33	155	75	16	155	147	136	151	135	155	140	155	154	155	153	146	42	141		S

Revett Formation (699 samples)

	Fe	Mg	Ca	Ti	Mn	B	Ba	Be	Co	Cr	La	Nb	Ni	Sc	Sr	V	Y	Zr	[1]Hg	[2]Cu	[2]Pb	[2]Zn	[2]Ag	[2]Cd	[3]As	[3]Sb	[4]S	
Fe		54	40	54	16	6	14	6	10	17	1	9	30	18	32	36	0	10	−1	15	12	−3	6	−8	−17	−13	×	Fe
Mg	693		39	40	16	7	21	−5	4	20	−4	−2	32	28	37	28	0	3	−1	8	2	3	1	−6	−13	−9	×	Mg
Ca	693	693		34	26	−13	16	3	−1	−9	−13	−3	13	15	41	22	−11	−9	−5	11	1	0	3	0	−3	−8	×	Ca
Ti	642	642	642		13	6	22	25	−4	12	8	10	19	15	23	17	2	28	−8	12	15	−2	3	−4	−7	−2	×	Ti
Mn	674	674	674	626		10	32	9	18	4	−9	11	19	6	15	7	0	3	16	10	8	15	10	18	2	1	×	Mn
B	683	683	683	632	664		24	−3	24	34	41	21	39	39	−4	6	61	39	6	−2	0	−3	4	−7	6	1	×	B
Ba	693	693	693	642	674	683		2	6	26	7	3	26	23	12	7	16	9	6	5	1	2	0	7	−2	2	×	Ba
Be	476	476	476	469	468	475	476		2	1	21	−5	−4	2	14	−5	4	18	4	9	14	0	5	11	8	1	×	Be
Co	377	377	377	370	371	375	377	348		25	27	16	25	36	23	11	29	11	30	34	6	−2	15	8	10	26	×	Co
Cr	692	692	692	641	673	682	692	476	377		24	14	51	42	−3	30	34	25	8	3	7	0	1	0	−4	1	×	Cr
La	495	495	495	467	485	494	495	397	346	494		26	18	38	−3	6	62	33	7	0	−2	−7	−2	−6	17	0	×	La
Nb	250	250	250	250	249	250	250	232	199	250	213		16	19	−2	11	22	19	12	0	0	−2	−3	−10	5	−2	×	Nb
Ni	692	692	692	641	673	682	692	476	377	692	494	250		50	17	20	37	14	7	6	6	14	4	0	−1	−6	×	Ni
Sc	687	687	687	636	669	678	687	476	377	687	494	250	687		22	19	59	18	15	3	0	1	4	−7	4	−6	×	Sc
Sr	592	592	592	541	575	584	592	413	336	592	418	236	592	590		7	−4	6	−7	24	6	6	5	0	−2	−1	×	Sr
V	693	693	693	642	674	683	693	476	377	692	495	250	692	687	592		3	5	−10	2	0	−5	0	−7	−17	−10	×	V
Y	624	624	624	598	610	619	624	468	371	624	477	249	624	623	529	624		37	33	4	1	0	7	−3	11	3	×	Y
Zr	689	689	689	639	671	679	689	474	376	588	491	248	688	683	590	689	620		5	14	12	−7	−3	−10	1	17	×	Zr
[1]Hg	635	635	635	620	620	625	635	471	370	634	468	249	634	629	536	635	501	632		30	23	20	11	18	21	7	×	Hg
[2]Cu	690	690	690	639	671	680	690	473	376	689	492	250	689	684	592	690	621	687	634		10	2	8	2	9	62	×	Cu
[2]Pb	655	655	655	604	636	645	655	452	367	654	472	229	654	649	567	655	587	652	599	659		35	45	33	9	11	×	Pb
[2]Zn	654	654	654	603	636	644	654	438	348	653	458	249	653	648	573	654	586	651	599	659	624		19	44	13	7	×	Zn
[2]Ag	661	661	661	611	644	651	661	456	362	661	473	238	661	656	569	661	599	658	609	664	631	631		26	12	14	×	Ag
[2]Cd	614	614	614	572	595	604	614	436	347	613	431	231	613	609	529	614	555	611	565	613	582	584	587		5	8	×	Cd
[3]As	315	315	315	300	312	309	315	227	178	314	212	149	314	312	279	315	294	314	293	315	287	310	303	300		18	×	As
[3]Sb	616	616	616	565	597	608	616	434	344	615	449	226	615	610	524	616	551	612	559	613	588	578	585	550	260		×	Sb
[1]S	×	×	×	×	×	×	×	×	×	×	×	×	×	×	×	×	×	×	×	×	×	×	×	×	×	×		S

See footnotes at the end of table.

TABLE 4.—*Correlation coefficients of selected elements in soils in the Coeur d'Alene district, by formation*—Continued

	Burke Formation (573 samples)																										
	Fe	Mg	Ca	Ti	Mn	B	Ba	Be	Co	Cr	La	Nb	Ni	Sc	Sr	V	Y	Zr	[1]Hg	[2]Cu	[2]Pb	[2]Zn	[2]Ag	[2]Cd	[3]As	[3]Sb	[4]S	
Fe		54	16	51	18	34	26	−16	16	40	10	3	37	25	12	36	−8	25	−40	10	3	−3	17	−13	−16	22	15	Fe
Mg	565		49	44	35	10	58	0	13	48	4	4	54	36	38	38	8	19	−17	5	−17	6	−7	−3	4	−5	−8	Mg
Ca	565	565		31	46	−24	50	14	8	6	−13	7	34	17	64	12	−7	6	−2	11	−11	19	−1	21	6	−12	19	Ca
Ti	525	525	525		24	17	41	14	22	37	15	27	41	37	20	33	12	41	−12	1	0	9	8	3	−12	23	−15	Ti
Mn	555	555	555	517		7	39	4	7	18	−12	17	36	19	40	27	2	13	12	16	5	33	6	24	18	5	−5	Mn
B	555	555	555	515	545		19	14	19	38	46	16	27	39	−7	11	47	44	−7	12	24	0	16	−11	3	19	26	B
Ba	565	565	565	525	555	555		20	13	48	13	25	60	46	43	30	30	29	−2	12	−10	17	−14	8	8	−13	−14	Ba
Be	496	496	496	489	492	487	496		24	3	33	14	8	22	24	−10	33	29	0	14	16	17	9	20	15	13	−11	Be
Co	558	558	558	518	548	549	558	490		28	38	16	30	49	10	7	36	22	17	27	2	4	6	0	8	16	−27	Co
Cr	563	565	565	523	553	554	563	494	557		34	31	60	52	12	40	39	29	0	14	2	0	−3	−6	1	7	−9	Cr
La	511	511	511	471	502	503	511	447	505	510		10	15	42	−3	−3	57	36	9	15	17	−8	12	−7	5	16	−8	La
Nb	323	323	323	321	322	320	323	322	318	323	294		25	31	14	35	28	32	10	5	0	11	−13	5	−2	5	4	Nb
Ni	564	564	564	524	554	554	564	496	558	562	511	323		53	29	37	34	23	−1	28	0	28	−4	8	12	−5	22	Ni
Sc	565	565	565	525	555	555	565	496	558	563	511	323	564		30	35	60	36	9	22	−10	−4	−3	−16	5	−1	−10	Sc
Sr	529	525	525	491	519	519	529	462	524	527	478	299	528	529		25	−1	26	−9	9	−19	13	−3	10	13	−2	6	Sr
V	561	561	561	521	551	551	561	492	554	559	509	323	560	561	525		13	21	−3	5	−15	−4	−7	−11	−5	−2	−15	V
Y	565	565	565	525	555	555	565	496	558	563	511	323	564	565	529	561		31	29	17	3	−3	−3	−13	1	24	−7	Y
Zr	559	559	559	523	549	549	559	495	552	557	505	322	558	559	523	555	559		−16	1	3	−2	4	−5	24	−5	−33	Zr
[1]Hg	557	557	557	518	547	547	557	488	550	555	503	317	556	557	523	553	557	551		19	9	18	−1	20	24	−5	−33	Hg
[2]Cu	460	560	560	460	456	450	460	451	453	458	416	306	459	460	426	460	460	459	454		26	33	21	29	15	32	0	Cu
[2]Pb	447	447	447	447	443	437	447	437	440	445	405	286	446	447	415	443	447	446	443	434		53	44	44	0	50	15	Pb
[2]Zn	542	542	542	542	532	533	542	474	535	540	495	307	541	542	507	541	542	536	536	459	441		28	60	23	28	17	Zn
[2]Ag	537	537	537	537	527	527	537	468	530	535	489	305	536	537	504	535	537	531	531	457	442	532		28	3	46	−4	Ag
[2]Cd	553	553	553	553	543	543	553	487	546	551	499	317	552	553	517	549	553	547	545	451	438	531	526		6	31	−1	Cd
[3]As	304	304	304	304	302	302	304	287	303	304	261	197	303	304	283	303	304	301	301	267	255	288	288	300		−2	29	As
[3]Sb	497	497	497	497	488	488	497	429	491	495	449	279	496	497	463	493	497	491	489	395	391	476	472	486	260		−17	Sb
[4]S	94	94	94	94	92	86	94	90	91	93	91	62	94	94	92	90	94	94	92	86	94	90	90	94	11	83		S

Prichard Formation (1,705 samples)

	Fe	Mg	Ca	Ti	Mn	B	Ba	Be	Co	Cr	La	Nb	Ni	Sc	Sr	V	Y	Zr	[1]Hg	[2]Cu	[2]Pb	[2]Zn	[2]Ag	[2]Cd	[3]As	[3]Sb	[4]S	
Fe		56	30	35	5	32	26	−6	37	42	21	13	43	45	15	27	37	28	−17	28	−5	−5	11	−20	11	0	12	Fe
Mg	1,441		46	40	24	27	54	−6	21	47	0	15	50	47	35	46	34	38	−10	8	−8	8	0	−9	4	−20	1	Mg
Ca	1,439	1,439		22	26	−12	39	−5	11	−2	−13	−8	24	11	61	7	−3	6	−8	6	−8	12	0	−3	−1	−21	11	Ca
Ti	1,425	1,425	1,423		15	20	51	24	21	43	21	27	29	43	19	40	36	47	0	−16	3	−1	−6	7	6	4	−15	Ti
Mn	1,438	1,438	1,436	1,422		−4	36	10	30	14	−23	−4	44	13	20	35	3	15	29	25	17	40	5	32	−3	−1	6	Mn
B	1,440	1,440	1,439	1,424	1,437		20	16	9	43	38	42	18	50	−13	22	63	50	−3	0	8	−4	2	−7	12	10	29	B
Ba	1,441	1,441	1,439	1,425	1,438	1,440		13	0	37	0	11	37	38	41	45	27	45	3	−12	−6	8	−10	6	1	−12	4	Ba
Be	1,422	1,422	1,420	1,406	1,419	1,421	1,422		16	20	34	22	7	23	4	6	27	17	6	−2	9	1	0	14	−1	12	−6	Be
Co	1,432	1,432	1,431	1,416	1,429	1,432	1,432	1,413		31	18	2	46	30	0	10	24	2	12	47	13	18	15	1	7	7	−2	Co
Cr	1,436	1,436	1,434	1,420	1,433	1,435	1,436	1,417	1,429		32	29	45	54	−2	48	49	37	9	4	7	0	−2	5	3	9	−14	Cr
La	1,354	1,354	1,353	1,338	1,351	1,354	1,354	1,320	1,346	1,351		19	0	32	−14	−15	53	21	0	0	8	−21	11	−11	2	18	−8	La
Nb	901	901	900	901	899	901	901	893	900	901	880		6	41	−9	27	46	39	−16	−12	−4	−6	−2	−5	3	−2	0	Nb
Ni	1,441	1,441	1,439	1,425	1,438	1,440	1,441	1,422	1,432	1,436	1,354	901		45	26	52	31	28	−1	31	−5	23	−1	0	10	−12	−9	Ni
Sc	1,437	1,437	1,436	1,421	1,434	1,437	1,437	1,418	1,431	1,434	1,351	900	1,437		20	50	65	51	−14	6	−8	−1	−12	−14	10	−9	−5	Sc
Sr	1,331	1,331	1,331	1,315	1,328	1,331	1,331	1,312	1,326	1,327	1,255	836	1,331	1,328		18	0	8	−11	0	−21	7	−14	−7	−1	−28	−6	Sr
V	1,441	1,441	1,439	1,425	1,438	1,440	1,441	1,422	1,432	1,436	1,354	901	1,441	1,437	1,331		29	45	−6	−3	−11	9	−19	3	7	−18	−8	V
Y	1,438	1,438	1,437	1,422	1,435	1,438	1,438	1,419	1,431	1,434	1,352	900	1,438	1,436	1,329	1,438		52	−5	1	0	−12	−5	−14	6	2	−4	Y
Zr	1,418	1,418	1,416	1,402	1,415	1,417	1,418	1,399	1,409	1,413	1,336	891	1,418	1,414	1,319	1,418	1,415		−3	−13	0	0	−9	0	2	−2	13	Zr
[1]Hg	1,404	1,404	1,402	1,388	1,401	1,403	1,404	1,385	1,395	1,399	1,319	873	1,404	1,400	1,297	1,404	1,401	1,381		18	60	44	34	63	0	49	16	Hg
[2]Cu	1,325	1,325	1,324	1,322	1,322	1,325	1,325	1,313	1,318	1,320	1,245	834	1,325	1,322	1,224	1,325	1,324	1,302	1,315		30	37	43	8	15	18	35	Cu
[2]Pb	1,402	1,402	1,400	1,399	1,399	1,401	1,402	1,385	1,393	1,397	1,317	885	1,402	1,398	1,296	1,402	1,399	1,379	1,368	1,548		55	53	66	9	63	37	Pb
[2]Zn	1,438	1,438	1,436	1,422	1,435	1,437	1,438	1,419	1,429	1,433	1,351	898	1,438	1,434	1,328	1,438	1,435	1,415	1,402	1,584	1,637		39	62	10	26	28	Zn
[2]Ag	1,408	1,408	1,407	1,392	1,405	1,407	1,408	1,389	1,399	1,404	1,323	878	1,408	1,404	1,302	1,408	1,405	1,385	1,372	1,444	1,509	1,556		32	11	44	38	Ag
[2]Cd	1,428	1,428	1,426	1,412	1,425	1,427	1,428	1,409	1,419	1,423	1,342	890	1,428	1,424	1,319	1,428	1,425	1,405	1,392	1,313	1,340	1,426	1,398		2	54	20	Cd
[3]As	1,012	1,012	1,012	1,011	1,009	1,012	1,012	1,003	1,010	1,010	940	706	1,012	1,011	934	1,012	1,011	1,003	978	938	993	1,010	992	1,009		14	7	As
[3]Sb	1,341	1,341	1,339	1,325	1,338	1,340	1,341	1,323	1,332	1,336	1,264	851	1,341	1,337	1,234	1,341	1,338	1,318	1,309	1,227	1,309	1,339	1,310	1,329	920		32	Sb
[4]S	416	416	415	406	414	415	416	405	408	413	410	195	416	413	390	416	414	416	415	366	405	416	408	414	124	413		S

See footnotes at the end of table.

TABLE 4.—*Correlation coefficients of selected elements in soils in the Coeur d'Alene district, by formation*—Continued

Belt (987 samples)																												
	Fe	Mg	Ca	Ti	Mn	B	Ba	Be	Co	Cr	La	Nb	Ni	Sc	Sr	V	Y	Zr	^{1}Hg	^{2}Cu	^{2}Pb	^{2}Zn	^{2}Ag	^{2}Cd	^{3}As	^{3}Sb	^{4}S	
Fe		42	32	49	15	−12	29	19	19	39	0	18	47	31	3	53	6	−4	11	39	14	16	0	−11	6	−13	×	Fe
Mg	987		21	13	−1	19	44	−1	20	36	6	18	51	36	11	32	26	−10	−19	16	−4	3	3	1	1	−11	×	Mg
Ca	987	987		23	23	−48	21	−14	−4	−6	−34	9	10	8	60	21	−20	−28	18	27	−4	13	22	4	9	−27	×	Ca
Ti	982	982	982		14	−20	31	7	2	42	−5	22	34	22	−9	53	5	35	18	30	−11	2	7	−11	−22	−14	×	Ti
Mn	985	985	985	980		−5	5	14	25	10	−8	12	16	12	2	25	0	0	33	26	29	32	5	16	13	6	×	Mn
B	970	970	970	965	968		13	15	29	38	55	7	33	29	−45	4	53	33	−28	−11	21	8	−29	10	15	40	×	B
Ba	987	987	987	982	985	970		15	13	46	17	2	37	32	25	37	27	17	−21	11	−3	6	−7	−4	−10	12	×	Ba
Be	832	832	832	827	830	825	832		11	18	26	3	14	16	−17	8	15	14	0	15	22	12	−21	−11	−17	15	×	Be
Co	720	720	720	715	718	709	720	662		33	28	16	48	40	−6	31	34	13	−2	38	32	26	−5	16	17	24	×	Co
Cr	971	971	971	966	969	961	971	825	709		35	20	59	54	−26	62	41	43	−7	14	19	19	−16	0	−1	24	×	Cr
La	760	760	760	755	758	756	760	725	619	755		1	25	35	−29	6	59	42	−28	1	22	3	−36	0	10	31	×	La
Nb	372	372	372	369	370	371	372	362	328	372	351		20	18	7	23	3	1	9	10	18	22	2	−14	57	−1	×	Nb
Ni	987	987	987	982	985	970	987	832	720	971	760	372		50	−18	56	43	22	−12	35	22	27	−7	3	−5	8	×	Ni
Sc	985	985	985	980	983	969	985	831	720	969	760	371	985		0	49	47	23	−9	21	13	15	2	9	10	16	×	Sc
Sr	723	723	723	718	722	708	723	644	581	708	569	274	723	723		−6	−19	−36	−1	0	−14	−4	22	−5	13	−18	×	Sr
V	987	987	987	982	985	970	987	832	720	971	760	372	987	985	723		15	18	8	31	23	30	6	−5	3	0	×	V
Y	983	983	983	978	981	967	983	832	720	967	760	372	983	982	721	983		41	−29	19	6	−2	−14	14	1	26	×	Y
Zr	977	977	977	972	975	960	977	822	714	961	750	364	977	975	721	977	973		−11	5	−4	−8	−18	4	−15	29	×	Zr
^{1}Hg	971	971	971	966	969	959	971	828	711	956	753	371	971	969	712	971	967	961		14	11	19	12	3	22	−11	×	Hg
^{2}Cu	975	975	975	970	973	966	975	827	712	966	756	371	975	973	713	975	971	966	961		12	5	9	8	9	4	×	Cu
^{2}Pb	960	960	960	955	958	947	960	813	703	947	743	360	960	958	711	960	956	951	946	953		55	−17	6	12	25	×	Pb
^{2}Zn	937	937	937	932	935	920	937	782	680	922	714	369	937	935	704	937	933	927	921	926	913		3	11	36	9	×	Zn
^{2}Ag	868	868	868	864	866	851	868	715	645	852	672	358	868	866	618	868	864	858	852	856	841	821		5	38	−16	×	Ag
^{2}Cd	788	788	788	786	787	771	788	633	576	772	618	313	788	786	535	788	784	778	772	777	763	747	767		21	10	×	Cd
^{3}As	189	189	189	188	189	186	189	79	83	188	77	39	189	188	82	189	185	189	183	189	184	184	184	167		22	×	As
^{3}Sb	777	777	777	773	775	768	777	710	602	772	649	334	777	775	580	777	774	768	765	772	761	728	692	614	119		×	Sb
^{4}S	×	×	×	×	×	×	×	×	×	×	×	×	×	×	×	×	×	×	×	×	×	×	×	×	×	×		S

All Formations (8,713 samples)

	Fe	Mg	Ca	Ti	Mn	B	Ba	Be	Co	Cr	La	Nb	Ni	Sc	Sr	V	Y	Zr	[1]Hg	[2]Cu	[2]Pb	[2]Zn	[2]Ag	[2]Cd	[3]As	[3]Sb	[4]S	
Fe		51	38	50	21	17	31	−3	19	29	5	13	40	31	22	40	8	15	−10	26	0	−1	4	−13	−3	−1	1	Fe
Mg	8,248		36	39	11	17	39	−3	22	41	4	12	42	37	26	35	23	17	−13	17	−3	−1	1	−6	0	−13	−1	Mg
Ca	8,242	8,243		36	33	−14	31	−7	12	0	−16	3	26	17	53	21	−5	0	3	19	−1	11	9	6	−10	−11	10	Ca
Ti	7,946	7,947	7,941		20	6	43	13	17	39	11	24	35	33	16	36	21	40	3	20	1	−1	−1	3	0	1	−3	Ti
Mn	8,022	8,022	8,016	7,746		13	32	4	18	8	−12	6	31	16	18	21	4	11	21	24	19	28	11	25	2	16	19	Mn
B	8,172	8,173	8,168	7,871	7,946		19	13	1	26	28	28	32	27	−10	10	39	35	−4	6	18	10	8	0	9	30	−1	B
Ba	8,247	8,247	8,241	7,945	8,021	8,171		11	18	43	7	12	38	34	29	29	30	32	0	19	15	13	2	11	7	12	3	Ba
Be	7,559	7,559	7,554	7,363	7,375	7,507	7,559		20	12	28	15	12	19	4	1	25	18	4	15	17	6	0	16	−1	12	−6	Be
Co	8,122	8,123	8,121	7,825	7,898	8,061	8,121	7,456		36	24	15	43	45	11	16	38	14	25	24	8	16	1	13	13	9	−10	Co
Cr	8,173	8,174	8,169	7,872	7,947	8,113	8,172	7,502	8,061		20	21	43	47	1	43	41	37	0	14	15	2	0	6	10	11	−4	Cr
La	7,313	7,314	7,310	7,026	7,096	7,265	7,312	6,782	7,219	7,274		21	11	28	−5	−1	47	24	0	2	2	−6	−2	−7	5	12	−10	La
Nb	4,153	4,153	4,149	4,145	4,067	4,135	4,153	4,047	4,104	4,141	3,825		24	35	3	23	34	23	8	7	7	11	0	3	7	3	−20	Nb
Ni	8,235	8,236	8,231	7,934	8,009	8,161	8,234	7,551	8,118	8,166	7,308	4,151		46	16	39	38	21	7	32	17	30	7	17	11	10	0	Ni
Sc	8,232	8,233	8,229	7,932	8,008	8,160	8,231	7,549	8,115	8,164	7,304	4,151	8,224		26	40	53	33	3	24	7	11	4	1	11	2	−5	Sc
Sr	7,537	7,537	7,537	7,237	7,322	7,466	7,536	6,895	7,445	7,473	6,651	3,796	7,531	7,528		9	0	6	−13	14	−1	12	5	3	−6	−6	2	Sr
V	8,234	8,235	8,229	7,933	8,008	8,159	8,233	7,546	8,109	8,160	7,304	4,150	8,222	8,219	7,523		18	23	−4	22	5	3	−3	0	1	−7	14	V
Y	8,216	8,217	8,212	7,915	7,990	8,147	8,215	7,545	8,101	8,150	7,300	4,147	8,209	8,208	7,515	8,204		36	15	15	5	1	0	1	13	11	−14	Y
Zr	8,199	8,200	8,194	7,903	7,977	8,124	8,198	7,518	8,075	8,125	7,270	4,129	8,190	8,184	7,511	8,186	8,168		−11	16	8	−7	0	−1	4	14	6	Zr
[1]Hg	8,049	8,049	8,043	7,753	7,830	7,973	8,048	7,387	7,925	7,974	7,133	4,103	8,036	8,034	7,351	8,035	8,017	8,000		7	21	31	7	38	14	24	5	Hg
[2]Cu	8,206	8,207	8,201	7,907	7,981	8,141	8,205	7,528	8,084	8,141	7,286	4,133	8,194	8,192	7,510	8,193	8,176	8,160	8,035		22	17	20	14	18	14	3	Cu
[2]Pb	8,071	8,072	8,067	7,773	7,851	8,000	8,071	7,397	7,950	8,000	7,183	4,031	8,059	8,057	7,393	8,058	8,040	8,025	7,897	8,464		52	34	54	13	44	10	Pb
[2]Zn	8,018	8,019	8,014	7,719	7,794	7,945	8,017	7,342	7,901	7,946	7,107	4,085	8,006	8,004	7,394	8,009	7,988	7,972	7,853	8,436	8,283		20	58	14	30	5	Zn
[2]Ag	7,498	7,499	7,497	7,227	7,278	7,424	7,497	6,929	7,385	7,428	6,654	4,034	7,488	7,485	6,854	7,487	7,468	7,452	7,333	7,802	7,658	7,664		22	12	28	12	Ag
[2]Cd	6,652	6,653	6,648	6,390	6,526	6,580	6,651	6,014	6,559	6,591	5,855	3,168	6,642	6,637	6,013	6,639	6,621	6,609	6,482	6,638	6,501	6,489	6,097		11	41	17	Cd
[3]As	3,480	3,481	3,480	3,440	3,419	3,468	3,479	3,292	3,449	3,469	3,014	2,294	3,477	3,478	3,189	3,473	3,470	3,466	3,406	3,486	3,368	3,430	3,413	2,981		14	4	As
[3]Sb	7,430	7,431	7,426	7,136	7,207	7,377	7,429	6,803	7,323	7,380	6,673	3,730	7,419	7,416	6,756	7,419	7,403	7,383	7,271	7,413	7,314	7,239	6,769	6,011	3,083		10	Sb
[4]S	758	758	757	662	737	746	758	664	751	751	670	297	758	754	689	745	745	758	754	757	757	738	748	729	271	711		S

[1] Mercury-vapor detector analysis.
[2] Atomic-absorption analysis.
[3] Colormetric analysis.
[4] Leco combustion analysis.

TABLE 5.—*Percentile distribution of elements in rocks in the Coeur d'Alene district, by formation*

[Values are in parts per million except as indicated. Analyses are spectrographic unless otherwise indicated]

Element	Monzonite (106 samples)					Wallace (998 samples)					Element
	Valid Observations	25th	50th	75th	90th	Valid Observations	25th	50th	75th	90th	
Iron[1]	106	1.7	2.5	3.4	5.4	993	1	2.4	4	6.8	Iron
Magnesium[1]	106	.21	.31	.4	.54	993	.16	.48	1.2	2.2	Magnesium
Calcium[1]	106	.5	.7	1.0	1.8	993	---	.05	.43	2.2	Calcium
Titanium[1]	106	.12	.16	.25	.39	993	.11	.21	.31	.44	Titanium
Manganese	106	344	610	833	1,130	993	168	360	819	1,883	Manganese
Boron	106	---	---	---	---	993	17	47	109	221	Boron
Barium	106	478	675	923	1,661	993	171	378	694	1,088	Barium
Beryllium	106	---	---	1.7	2.4	993	---	.89	1.7	2.4	Beryllium
Cobalt	106	---	---	8.3	13	993	---	3.9	9.1	15.9	Cobalt
Chromium	106	---	---	10	25	993	10.8	23.8	39.2	55.8	Chromium
Lanthanum	106	---	32	57	92	993	---	26	40	54	Lanthanum
Molybdenum	106	---	---	---	---	993	---	---	---	---	Molybdenum
Nickel	106	---	---	4.8	9.6	993	5.9	11	21	29	Nickel
Scandium	106	---	---	6.5	9.8	993	3.8	6.9	10	14	Scandium
Strontium	106	603	891	1,278	1,873	993	---	---	---	---	Strontium
Vanadium	106	40	57	95	207	993	20	36	60	97	Vanadium
Yttrium	106	9.8	13	20	32	993	12	22	34	51	Yttrium
Zirconium	106	60	87	120	183	993	100	189	277	379	Zirconium
Sulfur[1, 2]	12	.002	.006	.008	.01	971	.006	.009	.01	.03	Sulfur
Mercury[3]	106	.02	.04	.06	.1	988	.02	.04	.08	.19	Mercury
Copper[4]	105	---	18	36	69	980	---	11	26	76	Copper
Lead[4]	106	18	24	34	51	993	10	23	52	188	Lead
Zinc[4]	106	33	50	72	108	933	16	41	83	209	Zinc
Silver[4]	106	---	.2	.5	.9	990	---	.3	.6	1.1	Silver
Cadmium[4]	106	---	.42	.67	.96	987	---	.5	.8	1.3	Cadmium
Arsenic[5]	---	---	---	---	---	993	---	---	17	27	Arsenic
Antimony[5]	106	---	---	---	1.1	992	---	1.1	2.8	7.4	Antimony

Element	St. Regis (839 samples)					Revett (455 samples)					Element
	Valid Observations	25th	50th	75th	90th	Valid Observations	25th	50th	75th	90th	
Iron[1]	839	1.1	2.4	4.1	7.1	455	0.47	1.4	3.1	5.5	Iron
Magnesium[1]	839	.07	.19	.44	1	455	.02	.05	.1	.25	Magnesium
Calcium[1]	839	---	---	.05	.17	455	---	---	---	---	Calcium
Titanium[1]	839	.1	.19	.3	.4	455	.06	.13	.24	.36	Titanium
Manganese	839	212	600	1,715	4,760	455	97	381	1,329	4,723	Manganese
Boron	839	17	47	116	236	455	16	38	85	131	Boron
Barium	839	289	543	924	1,780	455	110	235	575	1,030	Barium
Beryllium	839	---	.9	1.8	2.5	455	---	---	1	1.8	Beryllium
Cobalt	839	---	---	9	15	455	---	---	---	8.8	Cobalt
Chromium	839	---	20	32	50	455	---	8.3	19	31	Chromium
Lanthanum	839	---	25	37	53	455	---	25	40	55	Lanthanum
Molybdenum	839	---	---	---	---	455	---	---	---	---	Molybdenum
Nickel	839	5	10	20	25	455	---	4.2	9.4	15	Nickel
Scandium	839	---	5	9	12	455	---	---	6.5	10	Scandium
Strontium	839	---	---	---	---	455	---	---	---	---	Strontium
Vanadium	839	20	30	50	75	455	8.6	20	33	50	Vanadium
Yttrium	839	13	20	30	45	455	9	15	25	36	Yttrium
Zirconium	839	123	207	312	477	455	113	244	455	1,095	Zirconium
Sulfur[1, 2]	795	.003	.007	.01	.025	423	.004	.006	.009	.01	Sulfur
Mercury[3]	828	---	.03	.07	.16	453	---	.03	.06	.15	Mercury
Copper[4]	834	---	9	25	70	449	---	8	20	45	Copper
Lead[4]	839	---	11	26	111	455	---	10	28	301	Lead
Zinc[4]	832	10	20	50	90	452	5	15	40	70	Zinc
Silver[4]	831	---	.2	.46	1	452	---	.2	.5	.9	Silver
Cadmium[4]	834	---	.4	.6	.9	453	---	.3	.5	.7	Cadmium
Arsenic[5]	832	---	---	---	18	455	---	---	---	20	Arsenic
Antimony[5]	830	.9	2.2	5	9.5	452	---	1.6	4	10	Antimony

See footnotes at the end of table.

TABLE 5.—*Percentile distribution of elements in rocks in the Coeur d'Alene district, by formation*—Continued

Element	Burke (402 samples)					Prichard (727 samples)					Element
	Valid Observations	25th	50th	75th	90th	Valid Observations	25th	50th	75th	90th	
Iron[1]	402	0.8	1.8	3.5	6.2	727	2	3	5	7	Iron
Magnesium[1]	402	.04	.1	.29	.5	727	.13	.4	.7	.9	Magnesium
Calcium[1]	402	---	---	---	.15	727	---	---	.05	.1	Calcium
Titanium[1]	402	.07	.19	.31	.46	727	.17	.3	.4	.5	Titanium
Manganese	402	119	386	978	2,086	727	121	224	475	1,083	Manganese
Boron	402	11	33	68	110	727	18	35	66	105	Boron
Barium	402	161	360	642	903	727	193	343	512	708	Barium
Beryllium	402	---	---	1.3	2.2	727	---	1.3	2	2.9	Beryllium
Cobalt	402	---	---	6.1	11	727	---	5	11	18	Cobalt
Chromium	402	---	13	27	46	727	15	40	60	80	Chromium
Lanthanum	402	---	28	40	53	727	---	34	50	70	Lanthanum
Molybdenum	402	---	---	---	---	727	---	---	---	---	Molybdenum
Nickel	402	---	5.5	13	21	727	---	10	17	29	Nickel
Scandium	402	---	3.9	8.8	11	727	5	10	15	19	Scandium
Strontium	402	---	---	---	---	727	---	---	---	---	Strontium
Vanadium	399	11	26	43	69	727	27	54	86	128	Vanadium
Yttrium	402	10	21	31	43	727	19	28	37	58	Yttrium
Zirconium	402	129	266	385	835	727	133	200	300	415	Zirconium
Sulfur[1,2]	394	.004	.007	.01	.04	720	.007	.01	.02	.1	Sulfur
Mercury[3]	401	---	---	.05	.09	701	---	.03	.06	.1	Mercury
Copper[4]	401	---	6.2	18	45	726	12	22	38	69	Copper
Lead[4]	402	---	14	41	216	727	20	34	55	125	Lead
Zinc[4]	400	12	31	55	118	724	40	60	90	138	Zinc
Silver[4]	401	.17	.36	.67	1.2	725	.2	.4	.6	1	Silver
Cadmium[4]	399	---	.3	.6	.8	724	.3	.5	.8	1.5	Cadmium
Arsenic[5]	393	---	---	---	19	726	---	---	21	40	Arsenic
Antimony[5]	402	---	1.1	3.7	11	726	.5	1.9	4.2	7.8	Antimony

Element	Belt (446 samples)					All Formations (3,979 samples)					Element
	Valid Observations	25th	50th	75th	90th	Valid Observations	25th	50th	75th	90th	
Iron[1]	446	0.8	2.1	3.9	7.2	3,979	1	2.4	4.1	6.9	Iron
Magnesium[1]	446	.09	.45	1.1	2	3,979	.07	.25	.65	1.2	Magnesium
Calcium[1]	446	---	.04	.4	2	3,979	---	---	.08	.86	Calcium
Titanium[1]	446	.12	.21	.32	.46	3,979	.1	.2	.3	.4	Titanium
Manganese	446	145	357	845	1,844	3,979	147	366	938	2,508	Manganese
Boron	446	11	30	61	115	3,979	13	38	84	166	Boron
Barium	446	153	312	597	878	3,979	182	383	677	1,085	Barium
Beryllium	446	---	.85	1.3	2	3,979	---	.8	1.7	2.4	Beryllium
Cobalt	446	---	4.8	8.8	16	3,979	---	---	8.9	15	Cobalt
Chromium	446	8.6	20	37	61	3,979	---	20	37	60	Chromium
Lanthanum	446	18	26	36	50	3,979	---	27	41	56	Lanthanum
Molybdenum	446	---	---	---	---	3,979	---	---	---	---	Molybdenum
Nickel	446	4.7	9.9	19	29	3,979	---	9	17	25	Nickel
Scandium	446	3.9	6.4	10	14	3,979	---	6	10	14	Scandium
Strontium	446	---	---	---	---	3,979	---	---	---	---	Strontium
Vanadium	446	15	31	59	104	3,970	17	34	58	97	Vanadium
Yttrium	446	13	22	33	48	3,979	12	21	33	48	Yttrium
Zirconium	446	94	166	257	361	3,979	108	198	310	489	Zirconium
Sulfur[1,2]	409	.003	.007	.01	.05	3,735	.005	.008	.01	.04	Sulfur
Mercury[3]	434	.02	.05	.07	1.1	3,922	---	.03	.06	.14	Mercury
Copper[4]	445	8.6	16	38	109	3,950	---	12	29	69	Copper
Lead[4]	446	9.2	14	27	58	3,979	8	19	43	140	Lead
Zinc[4]	445	9	21	50	100	3,963	12	36	68	130	Zinc
Silver[4]	445	---	---	.2	.6	3,961	---	.2	.5	1	Silver
Cadmium[4]	445	---	---	.44	.79	3,959	---	.4	.7	1.1	Cadmium
Arsenic[5]	445	---	---	---	20	3,969	---	---	9	24	Arsenic
Antimony[5]	446	---	.95	1.9	3.5	3,965	---	1	3.5	7.9	Antimony

---

[1] In percent.

[2] Leco combustion analysis.

[3] Mercury vapor detector analysis.

[4] Atomic absorption analysis.

[5] Colorimetric analysis.

TABLE 6.—*Percentile distribution of elements in soils in the Coeur d'Alene district, by formation*

[Values are in parts per million except as indicated. Analyses are spectrographic unless otherwise indicated. Leaders (---). no data]

Element	Monzonite (192 samples)					Wallace (2,298 samples)					Element
	Valid Observations	25th	50th	75th	90th	Valid Observations	25th	50th	75th	90th	
Iron[1]	192	2.7	3.3	4.1	5.0	2,175	2.8	3.7	5.3	6.9	Iron
Magnesium[1]	192	.41	.52	.68	.80	2,175	.4	.6	.8	1.1	Magnesium
Calcium[1]	192	.54	.65	.76	.92	2,175	.4	.6	.8	1.1	Calcium
Titanium[1]	192	.29	.37	.47	.54	2,175	.3	.4	.6	.8	Titanium
Manganese	192	473	781	1,340	1,946	2,175	795	1,377	2,308	3,675	Manganese
Boron	192	10	15	21	25	2,175	22	37	66	109	Boron
Barium	192	350	527	705	838	2,175	416	586	756	996	Barium
Beryllium	192	1.0	1.3	2.0	2.5	2,175	.8	1.2	1.6	2.1	Beryllium
Cobalt	192	8	11	14	17	2,175	---	9.4	14.5	19	Cobalt
Chromium	192	18	25	35	49	2,175	23	32	43	55	Chromium
Lanthanum	192	21	28	36	50	2,175	---	25	35	47	Lanthanum
Molybdenum	---	---	---	---	---	---	---	---	---	---	Molybdenum
Niobium	---	---	---	---	---	2,000	---	8	10	13	Niobium
Nickel	192	13	16	21	27	2,175	17	24	32	43	Nickel
Scandium	192	7	9	11	14	2,175	10	13	---	---	Scandium
Strontium	192	182	277	387	518	2,175	104	154	214	265	Strontium
Vanadium	192	55	74	108	153	2,170	71	94	120	155	Vanadium
Yttrium	192	14	18	25	33	2,175	16	22	30	39	Yttrium
Zirconium	192	118	151	198	248	2,175	153	203	269	347	Zirconium
Mercury[2]	192	.05	.08	.13	.23	2,176	.05	.13	.24	.39	Mercury
Copper[3]	177	14	21	34	65	2,293	22	29	35	47	Copper
Lead[3]	192	22	34	51	139	2,296	29	45	75	149	Lead
Zinc[3]	192	74	107	181	452	2,295	70	115	203	365	Zinc
Silver[3]	192	.4	.6	.8	1.1	2,292	.5	.6	.8	1.1	Silver
Cadmium[3]	192	.6	.8	1.1	2.2	2,142	---	.5	1	1.7	Cadmium
Arsenic[4]	192	---	---	11	21	2,178	---	---	10	20	Arsenic
Antimony[4]	192	.4	.8	1.6	3	2,178	.8	1.1	2.8	5.3	Antimony
Sulfur[1] [5]	31	.019	.029	---	---	395	.038	.046	.055	.070	Sulfur

Element	St. Regis (1,586 samples)					Revett (699 samples)					Element
	Valid Observations	25th	50th	75th	90th	Valid Observations	25th	50th	75th	90th	
Iron[1]	1,544	2.7	3.7	5.1	6.7	693	2.9	3.8	5.3	6.9	Iron
Magnesium[1]	1,544	.4	.6	.8	1	693	.4	.5	.7	.8	Magnesium
Calcium[1]	1,544	.4	.6	.8	1	693	.3	.5	.7	.9	Calcium
Titanium[1]	1,544	.3	.5	.7	1	693	.4	.5	.7	1	Titanium
Manganese	1,544	993	1,809	3,241	5,198	693	961	1,730	2,504	3,829	Manganese
Boron	1,544	19	31	55	145	693	20	30	48	79	Boron
Barium	1,544	486	684	979	1,431	693	454	616	812	1,125	Barium
Beryllium	1,544	---	1.1	1.6	2.2	693	---	1	1.5	2	Beryllium
Cobalt	1,544	---	9.5	1.4	19	693	---	8.8	13	17	Cobalt
Chromium	1,544	27	34	46	57	693	27	34	45	54	Chromium
Lanthanum	1,544	---	25	34	45	693	---	27	36	51	Lanthanum
Molybdenum	---	---	---	---	---	---	---	---	---	---	Molybdenum
Niobium	1,255	---	---	10	11	553	---	---	10	11	Niobium
Nickel	1,544	15	21	29	35	693	15	20	25	33	Nickel
Scandium	1,544	.8	10	12	15	693	8.5	10	12	16	Scandium
Strontium	1,544	117	164	222	275	693	105	157	220	282	Strontium
Vanadium	1,539	67	90	114	148	693	76	97	117	153	Vanadium
Yttrium	1,544	15	21	27	36	693	14	20	28	37	Yttrium
Zirconium	1,544	179	234	312	374	693	196	269	356	500	Zirconium
Mercury[2]	1,445	.05	.1	.2	.4	692	.04	.08	.18	.31	Mercury
Copper[3]	1,584	22	30	42	60	698	21	29	38	53	Copper
Lead[3]	1,584	24	39	71	195	698	27	41	76	218	Lead
Zinc[3]	1,584	57	86	141	250	697	50	77	117	218	Zinc
Silver[3]	1,583	.4	.6	.8	1.1	697	.4	.6	.7	1	Silver
Cadmium[3]	1,480	.4	.7	1.1	2.8	654	.4	.7	1.1	2.3	Cadmium
Arsenic[4]	1,544	---	---	9.8	20	693	---	---	10	20	Arsenic
Antimony[4]	1,544	.9	1.9	3.8	7	693	.9	1.8	2.8	5.7	Antimony
Sulfur[1] [5]	155	.039	.049	.063	.078	55	.044	.053	.071	.095	Sulfur

See footnotes at end of table.

TABLE 6.—*Percentile distribution of elements in soils in the Coeur d'Alene district, by formation*—Continued

Element	Burke (573 samples)					Prichard (1,705 samples)					Element
	Valid Observations	25th	50th	75th	90th	Valid Observations	25th	50th	75th	90th	
Iron[1]	565	2.6	3.3	4.4	5.6	1,441	2.5	3.1	3.9	5.1	Iron
Magnesium[1]	565	.45	.60	.73	.84	1,441	.46	.61	.74	.86	Magnesium
Calcium[1]	565	.42	.59	.80	1	1,441	.39	.57	.75	.98	Calcium
Titanium[1]	565	.40	.49	.70	1	1,441	.43	.56	.72	.88	Titanium
Manganese	565	829	1,373	2,249	3,313	1,441	766	1,285	2,034	3,010	Manganese
Boron	565	19	29	44	74	1,441	20	28	41	62	Boron
Barium	565	475	647	822	1,065	1,441	473	647	828	1,090	Barium
Beryllium	565	.9	1.1	1.5	2.0	1.441	1.1	1.4	1.8	2.3	Beryllium
Cobalt	562	8	10	14	18	1,436	10	14	20	28	Cobalt
Chromium	565	24	32	43	54	1,441	31	43	50	78	Chromium
Lanthanum	565	20	25	34	47	1,441	22	29	37	51	Lanthanum
Molybdenum	---	---	---	---	---	---	---	---	---	---	Molybdenum
Niobium	490	---	9	11	12	1,423	---	9	11	15	Niobium
Nickel	565	15	21	29	35	1,441	20	29	38	51	Nickel
Scandium	565	8	10	12	16	1,441	9	11	14	17	Scandium
Strontium	565	117	178	239	310	1,441	114	159	215	256	Strontium
Vanadium	561	66	90	112	141	1,441	71	98	131	160	Vanadium
Yttrium	565	15	21	30	38	1,441	19	25	33	41	Yttrium
Zirconium	565	179	252	343	472	1,418	187	253	330	395	Zirconium
Mercury[2]	562	.04	.09	.16	.26	1,417	.07	.13	.24	.50	Mercury
Copper[3]	476	15	20	24	31	1,586	17	21	28	37	Copper
Lead[3]	449	23	35	54	108	1,642	35	54	107	237	Lead
Zinc[3]	566	63	89	125	176	1,697	89	140	220	339	Zinc
Silver[3]	567	.4	.6	.8	1.1	1,632	.4	.5	.7	1.1	Silver
Cadmium[3]	559	.5	.7	1.1	1.9	1,440	.8	1.3	2.8	5.7	Cadmium
Arsenic[4]	565	---	8.6	11	22	1,441	---	10	21	28	Arsenic
Antimony[4]	564	.5	1	2	4	1,442	.8	1	4	8	Antimony
Sulfur[1][5]	143	.023	.035	.051	.07	421	.019	.029	.044	.060	Sulfur

Element	Belt (987 samples)					All Formations (8,713 samples)					Element
	Valid Observations	25th	50th	75th	90th	Valid Observations	25th	50th	75th	90th	
Iron[1]	987	2.8	3.7	5.1	7	8,249	2.7	3.6	4.9	6.5	Iron
Magnesium[1]	987	.5	.7	1.1	1.5	8,249	.47	.65	.81	1.1	Magnesium
Calcium[1]	987	.3	.5	.7	1	8,249	.41	.60	.82	1	Calcium
Titanium[1]	987	.3	.5	.7	.9	8,249	.38	.52	.73	1	Titanium
Manganese	987	599	866	1,387	2,040	8,248	777	1,333	2,242	3,597	Manganese
Boron	987	19	32	55	84	8,247	19	30	50	90	Boron
Barium	987	396	528	696	821	8,248	446	628	824	1,109	Barium
Beryllium	987	.9	1.3	1.6	1.9	8,249	.9	1.2	1.6	2.1	Beryllium
Cobalt	987	---	10	14	17	8,207	8.5	11	15	20	Cobalt
Chromium	987	26	36	50	66	8,249	27	35	43	64	Chromium
Lanthanum	987	18	27	38	50	8,249	20	26	35	48	Lanthanum
Molybdenum	---	---	---	---	---	---	---	---	---	---	Molybdenum
Niobium	987	---	---	9.5	11	7,530	---	8.6	10	12	Niobium
Nickel	987	15	21	29	35	8,249	16	23	31	38	Nickel
Scandium	987	7.5	9.5	11	14	8,249	8.3	10	12	16	Scandium
Strontium	987	---	111	157	214	8,249	109	156	218	276	Strontium
Vanadium	987	64	86	120	156	8,235	69	93	118	154	Vanadium
Yttrium	987	16	22	31	37	8,241	16	22	30	37	Yttrium
Zirconium	987	167	237	319	378	8,226	169	229	310	377	Zirconium
Mercury[2]	978	.04	.07	.1	.2	8,124	.05	.1	.2	.3	Mercury
Copper[3]	987	20	27	36	49	8,695	21	28	37	53	Copper
Lead[3]	987	22	31	43	55	8,514	28	43	75	171	Lead
Zinc[3]	987	43	62	85	118	8,684	61	95	161	280	Zinc
Silver[3]	986	.4	.5	.7	.9	8,611	.4	.6	.7	1.1	Silver
Cadmium[3]	987	.4	.7	1	1.2	7,167	.5	.8	1.3	2.7	Cadmium
Arsenic[4]	987	---	---	---	18	8,265	---	---	10	22	Arsenic
Antimony[4]	987	.4	.8	1.1	2.3	8,153	.8	1.1	2.9	5.8	Antimony
Sulfur[1][5]	---	---	---	---	---	759	.039	.047	.057	.073	Sulfur

[1] In Percent.

[2] Mercury vapor detector analysis.

[3] Atomic absorption analysis.

[4] Colorimetric analysis.

[5] Leco combustion analysis.

☆ U.S. GOVERNMENT PRINTING OFFICE: 1980—678–525